Graphic design: Communication Division, UiB / Print: Skipnes Kommunikasjon AS

uib.no

ISBN: 978-82-308-3854-9

2017

Deglaciation of the Norwegian fjords • Henning Åkesson

Deglaciation of the Norwegian fjords

Henning Åkesson

Thesis for the Degree of Philosophiae Doctor (PhD)
University of Bergen, Norway
2017

UNIVERSITY OF BERGEN

Deglaciation of the Norwegian fjords

Henning Åkesson

Thesis for the Degree of Philosophiae Doctor (PhD)
at the University of Bergen

2017

Date of defence: 09.01.2018

Year: 2017

Title: Deglaciation of the Norwegian fjords

Name: Henning Åkesson

Print: Skipnes Kommunikasjon / University of Bergen

Acknowledgements

This thesis is the outcome of three full years of work, something that would have been impossible without a number of very talented and generous people.

First of all, I would like to thank my supervisors Kerim, John-Inge and Mathieu for being supportive, interested, excited, and inclusive, and for giving me the opportunity to explore various scientific paths, while pointing me in the right direction when needed. A special thanks to Kerim, you reminded me to go beyond my own narrow field, and opened doors to pursue the interdisciplinary science that this thesis is a taste of.

I would like to thank John-Inge for sharing your immense knowledge of the climate and ice sheet history in Norway, and for putting together and leading the successful EISCLIM project, funded by the Research Council of Norway, that have supported me over these years. I am also indebted to all the other EISCLIM project members; thank you Jan, Anna, Kristian, Haflidi, Aage, Richard, Jason, Dale, Brent, and Lev.

Mathieu, it is difficult to express how grateful I am for the tremendous help and support you have given me. And in particular, for hosting me for a research stay at University of California, Irvine. Also thanks to Romain, Johannes, Yannick, Jeremie, Hélène, Anders, and Bernd for making my stay in Irvine great, I really enjoyed myself! This research stay was funded by the Research Council of Norway, the Meltzerfondet scholarship at the University of Bergen, and the Norwegian Research School in Climate Dynamics. The latter also funded a trip to Greenland for attending a conference and fieldwork.

I am thankful to Faezeh, you hosted me multiple times at Centre for Ice and Climate in Copenhagen and shared your experience on modelling calving glaciers. Rianne, you deserve a special mention for your fantastic contribution and support during our work on Hardangerjøkulen ice cap.

I am also very happy to have been a part of the unique scientific community at the Department of Earth Science and the Bjerknes Centre for Climate Research. Thank you all, and the people at SKD, you know who you are.

Thank you Petra and Anna, for jumping on the idea to start an ice dynamics journal club at University of Bergen, it's been real fun. Basile, Petra, and Nadine, you also contributed greatly to this thesis through our countless scientific discussions, and by giving feedback on an earlier version.

Finally, I would like to thank my family for always being supportive and encouraging, and Ida for being there for me and for being who you are.

Abstract

Melting glaciers and ice sheets are perhaps the most visible signs of a warming climate. Glaciers are retreating on every continent, ice sheets are shedding icebergs into a warming ocean at an accelerating rate, and the atmosphere melts more ice as temperatures rise. Despite these lines of evidence, and a growing scientific and public attention to melting ice; we are still not able to present robust numbers of future sea level rise.

While the overall picture is one of retreat and meltdown, complex patterns arise when we zoom in within a certain region. The geologic record testaments both collapse and periods of growth, and provides important clues to future mass loss. However, these records show that variable responses were present within regions exposed to the same climate forcing. This is also found in Greenland and Antarctica today, where observations reveal that neighbouring glaciers respond differently to the same climate warming. Caution is therefore needed when explaining the responses of these glaciers.

The instrumental record helps us to improve process understanding, yet is unable to assess changes over time scales longer than a few decades. The geologic record provides a longer perspective, but is not able to resolve short-lived variations. This time scale issue is critical because we need to understand both the short-term and long-term response to improve understanding of glacier and ice sheet dynamics and their sensitivity to climate change.

In this thesis, we use a suite of numerical model tools combined with geological data to assess how external forcing triggers and drives short- and long-term change. Equally important, we study how site-specific factors such as topography can prevent, delay, dampen, amplify, and override the ambient forcing. We assess theoretical cases as well as past and present glaciers in Norway and Greenland, with the goal to answer the overarching question: how do glaciers and ice sheets respond to climate change?

We move from the sensitivity of a Norwegian ice cap to Holocene climate change in Paper I, via the impact of fjord geometry on grounding line stability in Paper II, to the abrupt retreat of the nearby Hardangerfjorden glacier during the Younger Dryas cold period in Paper III. We continue with the most active glacier in Greenland in Paper IV, and finish with a comprehensive study of the triggers and drivers of the deglaciation of the Norwegian fjords in Paper V.

For marine-terminating glaciers, we find that grounding line dynamics and ice-ocean interactions are fundamental over time scales up to a century or two. Beyond this time frame, changes to the surface mass balance are likely to drive widespread, multi-centennial to millennial scale deglaciation. Based on the results presented in this thesis, we also suggest that topography is a factor that cannot be ignored. Once triggered, the response to climate change is to a large degree controlled by the underlying bed topography of ice caps (Paper I), and by the fjord bathymetry and width of marine-terminating glaciers (Papers II–V).

The implications are that continued intense studies of warming seas around Greenland and Antarctica are justified, but also that assessments of atmospheric-induced melt will be important to estimate long-term sea level change. The striking impact of topographic factors found in this thesis also shows a potential to use geometry to predict future evolution and estimate past retreat and advance.

List of papers

I. Åkesson, H., Nisancioglu, K. H., Giesen, R. H., and Morlighem, M. Simulating the evolution of Hardangerjøkulen ice cap in southern Norway since the mid-Holocene and its sensitivity to climate change, *The Cryosphere*, **11**, 281-302, https://doi.org/10.5194/tc-11-281-2017, 2017.

II. Åkesson, H., Nisancioglu, K. H., and Nick, F.M. Impact of fjord geometry on grounding line stability, *Frontiers of Earth Science: Cryosphere, in review*, 2017.

III. Åkesson, H., Gyllencreutz, R., Mangerud, J., Svendsen, J.I., Nick, F.M., and Nisancioglu, K.H. Fast retreat of a marine outlet glacier in western Norway at the last glacial termination, *manuscript prepared for submission*.

IV. Steiger, N., Nisancioglu, K. H., Åkesson, H., de Fleurian, B., and Nick, F. M. Non-linear retreat of Jakobshavn Isbræ since the Little Ice Age controlled by geometry, *The Cryosphere Discuss.*, https://doi.org/10.5194/tc-2017-151, *in review*, 2017.

V. Åkesson, H., Morlighem, M., Nisancioglu, K. H., Svendsen, J.I., and Mangerud, J. Deglaciation of the Norwegian fjords, *manuscript prepared for submission to Quaternary Science Reviews*.

Contents

Chapter 1

Scientific background and motivation

1.1 Why study land-ice?

If all land-based ice on Earth were to melt, global mean sea level would rise by 70 m. While this will not happen in our lifetime, glaciers and ice sheets are currently the largest contributors to sea level rise (Church et al., 2013). With future warming over the next century, sea level contributions from glaciers and small ice caps are projected to be larger than those from Greenland and Antarctica, and from thermal expansion of the ocean. Equally important, future change to glaciers and ice sheets flowing into the ocean is perhaps the least understood yet most potent wildcard concerning future rising seas (Mengel et al., 2016; Pattyn et al., 2017).

Melting ice also affects atmospheric circulation (Roe and Lindzen, 2001; Liakka et al., 2012; Löfverström et al., 2014), ocean freshwater budgets and ocean circulation (Tarasov and Peltier, 2005; Peck et al., 2006; Bamber et al., 2012; Dokken et al., 2013), as well as hydrology in mountain regions (Bliss et al., 2014), the latter with relevance for local biology, hydropower, tourism, and agriculture.

Glaciers and especially ice sheets were long thought to respond slowly to climate change; hence the expression 'with glacial pace'. However, this concept has been turned upside down over the last 15 years. Recent large calving events and accelerating ice loss in Greenland and Antarctica have transformed our view of ice sheets and we now know they can change over human time scales. New insight from the geologic record has further cemented this notion. Figure 1.1 outlines the numerous interactions between glaciers, ice sheets and the climate system.

1.2 Flow and mass balance of glaciers and ice sheets

1.2.1 Glaciers and ice sheets

A glacier is a moving body of perennial snow and ice. Glaciers and ice caps are typically $<$50,000 km^2 in area (Cogley et al., 2011), most of them considerably smaller. Valley glaciers flow downslope due to gravity down mountain valleys, while ice caps are features with a gently sloping interior covering the underlying topography, with outlet glaciers draining the interior. In contrast, continental ice sheets (area larger than 50,000 km^2) currently occupy Greenland and Antarctica, and have covered North

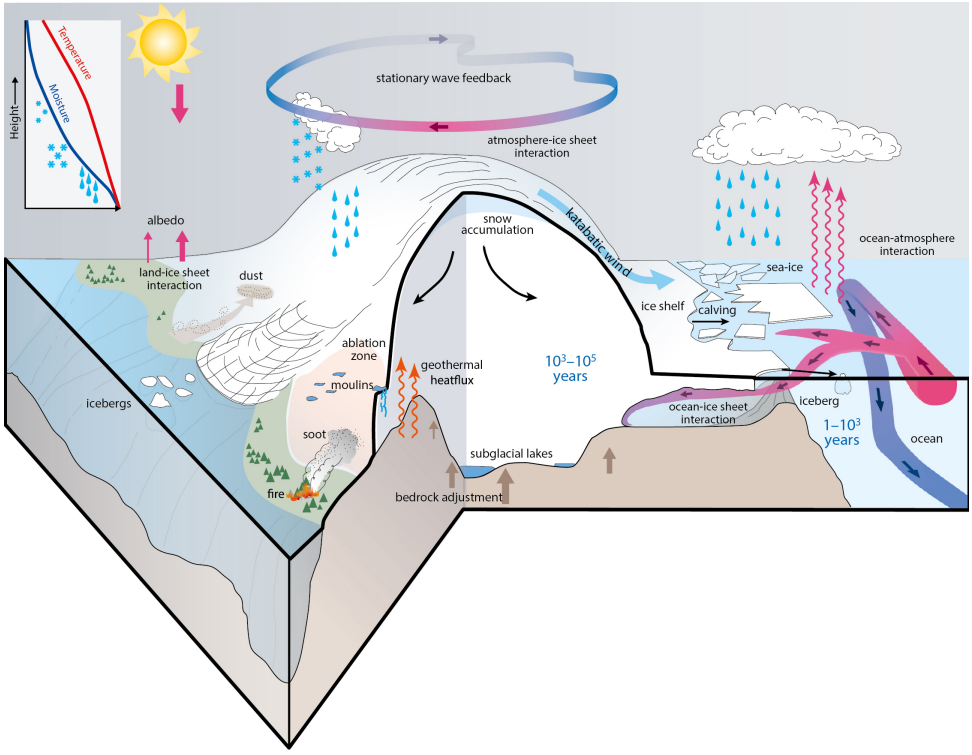

Figure 1.1: Overview of ice sheets in the climate system and approximate time scales of change involved. Figure from IPCC, 2013.

America (Laurentide Ice Sheet), and northern Europe and northern Asia (Eurasian Ice Sheet) during past glacial periods.

We distinguish between marine- and land-terminating ice margins. At margins of ice sheets, ice flow is often confined by deep troughs, constituting outlet glaciers terminating in fjords, or *marine-terminating glaciers*. These glaciers feature a suite of additional processes compared to glaciers terminating on land. A glacier with a grounded terminus, that is, with a vertical front, is called a *tidewater* glacier (Fig. 1.2a). In contrast, some glaciers have floating termini (Fig. 1.2b), or *ice shelves*. The boundary between grounded and floating ice is called the *grounding line*. In practice, there is not always a clear distinction between the two glacier types, and with time a glacier may change behaviour and geometry towards one or the other type.

1.2.2 Ice flow

Ice moves due to two mechanisms: ice deformation and basal slip (Cuffey and Paterson, 2010). The velocity we observe at the ice surface is hence the sum of these two components.

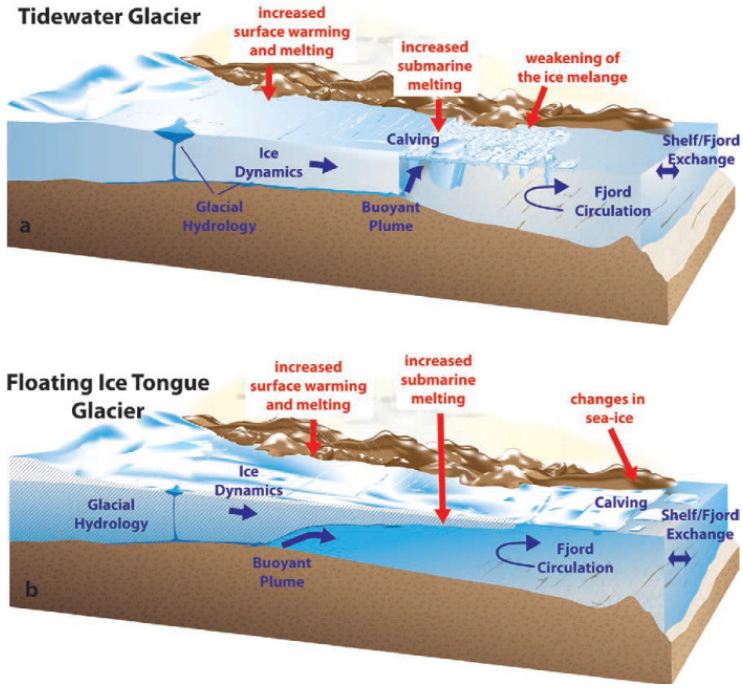

Figure 1.2: Overview of glaciological, oceanic and atmospheric processes involved for glaciers terminating in fjords, where we distinguish between (a) tidewater glaciers, with grounded termini, and (b) marine-terminating glaciers with floating termini. Figure from Straneo et al. (2013).

Ice deformation

Under enough weight, usually ice thicker than 30 m, ice starts to deform under its own weight, with deformation increasing with depth. Ice temperature largely controls deformation of ice, though ice fabric, impurities, and crystal orientations may also be important. Temperate (warm) ice found in maritime or relatively warm climates deforms more readily due to its lower viscosity, while cold ice found in continental cold climates tend to be more viscous and deform more moderately (Cuffey and Paterson, 2010).

Basal slip

In cold climates, glaciers may be frozen to their beds, in which case ice moves solely by internal deformation. In all other cases, glaciers slip along their beds (Cuffey and Paterson, 2010). Basal slip is a combination of sliding at the ice-bedrock or ice-sediment interface, and deformation of basal sediment (if present). The sliding speed is thought to be a function of basal roughness, sediment presence and characteristics, and basal hydrology. Basal slip is one of the most elusive problems in glaciology. Involved processes have key importance for glacier dynamics yet are extremely challenging to measure directly. In ice sheet models without explicit modelling of subglacial hydrol-

ogy, basal slip is normally parameterized as a function of a basal drag coefficient, which is meant to incorporate the aforementioned factors. Basal drag coefficients can be estimated using data assimilation methods for present-day ice sheets and glaciers, usually based on surface velocities measured from remotely sensed platforms (MacAyeal, 1993; Morlighem et al., 2010). When working with past or future ice masses, this velocity data is however not available to constrain basal conditions. The knowledge about both spatial and temporal evolution of basal drag remains poor, especially on interannual and longer time scales.

1.2.3 Surface mass balance and feedbacks

Surface mass balance is governed by the amount of winter snowfall and summer melt. Basal melt is usually negligible, except in geothermally active regions. Glaciers located in maritime regions, such as Norway, tend to have higher snowfall due to their proximity to moisture sources. With high winter snowfall, these glaciers can be sustained in a warmer climate with more summer melt. These glaciers have a larger mass throughput, since both winter and summer balance magnitudes are higher. This also makes them more responsive to external forcing (Johannesson et al., 1989).

The response of glaciers to climate change and their *equilibrium line altitude* (ELA) are tightly connected. The ELA marks the altitude where winter snowfall and summer melt balance each other, so that net annual surface mass balance is zero. With climate warming (cooling) the ELA rises (falls), and the glacier responds on time scales determined by the mass turnover, hypsometry (how glacier geometry varies with altitude) and ice dynamics (Johannesson et al., 1989; Harrison et al., 2001), see Fig. 1.3.

An important positive feedback exists between surface mass balance and altitude. This feedback is active both in a warming and cooling climate. In a warming scenario, surface melt increases, which lowers the glacier surface. Since air temperature normally decreases with altitude, the thinned surface is now located at a lower elevation and experiences a higher temperature, further accelerating melt. Conversely, a cooling climate causes less melt and glacier thickening up to higher altitudes, in turn reducing melt. There may be compensating effects, however. Warmer air can hold more moisture and increased winter precipitation can therefore counteract more melt in a warming climate. Increased snowfall caused a widespread advance of glaciers on the Norwegian west coast during the 1990s, in a period where glaciers elsewhere in the world were retreating due to atmospheric warming (Nesje and Matthews, 2012; Leclercq et al., 2014; Marzeion et al., 2014). In contrast, a cooling may starve the glacier of winter snowfall, offsetting the reduced melt.

The above points highlight that multiple glacier equilibria are possible for a given climate, or conversely, that a certain glacier state may be reached by several combinations of forcing. This also applies to ice dynamics (Sect. 1.2.2) and glacier geometry (Sect. 1.3.4).

1.3 Marine-terminating glaciers and their controls

The coasts of Patagonia, Alaska, Svalbard, and Greenland's western, southern and eastern coasts are dominated by tidewater glaciers, while Greenland's northern coast and

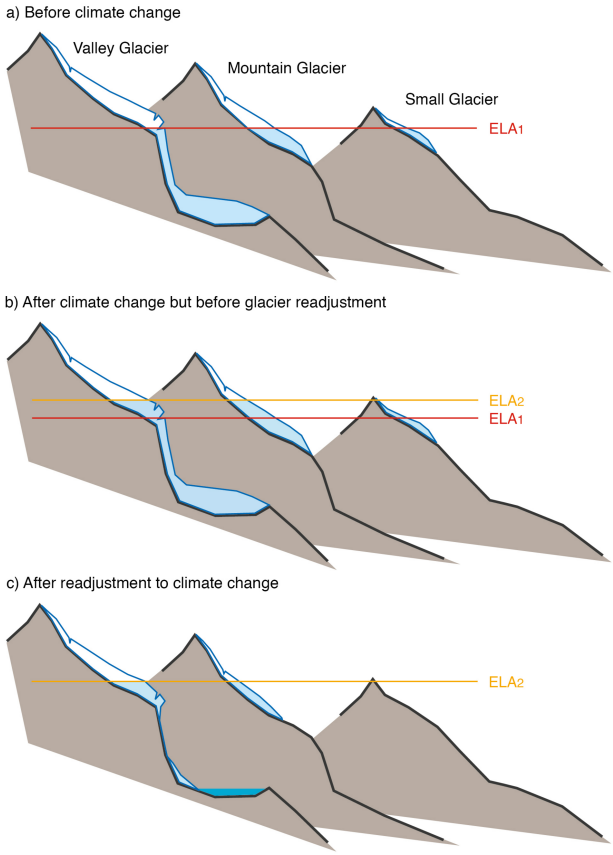

Figure 1.3: How glaciers in a certain climate (ELA_1) respond to climate warming and a new ELA_2. Note that if the ELA rises above the highest point of a glacier (small glacier in c)), net melt occurs over the entire glacier surface and the glacier will melt away completely. Figure from IPCC, 2013.

Antarctica mainly see glaciers with floating ice tongues or ice shelves (Fig. 1.2). Although marine-terminating glaciers are all calving, the style of calving is very different. Iceberg *calving* can be defined as blocks of ice being mechanically detached from a glacier front (Benn et al., 2007). Tidewater glaciers tend to produce icebergs created by crevassing near the calving front, while glaciers with floating termini often produce large, tabular icebergs caused by fractures originating farther upstream from the terminus (e.g. Falkner et al., 2011).

Another distinction is the type of controls of mass balance. Tidewater glacier mass balance is heavily controlled by seasonal calving. In contrast, mass balance for glaciers with floating ice tongues are mostly influenced by submarine melt, and their calving behaviour is thought to be affected by semi-permanent sea ice (Reeh et al., 2001; Straneo et al., 2013; Robel, 2017).

In the mid-1990s, acceleration, thinning and retreat of marine-terminating glaciers started in west and southeast Greenland (Luckman and Murray, 2005; Luckman et al.,

2006; Rignot and Kanagaratnam, 2006; Howat et al., 2007), and spread to the northwest during the mid-2000s (Khan et al., 2010). Speed-up and increased calving now also occur in the cold and dry northeastern part of Greenland, possibly initiated by a few years of reduced sea ice concentration and associated reduced back stress during 2002–2004 (Khan et al., 2014; Mouginot et al., 2015).

1.3.1 The atmosphere

Aforementioned recent changes in Greenland are broadly consistent with the observed warmer atmospheric and oceanic conditions (Bersch et al., 2007; Holland et al., 2008; Box et al., 2009). However, this pattern involves considerable spatial and temporal variability, even within the same regions (Howat et al., 2008; McFadden et al., 2011; Moon et al., 2012). Rising temperatures have caused a more negative surface mass balance and a lower surface albedo over the ice sheet (Fettweis et al., 2011; Hanna et al., 2013). At present, mass loss from Greenland is roughly equally split between surface melt (Van Den Broeke et al., 2009) and ice discharge from marine outlet glaciers (Howat et al., 2007; Straneo and Heimbach, 2013).

More surface melt means higher meltwater fluxes routed to the glacier bed. While providing a strong control of seasonal ice velocities through reorganization of the subglacial drainage system (e.g. Bartholomew et al., 2010; Schoof, 2010; Sole et al., 2011), the net effect of high subglacial water inputs on annual and interannual glacier velocities is less clear (Carr et al., 2013).

Meltwater may also enter surface crevasses and cause mechanical fracture (*hydrofracture*), as well as contribute to rheological weakening of the ice due to heat transfer from the warmer meltwater (Benn et al., 2007; Straneo et al., 2013; Pollard et al., 2015). These processes may affect both calving rates and enhance ice flow (Van Der Veen et al., 2011).

Links between climate and calving are complex (Post et al., 2011). Seasonally calving glaciers should experience higher annual calving rates as a result of any process that will extend the summer calving season. However, calving glaciers may act independent of ambient climate forcing (Pfeffer, 2003, 2007) and the degree of natural versus forced change is a key unknown that needs to be resolved.

Atmospheric-forced surface thinning is of key concern for ice sheet stability, since thinner ice shelves and floating termini may be more susceptible to fracture, calving, and collapse (Nick et al., 2010; Pollard et al., 2015). Thinning in the vicinity of grounding lines may also cause more ice to reach flotation, resulting in grounding line retreat (Sect. 1.3.4).

1.3.2 The ocean

To explain recent dynamic mass loss in Greenland, a leading hypothesis (Holland et al., 2008) is that submarine melt at the ice-ocean boundary triggered initial retreat (Vieli and Nick, 2011; Joughin et al., 2012). There are multiple lines of evidence supporting this idea, yet mechanisms linking a warming ocean to changing ice dynamics and retreat remain poorly understood. This is mainly due to insufficient understanding of physical processes and a pervasive lack of long-term studies connecting glacier activity to ocean forcing (Straneo et al., 2013). We also do not know on what time scales

ocean and atmospheric forcing are relevant, and what role they play in abrupt glacier changes. The observational record is too short to reconcile these issues, highlighting the need for long-term studies.

Submarine melt affects overall glacier mass balance and is important for ice shelves and floating termini, but it also undercuts the glacier terminus and thereby influence calving (Vieli and Nick, 2011; O'Leary and Christoffersen, 2013; Cook et al., 2014; Rignot et al., 2015; Benn et al., 2017). More surface melt increases subglacial discharge at the terminus, which in turn affects fjord circulation. A resulting meltwater plume rises buoyantly along the front, or along the ice shelf draft, if present. This enables entrainment of warm subsurface waters, melting the glacier from below (Jenkins, 2011; Straneo et al., 2011). The relationships between subglacial discharge, ocean warming, and submarine melt rates are however not straightforward. While difficult to directly observe, model studies have found that melt rates scale linearly with the ambient fjord temperature, and sub-linearly with subglacial discharge (Jenkins, 2011; Xu et al., 2012, 2013; Kimura et al., 2014; Slater et al., 2016).

In addition to plume dynamics and direct melting at the ice-ocean boundary, the exchange between continental shelf waters and fjords (e.g. Jackson et al., 2014) provides a link between changes in ocean dynamics, large scale climate dynamics, and ice sheet stability. Recent work has shown that warm Atlantic Water is able to access glacier fronts in particular in the deeper fjords in Greenland (Straneo et al., 2010). Such links are equally relevant in the past, for example between ocean conditions in the Nordic Seas and the deglaciation of the Norwegian fjords, as is the focus of this thesis.

1.3.3 Sea ice and ice mélange

Calving glaciers fill their host fjords with icebergs, which in winter are bound together by sea ice (Amundson et al., 2010). This semi-rigid mixture, called *ice mélange*, varies seasonally and is thought to affect calving rates and glacier stability, since it provides an additional buttressing force ('backstress') at the calving front, preventing calving to occur if the backstress is large enough (Howat et al., 2010; Vieli and Nick, 2011; Robel, 2017). Ice mélange can also dampen fjord circulation changes and tidal influence on the glacier front, as well as surface forcing such as wind stress (MacAyeal et al., 2012). For floating ice tongues, ice mélange and land-fast sea ice also affect calving (Reeh et al., 2001). Land-fast sea ice may prevent calved icebergs from being transported away from the glacier front, and thereby strengthen the ice mélange and promote glacier stability (Higgins, 1991; Reeh et al., 2001). When semi-permanent sea ice breaks up, rapid calving and mélange disintegration may take place (Higgins, 1991), as has happened more frequently in northeast Greenland (several times per decade; Hughes et al. (2011)) than in the decades before.

Carr et al. (2013) suggests that depending on the setting, sea ice decline may affect marine-terminating glacier dynamics in two ways. For seasonally ice-free fjords, less sea ice will extend the calving season. In fjords with perennial sea ice cover, sea ice decline may cause a transition from a semi-permanent cover with little calving to seasonally ice-free conditions with more vigorous calving.

1.3.4 Geometry and grounding line dynamics

Assessing glacier-specific factors such as geometry is key to understand glacier and ice sheet response to external forcing (Carr et al., 2013). The major Northern Hemisphere ice sheets during the last glacial period, the Laurentide and Eurasian Ice Sheets, both had extensive marine margins and fast-flowing ice streams (Sejrup et al., 2003; Stokes and Tarasov, 2010; Hughes et al., 2016). The bed topography of the Greenland Ice Sheet includes deep troughs below sea level extending far inland (Morlighem et al., 2014). The Antarctic Ice Sheet is also marine-based, with 45 % of the ice sheet area grounded below sea level (Fretwell et al., 2013; Millan et al., 2017), with especially the West Antarctic Ice Sheet being vulnerable to future mass loss and sea level rise (Mercer, 1978; Pollard et al., 2015). This concern has arisen from the geometry of West Antarctica's subglacial landscape, which deepens towards the interior of the ice sheet. Glaciers resting on these landward-sloping, or *retrograde*, beds have been considered inherently unstable (Weertman, 1974; Hughes, 1986; Pfeffer, 2007; Joughin et al., 2008). This instability is due to the fact that grounding line flux is thought to be proportional to some higher power (perhaps 4 or 5) of ice thickness at the grounding line (Schoof, 2007; Tsai et al., 2015). This means that with grounding line retreat along a retrograde bed follows an increased ice discharge through the grounding line, a positive feedback active as long as the bed deepens upstream. This situation is referred to as the *marine ice sheet instability* due to the self-sustaining flux feedback. It follows that this behaviour can cause retreat weakly correlated with or even independent of the ambient climate forcing (Weertman, 1974; Pfeffer, 2003; Goldberg et al., 2015; Pattyn et al., 2017).

Recent work suggests that grounding lines may stabilise even on retrograde beds (Nick et al., 2010; Gudmundsson et al., 2012; Jamieson et al., 2012; Enderlin et al., 2013; Carr et al., 2014). Ice shelf buttressing (Goldberg et al., 2009; Gudmundsson, 2013; Schoof et al., 2017) and/or topographic bottlenecks (Mercer, 1961; Jamieson et al., 2012; Stokes et al., 2014) may provide enough resistance to compensate for an otherwise unstable bed geometry. A related troublesome scenario is that loss of ice shelves (Scambos et al., 2004; Hogg and Gudmundsson, 2017) and floating ice tongues (Falkner et al., 2011; Mouginot et al., 2015) weakens or eliminates buttressing of inland ice, accelerating upstream ice discharge into the ocean with following sea level rise.

A potential stabilising feedback to long-term marginal mass loss is falling near-field sea level caused by bedrock uplift (Gomez et al., 2010). The latter is caused by loss of gravitational pull from the retreating ice sheet as well as from a declining ice load. Isostatic adjustment has also been shown to cause ice marginal oscillations over multi-millennial time scales in idealised marine ice sheet settings (Bassis et al., 2017).

Clearly, sea level change, grounding line dynamics and the role of geometry versus external forcing are among the big questions in glaciology and climate science, with populous coastlines worldwide in threat of future sea level rise. Even so, projections can still not present robust numbers on future mass loss, in part because analogous past ice sheet behaviour is still not well understood either.

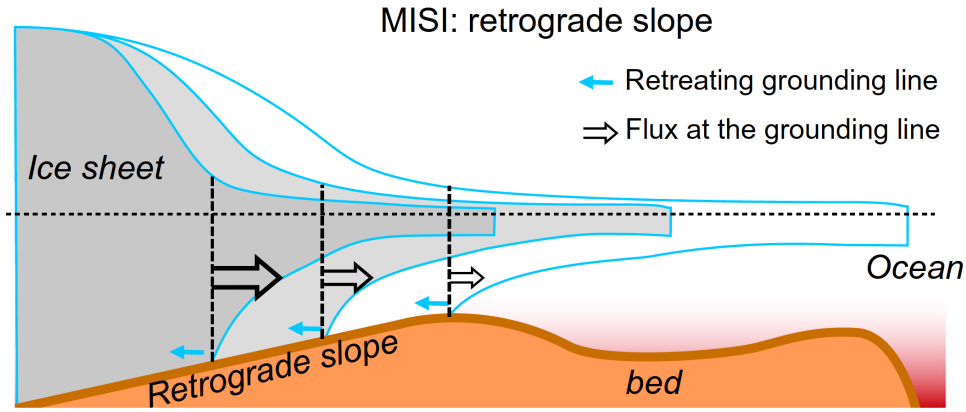

Figure 1.4: The Marine Ice Sheet Instability (MISI): a self-sustaining feedback that can cause unstable grounding line retreat. Grounding flux increases with ice thickness at the grounding line. For an inland-sloping (retrograde) bed, grounding line retreat leads to increased flux, thinning, loss of buttressing and more ice becoming afloat, moving the grounding line further inland where water is deeper and ice thicker. Further increased ice flux cause further thinning, and retreat. Figure modified after Pattyn et al. (2017).

1.4 The fjords of Norway and their deglacial and postglacial history

–*"Norway, the land of a thousand fjords."*

Norway[1] shares features with landscapes in Alaska, British Columbia, Patagonia, New Zealand, and Greenland, with deep fjords and valleys incised far inland into mountainous topography. Studying marine-based retreat in Norway during deglaciation thus provides valuable analogues for past and future mass loss from other fjord-incised coasts.

Ice sheets are the only means of eroding landscapes below sea level. Today's fjords have been carved out over multiple glacial cycles with enhanced erosion of the underlying bedrock (e.g. Kessler et al., 2008), though the time scales and their formation mechanisms are debated (Cook and Swift, 2012). Norway has 1,190 named fjords, the major ones typically 300–800 m deep, the deepest being Sognefjorden at 1308 m below sea level (Table 1.1). Topography is generally complex, with scattered islands, embayments, and multiple fjord arms. Land topography ranges from gently sloping areas up to a few hundred meters high close to the coast, to thousand meter high vertical rock walls. Mountains surrounding the fjords reach elevations of ∼1000–1200 m a.s.l., making a total relief of almost 2000 m at places. Since these areas were covered by the ice sheet during the last glacial period, ice thickness must have exceeded two kilometres in some fjords during the Last Glacial Maximum (LGM), 21–20 ka before present (BP). Further inland, the landscape transitions to mountain plateaus such as Hardangervidda, a gently undulating landscape characterised by exposed bedrock and little sediment cover. In the fjords, postglacial sediment infill is typically 10–100 m thick, but can be up to 200 m thick locally.

[1]This thesis focuses on the fjords of southwestern Norway; the description here is skewed accordingly.

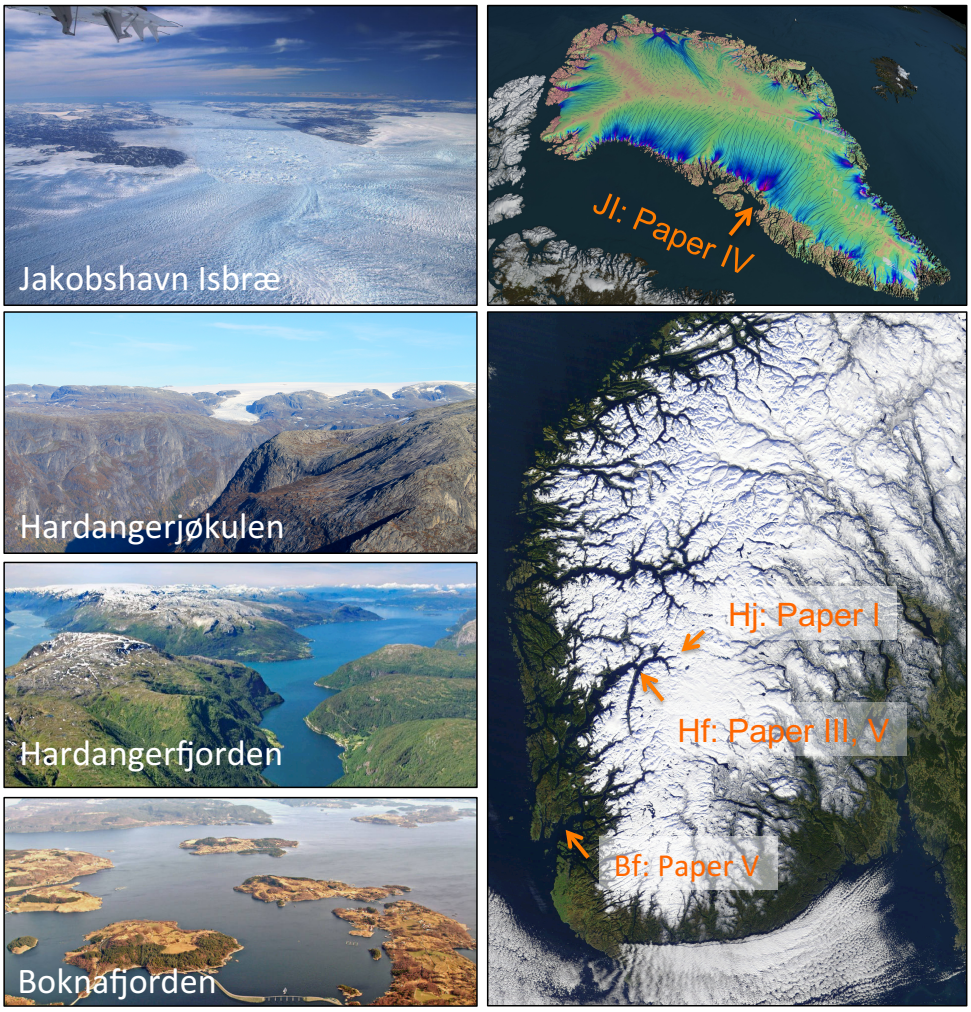

Figure 1.5: Top, left: Photo of the frontal region of Jakobshavn Isbræ, taken towards the fjord, studied in Paper IV. Note the calving front in the middle of the photo. Top, right: Map of ice surface velocity of the Greenland Ice Sheet. Below: Satellite image of southern Norway and key locations in this thesis: JI–Jakobshavn Isbræ (Paper IV), Hj–Hardangerjøkulen (Paper I), Hf–Hardangerfjorden (Paper III and V), and Bf–Boknafjorden (Paper V). These are typical landscapes for SW Norway, with Hardangerjøkulen situated in the transition zone between the fjords and the inland mountain plateau Hardangervidda. The valley depicted below Hardangerjøkulen continues into Hardangerfjorden further down (west). Credit: William Colgan (Jakobshavn), NASA (Greenland), Mads Erik Eriksson (Hardangerjøkulen), Finn Loftesnes (Hardangerfjorden), Statens Vegvesen (Boknafjorden).

Table 1.1: Characteristics of selected major fjords in Norway, sorted south to north. Numbers are typical and deviate locally. Fjord length may vary depending on exact points of measure. Map data from norgeskart.no/Norwegian Mapping Authority.

Fjord	Length (km)	Width (km)	Depth (m)	Sill depth (m)
Boknafjorden–Vindafjorden	120–130	5–10 (20)	200–700	200–300
Hardangerfjorden	180	5–10	400–800	300
Nordfjord	105	2–4	200–500	150
Sognefjorden	205	2–5 (10)	900–1200	200
Trondheimsfjorden	130	5–15	400–600	50–300
Skjerstadfjorden–Saltfjorden	65	(1) 2–6	300–400	no sill
Lyngen	82	3–10	75-300	no sill
The 'typical' Norwegian fjord	80–120	3–10	400–700	200–300

1.4.1 Deglaciation

At its maximum extent during the LGM ∼21–20 ka BP, the Eurasian Ice Sheet was more than three times more extensive than the present-day Greenland Ice Sheet (Svendsen et al., 2004; Hughes et al., 2016), and ∼40 % of the size of the modern Antarctic Ice Sheet. The North Sea was at least partly covered with ice connecting the Scandinavian Ice Sheet and the British-Irish Ice Sheet (Fig. 1.6). Southern Norway was entirely glaciated and glacial striations found in high-elevation bedrock indicate ice flow directions independent of the underlying topography, including flow perpendicular to fjord orientations (Hamborg and Mangerud, 1981; Sæle, 2017).

Off the Norwegian west coast, the Norwegian Channel Ice Stream was active sometime between 20–18 ka BP, possibly activated in stages, before it collapsed (Sejrup et al., 2003; Svendsen et al., 2015). This southeast-northwest oriented ice stream transported ice through a prominent 200-400 m deep, 50–100 km wide trough towards the shelf edge off the western coast of southern Norway (Fig. 1.6).

Following ice stream collapse, marginal retreat in southwestern Norway was limited between 18 and 15 ka BP. Sea surface temperatures in the Norwegian Sea were relatively stable during this time (Eldevik et al., 2014; Dokken et al., 2015). Since land areas were largely ice-covered, little information is available from terrestrial proxies. Greenland ice core records suggest a variable climate with little net change during this period (Rasmussen et al., 2014).

The timing and extent of marginal retreat appear to have varied significantly between nearby fjord systems. Reconstructions suggest that the Boknafjorden–Jæren region was the most sensitive in southwestern Norway, with retreat initiated ∼18 ka BP and accelerating around 16–15 ka BP (Svendsen et al., 2015; Johnsen, 2017; Gump et al., 2017). In contrast, the Hardangerfjorden region ∼60 km north was relatively stable, with little ice margin retreat until 14 ka BP.

The following Bølling-Allerød (BA) warm period c. 14.8–12.7 ka BP saw widespread ice sheet retreat. This notion is based on stratigraphic evidence (Mangerud, 1977; Lohne et al., 2007; Mangerud et al., 2011), since the subsequent Younger Dryas readvance c. 12.7–11.6 ka BP erased any geomorphological evidence from Allerød (c. 13.9–12.7 ka BP) minimum positions. The Allerød ice sheet margin in southwestern

Norway is thought to have been c. 40–50 km inland of the Younger Dryas maximum extent. The major Younger Dryas readvance in southwestern Norway is anomalous compared to other regions of the ice sheet, which saw smaller marginal change during this period. For example, evidence from Norway's southeastern coastal areas and around Oslo suggests readvances of up to 18 km (Sørensen, 1992; Bergstrøm, 1995). The maritime western sector's proximity to Atlantic moisture supply has been suggested to be responsible for the stronger readvances here (Stroeven et al., 2016). A particularly dynamic ice sheet margin in the west is also supported by several short-lived readvances and standstills, reflected by ice-marginal formations deposited after the Younger Dryas (e.g. Andersen, 1981). Such marginal features are absent in southern and eastern areas of the Scandinavian Ice Sheet (Stroeven et al., 2016).

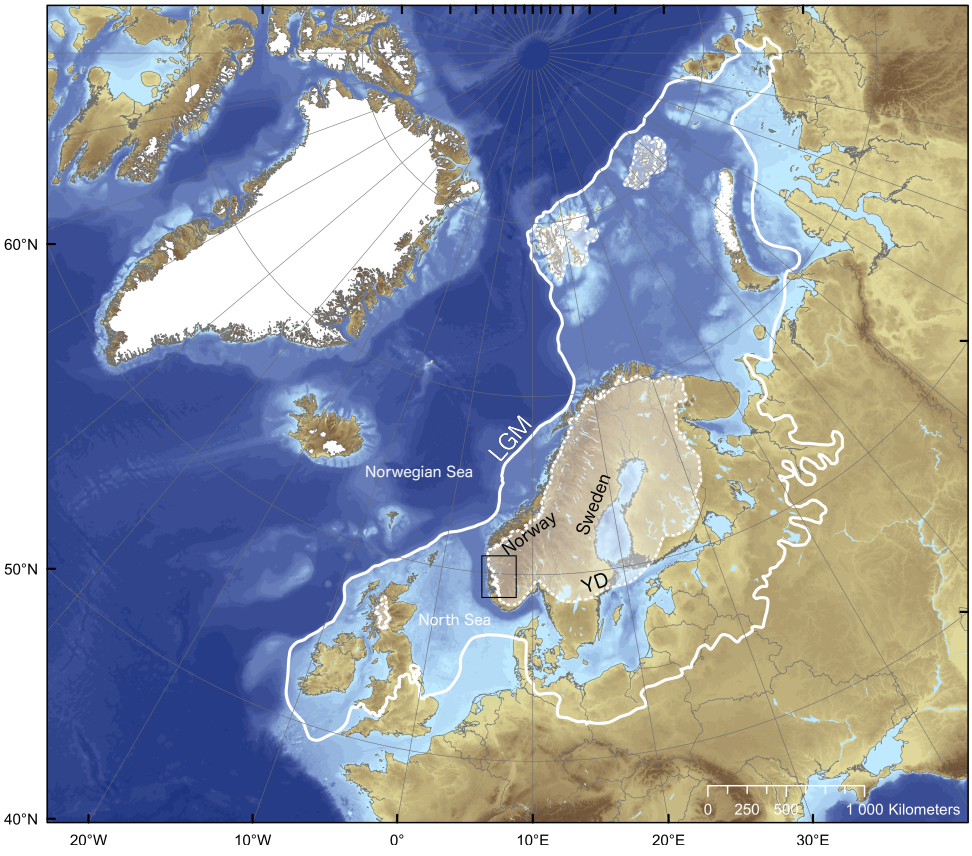

Figure 1.6: Overview map of the extent of the Eurasian Ice Sheet at the Last Glacial Maximum (LGM) c. 21–20 ka BP and the Younger Dryas (YD) c. 12 ka BP. Main focus area of this thesis is indicated (black rectangle). Figure from Paper III, modified after Svendsen et al. (2015) and Hughes et al. (2016).

1.4.2 Holocene history

Following the Younger Dryas, early Holocene warming rendered most of southern Norway ice-free by ∼10 ka BP (Hughes et al., 2016; Stroeven et al., 2016). For the remaining local ice caps and glaciers, ice retreat in response to a gradual warming and possibly drying trend occurred between c.10–6 ka BP (Nesje et al., 1994; Dahl and Nesje, 1994, 1996; Bakke et al., 2005; Bjune et al., 2005). During the mid-Holocene thermal maximum (c. 8 to 4 ka BP), temperatures were up to 2 °C higher than present (Bjune et al., 2005; Velle et al., 2005). All glaciers and ice caps in southern Norway melted away completely during this period (Nesje, 2009). Present-day glaciers in southern Norway are thus not remains from the Scandinavian Ice Sheet. Neoglaciation commenced c. 5–4 ka BP with a cooler and wetter climate towards the Little Ice Age, which in Norway is reflected by widespread glacier readvances in the 18th and 19th century (Kalela-Brundin, 1999; Nordli et al., 2003; Nesje and Dahl, 2003; Nesje et al., 2008a,b; Nesje, 2009; Rasmussen et al., 2010).

At present, numerous glaciers remain in southern Norway, the largest being Jostedalsbreen ice cap (474 km^2), Folgefonna ice cap (201 km^2), and Hardangerjøkulen ice cap (71 km^2) (Andreassen et al., 2012). These are all temperate ice bodies with gently sloping plateaus drained by steeper outlet glaciers. The glaciers have mass turnovers of around ∼2–3 m water equivalent (w.e.), reflecting their maritime location with relatively warm summers compensated by high winter snowfall (Andreassen et al., 2005; Kjøllmoen et al., 2011).

Chapter 2

Objectives and Methods

The main objective of this thesis is to improve our understanding of long-term glacier change and its relation to external forcing. Focus is on climate change in western Norway during deglaciation and the Holocene. This is a data-rich region featuring marine-terminating glaciers in the past and land-terminating glaciers at present, securing a high degree of transferability to other regions. My work aims to assess the responsible forcings and relevant time scales of change during deglaciation of the Norwegian fjords and postglacial variations of a local ice cap in the same region.

More specifically, this thesis attempts to answer the following questions:

- How sensitive are ice caps and glaciers to long-term climate change? (Paper I, V)
- How do past changes in atmospheric and oceanic conditions influence current and future ice mass loss? (Paper I, II, IV)
- What are the relative roles of climate forcing and fjord geometry in controlling marine-based glacier behaviour? (Paper II–V)
- How can detailed bed topography and fjord geometry be used to predict past and future glacier instability? (Paper I–V)

Paper I: *Long-term ice cap dynamics and sensitivity to climate change*

Paper I highlights the potential to combine paleo-data with ice flow models to understand long-term glacier change, and quantifies the sensitivity of the Hardangerjøkulen ice cap in Norway to climate change.

Paper II: *How fjord geometry controls behaviour of marine-terminating glaciers*

This work investigates the impact of synthetic fjord geometry on grounding line stability. The paper identifies key geometric characteristics with potential to improve understanding of past and ongoing changes, as well as to predict whether some marine-terminating glaciers are more vulnerable than others to future climate warming.

Paper III: *Abrupt marine-terminating glacier retreat – a lesson from the past*

Paper III studies the rapid retreat of a marine outlet glacier from the western Scandinavian Ice Sheet during the Younger Dryas cold-reversal. This paper identifies responsible triggers and drivers of retreat of marine outlet glaciers on decadal to centennial time scales. This work also highlights the advantages of combining well-constrained paleoglaciers with numerical ice flow models.

Paper IV: *Dynamics of the fastest-flowing glacier in the world since the Little Ice Age*

In this paper we focus on Jakobshavn Isbræ in western Greenland, and assess the role of regional warming versus fjord geometry and glaciological processes. Greenland is chosen because it is Norway's topographic cousin and a wildcard for sea level rise. Norway's paleo-fjord glaciers provide clues to recent and future mass loss in Greenlnad, and vice versa.

Paper V: *A high-resolution view of deglaciation of marine-based ice sheets*

In Paper V, we transiently simulate the deglaciation of a large region of western Norway. Thereby we aim to improve understanding of how fjord-type landscapes become ice-free, and specifically to investigate the triggers and controls of the deglaciation of the Norwegian fjords.

We employ two different numerical ice flow models. In Paper I, we study the land-terminating Hardangerjøkulen ice cap using the Ice Sheet System Model (ISSM; Larour et al. (2012)) with lower-order ice flow physics and a surface mass balance forcing validated by present-day observations. ISSM supports an adaptive mesh (Hecht, 2006), meaning model resolution can be refined in regions of special interest and kept low elsewhere, a key advantage for long paleo-simulations. We compare model results with evidence from direct ice front measurements, aerial photography, geomorphology, and paleoglaciological reconstructions from lacustrine sediments.

In paper II, III, and IV, we use a flowline model with parameterized width and lateral drag (Vieli et al., 2001; Nick et al., 2010, 2013) with a physically-based calving criterion (Benn et al., 2007; Nick et al., 2010) to study idealised and real-world marine-terminating glaciers in Norway and Greenland. This model allows for ensemble studies and simulations over long time scales at a minimal computational cost but does not capture complex geometry and multiple catchments well.

In Paper V, we study ice flow and deglaciation of a 320×150 km sector of south-western Norway. This region has incredibly complex topography with numerous fjord arms, islands, bays, coastal mountains and inland mountain plateaus. We therefore return to ISSM, using physics and numerical tools built to capture interactions between glacier catchments, fast marine-based ice flow and grounding line dynamics (Seroussi et al., 2014). We also exploit a wealth of empirical evidence available from what likely is the best documented region of the Eurasian Ice Sheet.

Chapter 3

Summary

Paper I: *Simulating the evolution of Hardangerjøkulen ice cap in southern Norway since the mid-Holocene and its sensitivity to climate change*

Paper I investigates the long-term dynamics and sensitivity to climate change of the Hardangerjøkulen ice cap. We use a numerical ice flow model constrained by glacier and climate reconstructions to simulate the evolution of this ice cap from 4,000 BP, through the Little Ice Age to the present-day. During our simulation from ice cap inception at 4,000 BP until today, Hardangerjøkulen grows non-linearly under our imposed linear climate forcing. The ice cap's outlet glaciers vary out-of-phase with each other for centuries at a time, implying that paleo-glacier reconstructions of entire ice cap changes should not be inferred from a single outlet glacier. We also find that present-day Hardangerjøkulen is exceptionally sensitive to climate change. This is due to a flat surface topography and an associated effective surface mass balance-elevation feedback. In addition, our experiments suggest that Hardangerjøkulen would not regrow in the modern climate, if the ice cap would melt away completely.

Paper II: *Impact of fjord geometry on grounding line stability*

In this paper, we use a simple ice flow model purpose-built for marine-terminating glaciers, including calving, to investigate how fjord geometry controls the stability of marine-terminating glaciers. Using a suite of idealised fjord geometries, representative of real-world glaciers, we show that identical warming ocean conditions may cause grounding line responses varying by several tens of kilometres depending on the fjord geometry. Our simulations highlight fjord width as fundamental to grounding line stability. In particular, glaciers in fjords with embayments or coalescent tributaries may exhibit rapid, irreversible retreat under ocean warming. In contrast, narrow bottlenecks promote stability and may prevent catastrophic grounding line migration.

Paper III: *Fast retreat of a marine outlet glacier in western Norway at the last glacial termination*

Paper III gives a decadal to centennial scale perspective of the abrupt retreat of Hardangerfjorden glacier at the Younger Dryas–Holocene transition, 11.6 – 11.1 ka BP. This

well-dated paleoglacier in western Norway is an excellent past analogue of Jakobshavn Isbræ in Greenland (Paper IV), and other similar outlet glaciers in Greenland, Alaska, and Patagonia. We continue with the ice flow model from Paper II, and find that high surface melt and warmer fjord waters are likely triggers and drivers of the reconstructed fast retreat. While geological point data can only give mean estimates of retreat rates, we add continuous detail to the retreat dynamics and suggest a highly variable retreat history paced by fjord bathymetry. Periods of high retreat rates above 250 m a^{-1} contribute significantly to the overall length of retreat, yet these rates are not sustainable for more than a few decades.

Paper IV: *Non-linear retreat of Jakobshavn Isbræ since the Little Ice Age controlled by geometry*

This work continues with the ice flow model used in Paper II and III, and shifts focus from Norway to the fastest flowing glacier in the world; Jakobshavn Isbræ in western Greenland. This glacier's floating tongue suddenly collapsed in the early 2000s, with a fast retreat and tripling in speed occurring since. Nonetheless, it is unclear to what extent Jakobshavn's past history influences its modern retreat. We therefore simulate the history of Jakobshavn from its Little Ice Age (LIA) maximum in year 1850, and find that the glacier responds non-linearly to a linear strengthening in external forcing. Surface mass balance has a negligible effect, whereas calving and ocean forcing are important drivers of retreat since the LIA. The changing forcing following the LIA triggers retreat, while fjord geometry controls the variability of our modelled non-linear retreat history. Paper IV also shows that because of intermittent grounding line stillstands at geometric pinning points, retreat may be delayed by several decades, only to be followed by an abrupt grounding line migration without additional forcing.

Paper V: *Deglaciation of the Norwegian fjords*

We now return to the model from Paper I, using a version that incorporates accurate grounding line dynamics and fast flow. Paper V studies the regional deglaciation of the fjords at the Norwegian west coast from 18–11 ka BP. Using a first-order climatology based on paleo-records, this approach suggests that multi-millennial deglaciation in this region was driven by surface melt. In contrast, a driving role of the ocean appears unlikely. However, their relative roles depend on the time scale of interest. Our simulations in fact suggest that the ocean is a highly potent trigger for swift decadal scale grounding line retreat. In addition, we find that fjord topography strongly controls the sensitivity of the marine ice sheet margin in this region. For example, our sensitivity experiments, deglaciation simulations and available geological reconstructions all suggest that the Boknafjorden area in the south was the most vulnerable to external forcing. This region features a stabilising, shallow outer sill and an inland wide, deep trough prone to grounding line instability. In contrast, glaciers in fjords further north with bottleneck inlets and/or shallow sills were significantly more resilient to ocean warming.

Main conclusions

Based on Papers I–V, the main conclusions of this thesis are (cf. Section 2):

- Ice caps like Hardangerjøkulen, studied in Paper I, are particularly sensitive to climate change due to their uneven distribution of mass with elevation, and a highly effective surface mass balance-elevation feedback.
- Past and contemporary mass loss cannot be viewed in isolation of its historic changes. Paper I shows that multiple equilibria are possible depending on the initial ice cap state. Rapid, irreversible changes occur in Paper II due to geometric influence. For a marine outlet glacier, Paper IV shows that sudden grounding line retreat can occur as a result of climate forcing occurring decades before.
- The topography of glaciers, ice caps, and fjords may mask climate signals and prevent, delay, or amplify response to external forcing. If not accounted for, this influence will bias interpretation of observed and reconstructed glacier changes. All papers in this thesis support this point. Paper II, IV, and V highlight fjord width as a previously partly overlooked factor, in comparison to the bed topography and fjord bathymetry, which are key controls in Paper I and III.
- The time scale of interest determines whether the ocean or the atmosphere drive glacier retreat. For short-term change over a century or two, ocean influence and grounding line dynamics are likely controls of marine outlet glaciers, as shown in Papers III, IV, and V. Surface mass balance, hereunder atmospheric warming and surface melt, will likely drive centennial and longer time scale change. This is the large scale picture. Nonetheless, ice-ocean interactions and geometric influence may punctuate the long-term response to the atmosphere, causing short-lived, abrupt changes.

Chapter 4

Future outlook

This thesis improves understanding of a number of unresolved challenges within glaciology, climate science, paleoclimate and paleoglaciology. However, many unanswered questions remain, and new ones have arisen.

All papers show that the underlying and surrounding topography of glaciers have the capacity to significantly alter or even override the effects of external climate forcing. Data collection to improve knowledge of subglacial topography and ocean bathymetry is therefore an important priority. We also need high-resolution models to capture grounding line dynamics, even on long-time scales.

We have also found that the relative importance of oceanic and atmospheric warming on the retreat and advance of marine outlet glaciers depends on the time scale of interest. Over decadal time scales, ice-ocean interactions are important controls of glacier retreat. On centennial and longer time scales, surface mass balance and its underlying ice-atmosphere interactions drive retreat. We emphasise that the extent to which the underlying bed is marine- or land-based is a fundamental control of mass loss, which again highlights the importance of accurate data of bed topography.

The papers in this thesis illustrate the potential to combine detailed model simulations with sediment records as well as with terrestrial and submarine geomorphology. Still, there is no straightforward answer to how we should do model-data integration. Our take has been to use simplified approaches to the complex system that is ice dynamics and climate interactions, and not to apply aggressive tuning towards data. The truth is that (almost) any model can be (over)fitted to data, with the result that we learn nothing. However, there are several possible routes in between. This thesis point out that simplified yet carefully constructed model simulations can complement and refine evidence of glacier behaviour from geological reconstructions. As theoretical understanding develops, more data becomes available, and parameterizations improve, we can add one detail at a time, hopefully without losing track of what models actually tell us about the underlying dynamics.

An expected objection from modellers of short (observational) time scales will be that the models in this thesis, and their parameterizations of key physical processes within, are too simplistic and lack important physics. I am inclined to agree in principle but disagree in practice, because these models are meant to develop our physical understanding of glacier systems and their response to climate change, rather than simulate physical processes in detail. Nonetheless, a number of processes are indeed poorly constrained in ice sheet models.

By reflection upon this thesis, a number of potential future avenues have also become increasingly captivating to the author.

For marine outlet glaciers, iceberg calving remains a process as elusive as ever. This area of research is strikingly active (e.g. Bassis and Walker, 2012; Åström et al., 2014; Benn et al., 2017), but a universal calving law applicable to modern marine-based glaciers is yet to arrive, let alone for paleo-glaciers. Calving as a process comes in so many different flavours, depending on the geometry and glaciological setting, that we may have to rethink the problem. A possible 'solution' may be calving laws that adapt over time, as calving styles evolve and boundary conditions change. However, this requires much more data than presently is available, both from the present-day and from the past, and development of a new generation of calving models suitable for longer time scales.

Another unsolved problem is how the atmosphere influences frontal ablation, hereunder submarine melt and calving. By this, I do not mean through water-filled crevasses or basal lubrication in response to higher meltwater input from the surface. We know that submarine melt of calving fronts and ice shelves scales with subglacial discharge and fjord temperatures. Subglacial discharge itself depends on the supply of surface meltwater produced by a warming atmosphere. This coupling between summer melt and calving activity through subglacial discharge remains largely untouched by the scientific literature.

There is also no doubt in my mind that the integration between ice flow models and sediment records in fjords and from offshore is in its infancy. For example, what does a record of Ice Rafted Debris (IRD) really tell us about grounding line and calving dynamics? How can we quantitatively connect calving fluxes and the number of sand grains in a sediment sample? The potential for new and existing records to be combined with models is clear, be it for Greenland, Norway, Patagonia, Svalbard, the British Isles, New Zealand, British Columbia, Arctic Canada, Novaya Zemlya, or Antarctica.

To me, collapse of paleo-ice shelves and its impact on ice sheet stability is also one of the more exciting remaining frontiers. Ice shelves of the past have been understudied for good reasons, because they do not leave as clear geomorphic imprints on the sea floor as grounding lines do. Now, several promising proxies and morphological techniques are emerging (Jakobsson et al., 2011; Yokoyama et al., 2016; Davies et al., 2017), waiting to be refined and complemented by ice sheet models.

Returning to Norway, this is a country where the number of sediment records from glacier-fed lakes must be one of the highest in the world, if not the highest. Many glaciers are accessible yet have not been studied exhaustively from an ice dynamical perspective. Continued studies of their long-term evolution, building on the conceptual groundwork from Paper I, appear logical and inevitable. Assessment of the underlying assumptions for records of past glacier activity is another challenge, with regards to basal conditions, thermal regime, the relationship between ice dynamics and erosion, and sediment transport.

Finally, we do not do science only because of science. Glaciers are disappearing in front of our eyes – let's continue to find out why and tell people what it means.

Chapter 5

Scientific results

Paper I

5.1 Simulating the evolution of Hardangerjøkulen ice cap in southern Norway since the mid-Holocene and its sensitivity to climate change

Åkesson, H., Nisancioglu, K. H., Giesen, R. H., and Morlighem, M. Simulating the evolution of Hardangerjøkulen ice cap in southern Norway since the mid-Holocene and its sensitivity to climate change, *The Cryosphere*, **11**, 281-302, https://doi.org/10.5194/tc-11-281-2017, 2017.

The Cryosphere, 11, 281–302, 2017
www.the-cryosphere.net/11/281/2017/
doi:10.5194/tc-11-281-2017

The Cryosphere Open Access EGU

Simulating the evolution of Hardangerjøkulen ice cap in southern Norway since the mid-Holocene and its sensitivity to climate change

Henning Åkesson[1,2], **Kerim H. Nisancioglu**[1,3], **Rianne H. Giesen**[4], **and Mathieu Morlighem**[2]

[1]Department of Earth Science, University of Bergen and Bjerknes Centre for Climate Research, Allégaten 70, 5007 Bergen, Norway
[2]University of California, Irvine, Department of Earth System Science, 3218 Croul Hall, Irvine, CA, 92697-3100, USA
[3]Centre for Earth Evolution and Dynamics, University of Oslo, Po. Box 1028 Blindern, 0315 Oslo, Norway
[4]Institute for Marine and Atmospheric research, Utrecht University, P.O. Box 80005, 3508 TA Utrecht, the Netherlands

Correspondence to: Henning Åkesson (henning.akesson@uib.no)

Received: 8 March 2016 – Published in The Cryosphere Discuss.: 29 April 2016
Revised: 22 December 2016 – Accepted: 28 December 2016 – Published: 27 January 2017

Abstract. Understanding of long-term dynamics of glaciers and ice caps is vital to assess their recent and future changes, yet few long-term reconstructions using ice flow models exist. Here we present simulations of the maritime Hardangerjøkulen ice cap in Norway from the mid-Holocene through the Little Ice Age (LIA) to the present day, using a numerical ice flow model combined with glacier and climate reconstructions.

In our simulation, under a linear climate forcing, we find that Hardangerjøkulen grows from ice-free conditions in the mid-Holocene to its maximum extent during the LIA in a nonlinear, spatially asynchronous fashion. During its fastest stage of growth (2300–1300 BP), the ice cap triples its volume in less than 1000 years. The modeled ice cap extent and outlet glacier length changes from the LIA until today agree well with available observations.

Volume and area for Hardangerjøkulen and several of its outlet glaciers vary out-of-phase for several centuries during the Holocene. This volume–area disequilibrium varies in time and from one outlet glacier to the next, illustrating that linear relations between ice extent, volume and glacier proxy records, as generally used in paleoclimatic reconstructions, have only limited validity.

We also show that the present-day ice cap is highly sensitive to surface mass balance changes and that the effect of the ice cap hypsometry on the mass balance–altitude feedback is essential to this sensitivity. A mass balance shift by +0.5 m w.e. relative to the mass balance from the last decades almost doubles ice volume, while a decrease of 0.2 m w.e. or more induces a strong mass balance–altitude feedback and makes Hardangerjøkulen disappear entirely. Furthermore, once disappeared, an additional +0.1 m w.e. relative to the present mass balance is needed to regrow the ice cap to its present-day extent. We expect that other ice caps with comparable geometry in, for example, Norway, Iceland, Patagonia and peripheral Greenland may behave similarly, making them particularly vulnerable to climate change.

1 Introduction

The 211 000 glaciers and ice caps (GICs) (Pfeffer et al., 2014; Arendt et al., 2015) in the world are relatively small compared to the Greenland and Antarctic ice sheets, but they constitute about half of the current cryospheric contribution to sea level rise (Shepherd et al., 2012; Vaughan et al., 2013), a distribution projected to remain similar throughout the 21st century (Church et al., 2013; Huss and Hock, 2015). Since areas of GICs are more readily available than their volume, scaling methods are commonly employed to estimate total ice volumes and their sea level equivalents (e.g., Bahr et al., 1997, 2015; Grinsted, 2013). Many of these GICs are ice caps, though little is known about their response to long-term climate change, how a particular ice cap geometry contributes to this sensitivity or how scaling methods perform for ice caps.

Table 1. Constants and parameter values used in this study.

Parameter	Symbol	Unit	Value
Ice density	ρ_i	$kg\,m^{-3}$	917
Gravitational acceleration	g	$m\,s^{-2}$	9.81
Flow factor	A	$s^{-1}\,Pa^{-3}$	0.95×10^{-24} to 2.4×10^{-24}
Sliding parameter	β	$m\,s^{-1}\,Pa^{-1}$	4×10^{-12} to 1×10^{-13}
Sliding law exponent	m		1
Glen's law exponent	n		3
Mesh resolution	Δx	m	200–500
Time step	Δt	a	0.02

Reconstructions of past climate and glacier variations contribute to our understanding of long-term glacier behavior. However, these studies often build on simple glaciological assumptions relating proxies, ice extent, ice volume and climate (e.g., Hallet et al., 1996). As glaciers are nonlinear systems with feedbacks, such relations are difficult to constrain without a numerical model. However, long-term reconstructions using ice flow models are rare. Most existing quantitative modeling studies of GICs are restricted to timescales of decades (e.g., Leysinger-Vieli and Gudmundsson, 2004; Raper and Braithwaite, 2009) or centuries (Jouvet et al., 2009; Giesen and Oerlemans, 2010; Aðalgeirsdóttir et al., 2011; Zekollari et al., 2014; Zekollari and Huybrechts, 2015; Ziemen et al., 2016). Only a very limited number of studies exist for the longer timescales (e.g., Flowers et al., 2008; Laumann and Nesje, 2014). Studies focusing on glacier evolution since the Little Ice Age (LIA) (e.g., Giesen and Oerlemans, 2010; Aðalgeirsdóttir et al., 2011; Zekollari et al., 2014) normally perturb a present-day glacier or ice cap with a climate anomaly relative to the modern and do not explicitly consider the ice cap history preceding the LIA.

In this study, we use a numerical ice flow model to provide a quantitative, long-term, dynamical perspective on the history and current state of the Hardangerjøkulen ice cap in southern Norway. These results are also relevant for our understanding of the history and future stability of similar ice masses in, e.g., Norway (Nesje et al., 2008a), Iceland (Aðalgeirsdóttir et al., 2006), Patagonia (Rignot et al., 2003), Alaska (Berthier et al., 2010) and peripheral Greenland (Jacob et al., 2012). We present a plausible ice cap history over several thousand years before the LIA (Sect. 4.1) and use this as a starting point for simulations from LIA to present day (Sect. 4.2). To evaluate the sensitivity of the ice cap to the choice of dynamical model parameters, we perform an ensemble of simulations with different dynamical model parameters (Sect. 4.2.1). Furthermore, we quantify the sensitivity of Hardangerjøkulen to climatic change (Sect. 4.3).

We find that Hardangerjøkulen is exceptionally sensitive to surface mass balance changes and that the surface mass balance–altitude feedback and ice cap hypsometry are crucial to this sensitivity. To constrain the assumptions made in glacier reconstructions and volume–area scaling applications, we assess the degree of linearity between ice cap volume and area (Sect. 4.4). We show that commonly used scaling relations overestimate ice volume and suggest that glacier and climate reconstructions could benefit from quantifying the impact on proxy records of bed topography, glacier hypsometry and the surface mass balance–altitude feedback (Sect. 5.5).

2 Hardangerjøkulen ice cap

2.1 Present-day geometry

2.1.1 Surface topography

Hardangerjøkulen (60°55′ N, 7°25′ E) has a present-day (year 2012) area of 73 km^2 (Andreassen et al., 2012) and is located at the western flank of the Hardangervidda mountain plateau. The ice cap is rather flat in the interior with steeper glaciers draining the plateau (Fig. 1). The largest outlet glaciers are Rembesdalskåka (facing W–SW; 17.4 km^2), Midtdalsbreen (NE; 6.8 km^2), Blåisen (NE; 6.6 km^2) and Vestre Leirbotnskåka (S–SE; 8 km^2). Surface elevation ranges from 1020 to 1865 m a.s.l. (Andreassen et al., 2016), with 80 % of the ice cap area and 70 % of Rembesdalskåka, situated above the mean equilibrium-line altitude (ELA) at 1640 m a.s.l. (1963–2007 average; Giesen, 2009). Rembesdalskåka drains towards the dammed lake Rembesdalsvatnet, located $\sim$ 1 km from the present-day glacier terminus (Kjøllmoen et al., 2011). Midtdalsbreen is a gently sloping outlet glacier ranging from 1380 to 1865 m a.s.l.

2.1.2 Ice thickness and bed topography

A number of surveys have mapped the ice thickness at Hardangerjøkulen (e.g., Sellevold and Kloster, 1964; Elvehøy et al., 1997; Østen, 1998, K. Melvold, unpublished data), with the highest measurement density for Midtdalsbreen (Fig. 2.12a in Giesen, 2009; Willis et al., 2012). In areas with dense measurements, ice thickness was interpolated using methods detailed in Melvold and Schuler (2008).

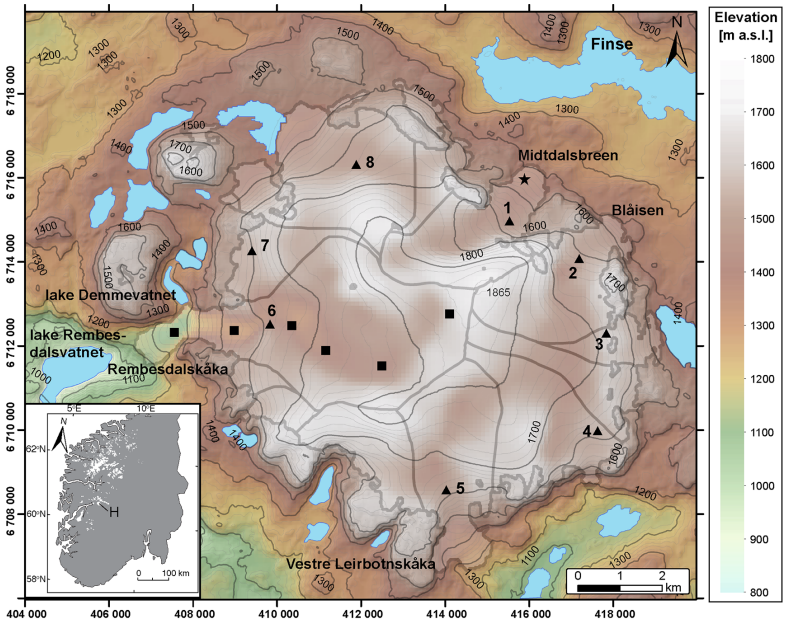

Figure 1. Bed (coloring) and surface (contours) topography of Hardangerjøkulen ice cap. Contour interval is 20 m and created from a digital elevation model by Statens Kartverk (1995). The reference system is UTM zone 32N (EUREF89). Ice cap outline and drainage basins from 2003 are indicated (data from cryoclim.net), as well as surrounding lakes (drawn after Statens Kartverk N50 1 : 50 000). Shown are GPS positions for velocity measurements (numbered triangles), mass balance stakes from NVE (squares) and location of the automatic weather station (star). Inset: map of southern Norway showing the location of Hardangerjøkulen (H).

In sparsely measured areas, ice thickness H was estimated directly from the surface slope α, assuming perfect plasticity (Paterson, 1994, p. 240). Based on detailed ice thickness measurements and information on the surface slope on Midtdalsbreen, a yield stress of 150–180 kPa was used, in agreement with other mountain glaciers (Cuffey and Paterson, 2010, p. 297; Zekollari et al., 2013). Over the flat areas near ice divides and ice ridges, as well as near ice margins, manual extrapolation was required to obtain a smooth ice surface (K. Melvold, personal communication, 2009). A map of bed topography (Fig. 1) was produced by combining the final ice thickness map with a surface DEM (year 1995) from the Norwegian Mapping Authority, derived from aerial photographs.

2.2 Past geometry

2.2.1 Holocene changes

Reconstructions show that glaciers in southern Norway did not survive the mid-Holocene thermal maximum (e.g., Bakke et al., 2005; Nesje, 2009). Based on lake sediments and terrestrial deposits, Hardangerjøkulen is estimated to have been absent from ca. 7500 to 4800 BP (Dahl and Nesje, 1994), although a short-lived glacier advance is documented for the southern side of the ice cap at ca. 7000 BP (Nesje et al., 1994). Some high-frequency glacier fluctuations of local northern glaciers occurred during the period 4800–3800 BP, after which Hardangerjøkulen has been present continuously (Dahl and Nesje, 1994). There are few quantitative constraints on ice cap extent for the period from ice cap inception 4000 BP until the LIA. However, interpretations of lake sediments and geomorphological evidence suggest a gradual growth of Hardangerjøkulen during this period (Dahl and Nesje, 1994, 1996).

2.2.2 Outlet glacier changes since the Little Ice Age

Length changes extracted from maps and satellite imagery, moraine positions and direct front measurements are combined to derive length records for two major outlet glaciers for the period 1750–2008. For Rembesdalskåka, we use the same flowline as the Norwegian Water and Energy Directorate (NVE) use for their mass balance measurements (H. Elvehøy, personal communication, 2014). The NVE flowline for Midtdalsbreen was slightly modified to better

correspond with the maximum ice velocities. Since changes are only made upglacier of the present-day margin, they do not interfere with the area where data of frontal changes exist.

The LIA maximum for Midtdalsbreen is dated to AD 1750 with lichenometry (Andersen and Sollid, 1971). For Rembesdalskåka, the outermost terminal moraine has not been dated but is assumed to originate from the LIA maximum.

Frontal observations for Rembesdalskåka began in 1917. These have been performed for 22 of the years during the period 1917–1995 and are done annually since 1995. For Midtdalsbreen, an annual length change record exists from 1982 onwards (Kjøllmoen et al., 2011). At present, Rembesdalskåka has retreated almost 2 km from its LIA maximum extent and Midtdalsbreen $\sim$ 1 km.

The two outlet glaciers considered advanced in response to snowy winters around 1990. The terminus change from 1988 to 2000 for Rembesdalskåka was +147 m and for Midtdalsbreen +46 m. By 2013, Rembesdalskåka and Midtdalsbreen had retreated 332 and 164 m, respectively, from their positions in 2000 (Andreassen et al., 2005, Kjøllmoen et al., 2011, Cryoclim.net, 2014).

2.3 Climate

2.3.1 Holocene and Little Ice Age climate

Reconstructions for southern Norway based on pollen and chironomids suggest that summer temperatures were up to 2 °C higher than present in the period between 8000 and 4000 BP, when solar insolation was higher (Nesje and Dahl, 1991; Bjune et al., 2005; Velle et al., 2005a). At 4000 BP, proxy studies suggest a drop in summer temperatures to 0.5 °C lower than present combined with a drier climate (Dahl and Nesje, 1996; Bjune et al., 2005; Velle et al., 2005b; Seppä et al., 2005).

Dahl and Nesje (1996) reconstructed Holocene summer temperatures for southern Norway based on former pine-tree limits. Using a well-established empirical relationship between summer temperature and winter precipitation at the ELA of Norwegian glaciers (Liestøl in Sissons, 1979; Sutherland, 1984), they estimated winter precipitation for the Hardangerjøkulen area from lake sediment-derived ELAs. These reconstructions suggest a close to linear cooling and wetting trend from 4000 BP until the LIA, including a possible warm event lasting for several centuries around 2000 BP (Velle et al., 2005a).

The LIA climate in southern Norway is likely to have experienced more precipitation (Nesje and Dahl, 2003; Nesje et al., 2008b; Rasmussen et al., 2010) and was ca. 0.5–1.0 °C colder than present (Kalela-Brundin, 1999; Nordli et al., 2003), although some reconstructions indicate milder summers during the first quarter of the 18th century (Kalela-Brundin, 1999).

2.3.2 Present climate

Southern Norway is located in the Northern Hemisphere westerly wind belt and is heavily influenced by moist, warm air picked up by the frequent storms coming off the Atlantic Ocean (Uvo, 2003). When these winds reach the mountainous west coast, orographic lifting occurs and precipitation falls as rain or snow, depending on elevation. Conversely, eastern Norway is located in the rain shadow of the coastal mountains and the high mountain plateau Hardangervidda.

This strong west–east precipitation gradient is illustrated by the mean annual precipitation for 1961–1990 over southern Norway. Precipitation in Bergen, 65 km west of Hardangerjøkulen, reaches 2250 mm a^{-1} (data from eklima.no, Norwegian Meteorological Institute). In contrast, Oslo in eastern Norway receives 763 mm precipitation per year. Liset, 17 km southeast of the summit of Hardangerjøkulen, receives 1110 mm a^{-1}, while Finse, 8 km northeast of the summit, experiences 1030 mm a^{-1}. Finse has a mean annual temperature of −2.1 °C, while temperature is not measured at Liset.

2.4 Surface mass balance

Glaciological mass balance measurements started on Rembesdalskåka in 1963. The mean net balance for the period 1963–2010 was slightly positive (+0.08 m w.e. – water equivalent), divided into a winter balance of +2.10 m w.e. and a summer balance of −2.03 m w.e. (Kjøllmoen et al., 2011).

For Midtdalsbreen, mass balance was only measured in 2000 and 2001 (Krantz, 2002). This 2-year time series is too short for a robust surface mass balance comparison between the two outlet glaciers.

Specific mass balance profiles for the entire elevation range of Rembesdalskåka exist for 35 of the 45 mass balance years (1 October–30 September) in the period 1963–2007. The interannual variability around the mean winter profile is similar at all elevations, while the range in summer balances increases from high to low elevations (Fig. 2.7a in Giesen, 2009). The decrease in mass balance at the highest elevations is a persistent feature of the winter mass balance and is strongest in years with large accumulation (Fig. 5.3 in Giesen, 2009). Its origin is, however, uncertain and long-term snow depth measurements on several outlet glaciers are needed to identify the underlying process.

The net balance profile has a similar shape for most years, and the relation between net mass balance and altitude is approximately linear from the terminus up to 1675 m a.s.l. (Fig. 2), with a mass balance gradient of 0.0097 m w.e. per meter altitude. The net mass balance is zero at 1640 m a.s.l., marking the ELA. Above the ELA, the mass balance gradient decreases with altitude and becomes negative at the highest elevations (Fig. 2).

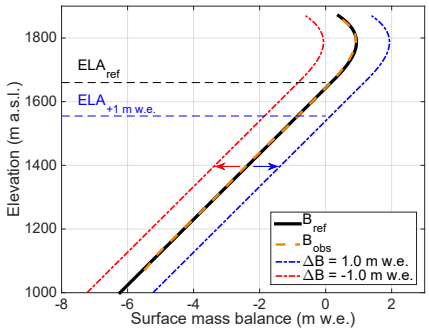

Figure 2. Reference net surface mass balance (B_{ref}) profile used in the model runs, based on the mean observed (B_{obs}) profile for 35 of the 45 years 1963–2007. At lower elevations, a linear gradient is used; for the highest elevations, a third-order polynomial is fitted to the observed values. Shown are also $\Delta B(t) = -1.0$ and $+1.0$ m w.e., examples of how temporal mass balance changes are imposed (Eq. 6), along with corresponding ELAs. For -1.0 m w.e., mass balance is negative at all elevations, and thus ELA is above the summit. Data from NVE.

2.5 Ice dynamics

2.5.1 Basal conditions

Although bed conditions are not well known, based on the sparse sediment cover in the surrounding areas (Andersen and Sollid, 1971) we assume Hardangerjøkulen to be hard-bedded, i.e., without any deformable subglacial sediments present.

Given its climatic setting and based on the radar investigations described in Sect. 2.1.2, Hardangerjøkulen can be characterized as a temperate ice cap. To the contrary, temperature measurements suggest that Midtdalsbreen has local cold-based areas at its terminus (Hagen, 1978; Konnestad, 1996; Reinardy et al., 2013). However, we expect that this has a minor effect on the large-scale ice flow of Midtdalsbreen and Hardangerjøkulen.

2.5.2 Surface velocities

Over the lower ablation zone of Midtdalsbreen, surface speeds of 4–40 m a^{-1} were measured during summer 2000 (Vaksdal, 2001). In addition, ice velocities were derived from Global Positioning System (GPS) units recording at nine locations on Hardangerjøkulen during the period May 2005–September 2007 (Giesen, 2009). One GPS was mounted on the automatic weather station (AWS) on Midtdalsbreen, the other eight were situated on stakes at the ELA of the main outlet glaciers (Fig. 1). These data show highest velocities for the largest outlet glacier Rembesdalskåka (46 m a^{-1}). Velocities at Midtdalsbreen, measured May 2005 to March 2006, were 33 m a^{-1} at the ELA and $\sim$ 20–22 m a^{-1} at the AWS, which is within the range of ablation zone summer velocities suggested by Vaksdal (2001).

Since velocities have only been measured for single years or shorter, these observations provide guidance rather than serving as calibration or validation data for our model. To the authors' knowledge, there are no high-resolution velocity data derived from remote sensing covering the area of interest.

3 Model description and setup

3.1 Ice flow model

We use the two-dimensional, vertically integrated shallow ice approximation (SIA) within the finite-element Ice Sheet System Model (ISSM; Larour et al., 2012). Only the capabilities of ISSM relevant for this paper are covered here; for a complete description, including a more comprehensive section on model numerics and architecture, we refer to Larour et al. (2012) and http://issm.jpl.nasa.gov.

The SIA is based on a scaling analysis of the Stokes stress balance (Hutter, 1983; Morland, 1984). This scaling argument assumes that the typical glacier length, L, is much larger than the typical ice thickness H. For this purpose, the aspect-ratio ϵ is defined as

$$\epsilon = \frac{[H]}{[L]}, \tag{1}$$

where ϵ describes the "shallowness" of an ice mass. An aspect ratio much smaller than unity is required for the SIA to be valid. Generally, the smaller the ϵ, the more accurate the SIA is (Le Meur et al., 2004; Greve and Blatter, 2009; Winkelmann et al., 2011). Based on outlet glacier length records from the LIA until today, the characteristic horizontal scale for Hardangerjøkulen is 4 to 10 km. Due to the highly variable bed topography, a typical vertical scale of $\sim$ 200 m is estimated qualitatively using ice thickness around the ELA. These scales give an ϵ between 0.02 and 0.05, which is acceptable for using the SIA (Le Meur and Vincent, 2003).

The SIA has proven accurate in representing glacier length and volume fluctuations on the decadal and longer timescales we are focusing on (Leysinger-Vieli and Gudmundsson, 2004). While higher order models may be needed in dynamic regions, even for paleosimulations (Kirchner et al., 2016), Hardangerjøkulen has relatively gentle surface slopes and lacks areas of very fast flow, making the SIA a viable choice.

Because of its simplicity, SIA is also computationally efficient (Rutt et al., 2009), enabling ensemble simulations over longer timescales.

3.1.1 Ice deformation and sliding

The constitutive relationship relating stress to ice deformation (strain rate) is Glen's flow law (Glen, 1955), which for

the special case of vertical shear stress τ_{xz} only (SIA) states

$$\dot{\epsilon} = A\tau_{xz}^{n}, \tag{2}$$

where $\dot{\epsilon}$ is the strain rate tensor, A is the flow factor accounting for ice rheology and $n = 3$ is Glen's flow law exponent. We use a spatially constant flow factor A, assuming homogeneous ice temperature T_{ice} and material properties across the ice cap.

In contrast to many other studies, where a tuned "best-fit" parameter combination is selected and used in all simulations, we perform ensemble runs for a parameter space of different flow factors and sliding parameters (described below), for both the calibration procedure and subsequent model runs.

SIA is strictly only valid for a no-slip bed (Guðmundsson, 2003; Hindmarsh, 2004). However, Hardangerjøkulen is a temperate ice cap, and summer speedups have been observed at Midtdalsbreen (Willis, 1995; Willis et al., 2012), indicating basal motion. We introduce sliding using a linear Weertman sliding formulation (Weertman, 1964), which for the SIA means basal velocities u_{b} are proportional to the basal shear stress τ_{b}:

$$u_{\mathrm{b}} = \beta\tau_{\mathrm{b}}^{m}, \tag{3}$$

where β is a (tuning) basal sliding parameter. β can be set spatially and temporally constant or be a function of temperature, basal water depth, basal water pressure, bed roughness or other factors, and m is the sliding law exponent, which equals one for the linear sliding law we apply.

In this study, the basal sliding parameter β is assumed spatially and temporally constant. We consider it speculative to apply ad hoc variations in basal sliding without proper validation. ISSM has capabilities to perform inversions for basal friction based on data assimilation techniques (e.g., MacAyeal, 1993; Morlighem et al., 2010), but this requires more extensive velocity data coverage than what is available for Hardangerjøkulen at present. More fundamentally, inverted friction fields may become inaccurate on the long timescales considered in this study.

3.1.2 Mass transport

For the vertically integrated ice flow model used in this study, the two-dimensional continuity equation states

$$\frac{\partial H}{\partial t} = -\nabla \cdot (\overline{u}H) + \dot{M}, \tag{4}$$

where $\overline{u}$ is the vertically averaged ice velocity ($\mathrm{m\,a^{-1}}$) and $\dot{M}$ the surface mass balance rate (m ice equivalent $\mathrm{a^{-1}}$). The basal melt rate is assumed negligible, and calving is not included in the model. Rembesdalskåka likely terminated in lake Rembesdalsvatnet during the LIA and the northwestern ice cap presently terminates in water, but we expect this to have minor effect on ice dynamics.

3.1.3 Mesh and time stepping

Following methods outlined in Hecht (2006) and Morlighem et al. (2011), an anisotropic mesh with resolution 200–500 m was constructed using local mesh refinement based on modeled velocities for a steady-state ice cap close to observed LIA extent. This ice cap was reached using our best-fit deformation and sliding parameters (Sect. 3.2.1) on a uniform mesh and a mass balance perturbation forcing the ice cap to advance to terminus positions close to the LIA extent. The anisotropic mesh adds accuracy around the LIA margins. When the glacier is smaller or larger, the accuracy is reduced (400–500 m).

The stress balance of SIA is local. Using a very high resolution for SIA hence increases the risk of unphysical stress gradients and velocities due to local variations in bed topography. We avoid this by smoothing the surface and bedrock DEMs to 200 m. This mesh resolution also enables us to carry out Holocene runs and our ensemble study at lower computational cost. Tests on mesh convergence using uniform 150 and 200 m meshes indicate that total volume varies by less than 5 % compared to our anisotropic 200–500 m mesh.

We use a finite difference scheme in time, where a time step of 0.02 years was found low enough to avoid numerical instabilities.

3.2 Experimental setup and calibration

3.2.1 Ensemble calibration of ice deformation and sliding parameters

To calibrate model parameters governing ice deformation and basal sliding, we use the 1995 surface DEM as the initial condition. We run the model with constant climate forcing, using our reference mass balance function ($\Delta B(t) = 0$ in Eq. 6 below), until a steady state is reached.

Since we run the model with a mass balance function averaged over several decades, it is important that there was no large climate–geometry imbalance for this period. Indeed, the ice cap was in close to steady state between the early 1960s and 1995, since surface elevation change from 1961 to 1995 was ± 10 m (Andreassen and Elvehøy, 2001).

In reality, an ice cap is never in exact steady state, but it is still a useful concept to understand model sensitivity (Aðalgeirsdóttir et al., 2011). To investigate model sensitivity to deformation and sliding parameters, and to find a best-fit combination for our historic runs, we run an ensemble of 24 possible parameter combinations (Table 1), well enclosed by values used in the literature. The flow factor A depends on ice temperature, as well on ice fabric, impurities and possibly other factors. Without an a priori assumption of ice temperature, we investigate values from $A = 0.95 \times 10^{-24}$ to $2.4 \times 10^{-24}\,\mathrm{s^{-1}\,Pa^{-3}}$, roughly corre-

sponding to $T_{ice} = 0$ to $-5\,^{\circ}C$ (Cuffey and Paterson, 2010, p. 73). For the sliding parameter, we perform runs using $\beta = 4 \times 10^{-12}$ to 1×10^{-13} m s^{-1} Pa^{-1}.

The best-fit combination is obtained by minimizing the root mean square error (RMSE) between the modeled (H_{mod}) and observed (H_{obs}) ice thickness:

$$\mathrm{RMSE} = \sqrt{\frac{\sum_{i=1}^{k} (H_{mod} - H_{obs})^2}{k}}, \quad (5)$$

where k is the number of vertices for which the RMSE is calculated.

Since the outlet glaciers Midtdalsbreen and Rembesdalskåka are of primary interest, we use the combined RMSE along their flowlines as the most important metric (Fig. 3). As an additional check, we also calculate the RMSE for ice thickness over the entire ice cap (not shown here). We consider our best-fit parameter combination to be $A = 2.0315 \times 10^{-24}$ s^{-1} Pa^{-3} and $\beta = 2 \times 10^{-12}$ m s^{-1} Pa^{-1} (Fig. 3).

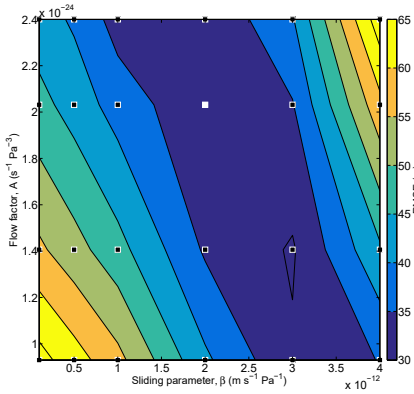

Figure 3. Root mean square error (RMSE) between modeled and observed present-day ice thickness along the flowlines of Midtdalsbreen and Rembesdalskåka, using an ensemble of sliding (β) and rheology (A) parameters. Shown are parameter combinations (black squares) and the "best-fit" parameter combination used in subsequent runs (white square).

3.2.2 Mass balance parameterization

A vertical reference mass balance function B_{ref} is derived from observed specific mass balance gradients, which exist for 35 of the 45 years spanning 1963–2007. The averaged net mass balance profile can be approximated by a combination of a linear function for elevations up to 1675 m a.s.l. and a third-order polynomial at higher elevations (Fig. 2). The resulting mass balance function gives an annual mass balance for Rembesdalskåka of -0.175 m w.e. We therefore shifted this profile by $+0.175$ m w.e. to obtain B_{ref}.

Mass balance $B(z, t)$ for any point in time is calculated by shifting B_{ref} by a mass balance anomaly $\Delta B(t)$ at all elevations (Oerlemans, 1997a):

$$B(z, t) = B_{ref}(z) + \Delta B(t). \quad (6)$$

A mass balance–altitude feedback is included in the model by recalculating the mass balance $B(z, t)$ at a specific point for each time step according to the updated surface elevation. The elevation of the maximum net mass balance is not adapted to changes in the ice cap summit elevation, as the effect on modeled ice volume is minor (Giesen, 2009).

3.2.3 Holocene mass balance

Reconstructions (Sect. 2.2.2) suggest that Hardangerjøkulen has been continuously present since ca. 3800 BP, with smaller local glacier activity during the millennium before. We therefore choose 4000 BP, with no ice cap present, as the starting point for our simulations.

Temperature proxies indicate a positive mass balance anomaly at 4000 BP, while precipitation reconstructions point to more negative mass balances (Sect. 2.2.2). Combined, these suggest mass balance conditions similar to present day. Accordingly, we start from $\Delta B(t) = 0$ and thereafter linearly increase mass balance to 0.4 m w.e. over the period 4000 to 400 BP (AD 1600). The final value of 0.4 m w.e. is chosen to produce an ice cap sized between the present-day and LIA extent. For this simulation, we use our best-fit deformation and sliding parameters obtained from the calibration ensemble.

It is possible to refine or alternate this simple forcing in several ways. However, applying such changes based on poorly constrained past climatic and mass balance conditions adds additional uncertainty. Our deliberately simple, linear forcing also allows us to isolate any nonlinear, asynchronous behavior in a clear manner.

3.2.4 Historic mass balance

Using our Holocene run ending at AD 1600 as initial conditions, we aim to reproduce the history of Hardangerjøkulen from the LIA until present day, as well as to assess model sensitivity to the choice of deformation and sliding parameters. For these purposes, we run the same parameter ensemble as used in the calibration process.

Since the mass balance record from Rembesdalskåka starts in 1963, mass balance has to be reconstructed for the period prior to this. A plausible mass balance history is found from AD 1600, through the LIA maximum in 1750 up to 1963, using a dynamic calibration (Oerlemans, 1997a, 2001). This approach is based on matching the model against the moraine evidence and length records of the outlet glaciers Midtdalsbreen and Rembesdalskåka, while adjusting $\Delta B(t)$ accordingly. We use a slightly modified mass balance history as ob-

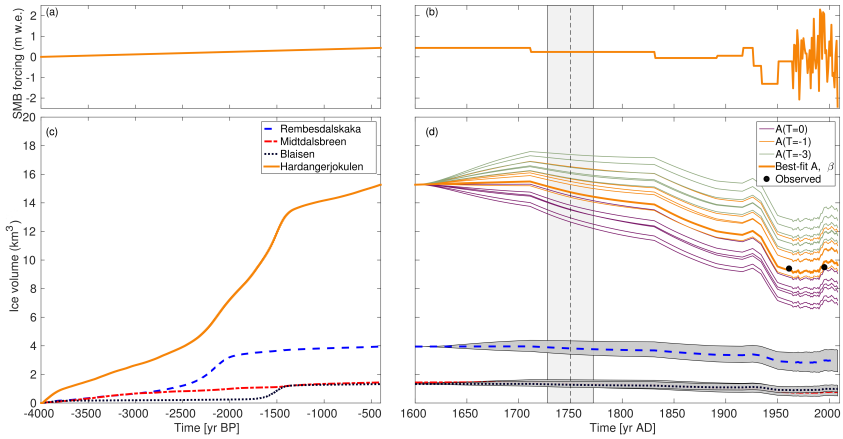

Figure 4. Mass balance forcing for **(a)** mid- to late Holocene (spinup period) and **(b)** AD 1600–2008. Ice volume response for **(c)** mid- to late Holocene and for **(d)** AD 1600–2008 using an ensemble of sliding and deformation parameter combinations (dark shading) and our "best-fit" combination obtained from independent calibration. Colors represent different outlet glaciers and the whole ice cap. The LIA maximum, as dated at Midtdalsbreen (dashed line), and its temporal uncertainties (light shading) are also shown, as well as ice volume observations from 1961 and 1995 (black dots). For details, see text.

tained for Hardangerjøkulen by Giesen (2009), using minimal tuning, since a key aim is to investigate parameter sensitivity, and mass balance is arbitrary before 1963.

3.2.5 Mass balance sensitivity and hysteresis

To investigate the sensitivity of present-day Hardangerjøkulen to changes in mass balance, steady-state experiments are performed with present-day ice cap topography as the starting point. These experiments are performed starting from the steady-state ice cap obtained with the best-fit parameters and no mass balance anomaly. From this state, we perturb the mass balance by anomalies between -0.5 and $+0.5$ m w.e. and run the model to a new equilibrium.

To investigate the role of the mass balance–altitude feedback in the ice cap response, we perform additional experiments excluding this feedback by keeping the spatial mass balance field fixed in time to the present-day surface topography.

Finally, we investigate dependence on initial conditions (hysteresis) by running experiments using ice-free initial conditions, with the mass balance–altitude feedback included.

4 Results

4.1 Mid- to late Holocene evolution of Hardangerjøkulen

Using a linear mass balance increase from 0 m w.e. at 4000 BP to 0.4 m w.e. at AD 1600 (Fig. 4a), we find an ice volume evolution for Hardangerjøkulen during the mid- to late Holocene that is far from linear and different between outlet glaciers (Fig. 4c). Starting from ice-free conditions, ice cap volume increases in a step-wise manner, with Hardangerjøkulen tripling its volume over a period of 1000 years (ca. 2300–1300 BP), before stabilizing at the end of the period.

Simulated snapshot thickness maps reveal patterns of ice cap growth (Fig. 5). Initially, ice grows on high bedrock ridges above the ELA (Fig. 5a, also see Fig. 1). During the period of linearly increasing ice volume (4000–3800 BP), Rembesdalskåka and Midtdalsbreen advance at similar rates. At this stage, Rembesdalskåka occupies an area with a gently sloping and partly overdeepened bed (Fig. 6).

After passing the lower edge of this overdeepening, Rembesdalskåka advances ~ 3.5 km in 400 years (2300–1900 BP), corresponding to a length increase of 60 % (Fig. 6). In contrast, Midtdalsbreen is already at an advanced position in 2300 BP and changes only modestly during this period.

Ice volume grows rapidly from 2300 to 1900 BP, but the advance and thickening of Rembesdalskåka alone cannot explain this ice volume increase. Rather, the bulk of Hardanger-

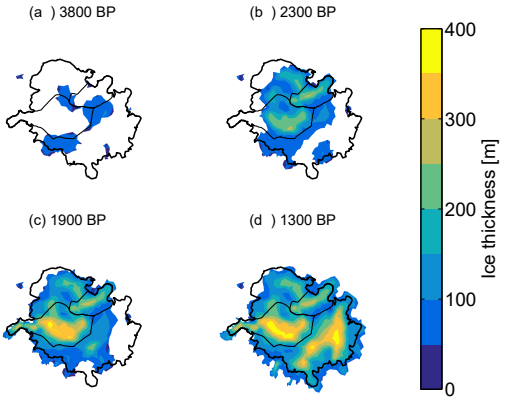

Figure 5. Modeled ice thickness at **(a)** 3800, **(b)** 2300, **(c)** 1900 and 1300 BP using our "best-fit" model parameters obtained from independent calibration. Shown are also ice cap extent in AD 1995 (black thick line) and corresponding drainage basins for outlet glaciers Rembesdalskåka (SW) and Midtdalsbreen (NE; black thin lines).

jøkulen's volume increase during this period is due to ice cap growth in the east and southeast, where deep bedrock basins are filled with ice up to 400 m thick (Fig. 5d, see also Fig. 1).

We tested alternative mass balance forcings (faster rate of linear increase and constant mass balance equal to the final value), and we found the spatial pattern of ice cap growth to be robust.

At the end of the spinup period (ca. 1300–400 BP), outlet glaciers stabilize their frontal positions and ice volume increase flattens out.

4.2 Hardangerjøkulen since the Little Ice Age

4.2.1 Parameter ensemble

From AD 1600, we continue the Holocene run using our ensemble of sliding and deformation parameter combinations, for one specific mass balance history. The ensemble modeled ice volumes at the LIA maximum (AD 1750) range from ca. 12.7 to 17.4 km^3 and vary between 6.9 and 13.4 km^3 for the present day (AD 2008; Fig. 4d). Parameter combinations including rate factors $A(T = -1\,°C)$ all give results $\pm 10\,\%$ from the observed ice volumes in 1961 and 1995. Using enhanced sliding and stiffer ice, or vice versa, it is possible to get close to the observed ice volume also for other rate factors. However, only using ice volume for validation is not sufficient. A simulated ice volume close to observations does not imply accurate ice extent and surface topography. The ~ 100 m spread in estimated surface elevation for the ice cap interior in 1995 (Fig. 7) illustrates the impact of parameter uncertainty on the dynamics and hence ice cap hypsometry.

4.2.2 Simulation using best-fit parameters

The LIA maximum ice volume using the best-fit parameter combination is modeled to 14.8 km^3 (Fig. 4d). It is not possible to obtain correspondence to observed lengths for both outlet glaciers simultaneously, not even by altering the dynamical parameters (Fig. 7). The mass balance history giving optimal results for Midtdalsbreen was chosen since its LIA maximum extent has been dated to AD 1750, while no dates exist for Rembesdalskåka. In addition, bed topography is more accurate for Midtdalsbreen. Using this setup, the LIA maximum length agrees reasonably well with moraine evidence, whereas Rembesdalskåka is too short (Fig. 8). Consistent with the results for Midtdalsbreen and Rembesdalskåka, the lengths of the southwestern outlet glaciers at the LIA maximum are underestimated in the model (Fig. 9a), while the extent of the northeastern outlet glaciers agrees well with moraine evidence.

During the early 1900s, outlet glacier lengths are too short (Figs. 8 and 9b), but the difference for Midtdalsbreen is only slightly larger than the model resolution (200 m). The ice cap margin after 1960 is reproduced with a high degree of detail (Fig. 9c and d). Most, but not all, discrepancies are close to the model resolution. One exception is the too small northwestern ice cap. However, ice thickness in the missing area is small (< 50 m), so this mismatch contributes little in terms of total ice volume.

The closest match with observed ice volume in 1961 and 1995 (Fig. 4d) within our ensemble is by the best-fit parameter combination obtained from calibration (Fig. 3). Modeled and observed ice volume for these years differ by 0.10 and 0.22 km^3, respectively, or 1.1 and 2.3 % of total observed ice volume, respectively. Modeled thickness in 1995 is generally in good agreement with the data, though the ice cap interior is somewhat too thin and the thickness along the eastern margin is overestimated (Fig. 9e).

The simulated continuous ice volume history of Hardangerjøkulen from 4000 BP through the LIA until today, including our ensemble from AD 1600 onwards, is shown in its entirety in Fig. 4c and d. The simulations show that Hardangerjøkulen has lost one-third of its volume between 1750 and the present day.

4.3 Mass balance sensitivity and hysteresis

We find that Hardangerjøkulen at present is exceptionally sensitive to mass balance changes (Figs. 10 and 11a). In particular, the ice cap is bound to disappear almost entirely for mass balance anomalies of -0.2 m w.e. or lower. Our parameter ensemble suggests a disappearance for anomalies between -0.5 and -0.1 m w.e., though this range is likely smaller as explained in Sect. 4.2.1. Our simulations show a close to linear relationship between positive mass balance perturbations and ice volume response (Fig. 10), while the

ice cap melts away partly or completely for the negative anomalies.

Further experiments show that the mass balance–altitude feedback is vital in explaining Hardangerjøkulen's high sensitivity to climate change. Without the feedback, the ice cap responds close to linearly to mass balance perturbations and thus is far less sensitive to climate change (Fig. 11b). For example, half of present-day ice volume ($4.9\,km^3$) is still present for a mass balance anomaly of -0.5 m w.e., while with $+0.5$ m w.e., ice volume increases by $\sim 35\,\%$. In stark contrast, when including the feedback, the ice cap disappears completely for the corresponding negative anomaly, and ice volume almost doubles ($+92\,\%$) for the positive anomaly (Fig. 11a).

Starting from ice-free conditions and including the mass balance–altitude feedback, we find that the Hardangerjøkulen's climatic response depends on the ice cap's initial state. For mass balance anomalies close to our reference mass balance for 1963–2007, between -0.2 and $+0.1$ m w.e., large differences occur between ice volumes reached from present-day and ice-free conditions (Fig. 10). When starting from a situation without ice, present-day mass balance conditions produce an ice cap that has only $20\,\%$ of the volume of today's ice cap. In addition to Hardangerjøkulen being bound to disappear almost completely for a slight decrease in the mass balance, this result implies that a positive mass balance anomaly is needed to regrow the ice cap to its present-day extent, once it has disappeared.

4.4 Volume–area phasing and scaling

Our Holocene simulations show that the ice volume evolution for three of the outlet glaciers (Rembesdalskåka, Midtdalsbreen, Blåisen) is asynchronous (Fig. 12). Midtdalsbreen's ice volume increases linearly over time, while Rembesdalskåka and Blåisen have distinct jumps in ice volume, related to their bed topography. The importance of bedrock troughs and overdeepenings is further illustrated by Hardangerjøkulen's nonlinear volume increase ca. 2300–1300 BP, a period when volume increases faster than area (Fig. 12). During this period, ice is thickening rather than expanding horizontally, which can largely be explained by ice growth in subglacial valleys in the eastern and southeastern parts of the ice cap (Fig. 1). These bed depressions fill up quickly because ice flow converges into them from surrounding high bedrock ridges, and the mass balance–altitude feedback amplifies the ice thickening.

We compare our steady-state mass balance perturbation experiments (Sect. 4.3) with volume–area scaling relations for steady-state ice caps from the literature (Fig. 13a) of the form $V = cA^{\gamma}$ (Bahr et al., 1997). For a consistent comparison, we group our perturbation experiments into those which produce a fully developed ice cap and those where ice is mainly present on high ridges and thus cannot be classified as a glacier or ice cap. We find that ice cap scaling relations from the literature overestimate the ice volume of the full-grown ice cap. Both the exponent and the scaling factor found for Hardangerjøkulen ($\gamma = 1.3738$ and $c = 0.0227$) are closer to literature values for valley glaciers (e.g Bahr et al., 2015).

During the first half of the Holocene simulation, a full ice cap does not develop, and volumes are up to $60\,\%$ smaller than ice volumes predicted from the volume–area relation derived from our steady-state experiments (Fig. 13b). Approaching the LIA and up to today, Hardangerjøkulen has a more developed shape, and our steady-state-derived volume–area relation fits well with simulated volumes. We discuss these results and their implications in Sect. 5.5.

5 Discussion

5.1 Sensitivity to sliding and deformation parameters

Running our parameter calibration ensemble, we aim to minimize the RMSE between observed and modeled present-day surface topography. Several parameter combinations give similar RMSEs (Fig. 3). Since both the rate factor (A) and sliding parameter (β) depend on driving stress (Flowers et al., 2008; Zekollari et al., 2013), one can keep the same surface velocities by reducing one parameter and increasing the other. Hence it is challenging to pick a unique combination without more empirical knowledge about their relative importance (Le Meur and Vincent, 2003; Aðalgeirsdóttir et al., 2011; Zekollari et al., 2013). This underlines the motivation behind keeping our ensemble after the calibration. A comparison with an ice velocity map, which is not available for Hardangerjøkulen, would more strongly constrain A and β.

Notwithstanding data deficiencies, a notable finding is that the impact of A on ice volume is relatively small at calibration (Fig. 3) but large during our transient simulation over several centuries (Fig. 4d). This disparity suggests that small differences in model rheology at initialization can propagate significantly with time. This time dependency has implications for other model studies of long-term dynamics of glaciers and ice caps. With growing availability of data, such studies may consider a "dynamic" or "transient" calibration (e.g., Oerlemans, 1997a; Davies et al., 2014; Goldberg et al., 2015), as opposed to a "snapshot" calibration. The "transient" method uses several sets of observations to infer model parameters, ideally at dynamically and climatically different states.

During the years following AD 1600, when including the ensemble of dynamical parameters, the ice cap response is a combined effect of climate forcing and adjustment to new parameter values. The period AD 1600–1710 can be viewed as a short spinup phase for the historic simulation, where the mass balance is kept constant at the end value of the Holocene simulation ($\Delta B(t) = 0.4$ m w.e.).

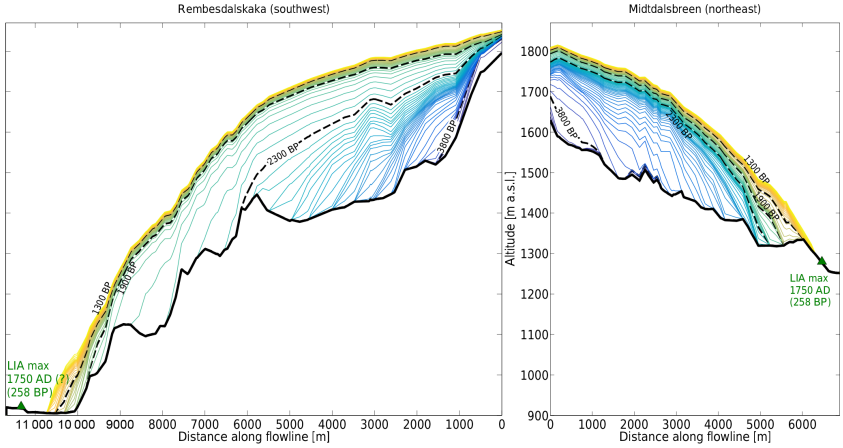

Figure 6. Modeled surfaces from 4000 BP to AD 1600, starting with no ice cap, shown every 50 years from older (dark blue) to younger (yellow). BP ages are relative to AD 2008. Note that the top of Rembesdalskåka (Hardangerjøkulen's summit) does not coincide with the top of Midtdalsbreen's flowline (see Fig. 9d).

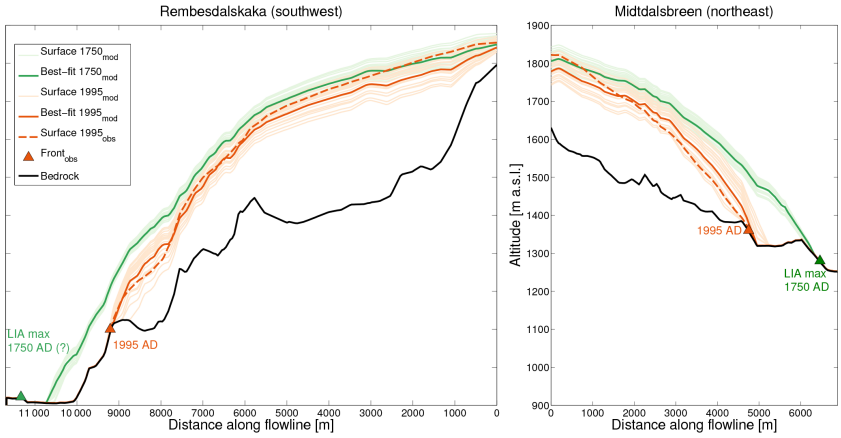

Figure 7. Modeled surfaces for AD 1750 (light green) and 1995 (light orange) for Rembesdalskåka and Midtdalsbreen, using an ensemble of different dynamical parameter combinations. Modeled surface using our "best-fit" parameter combination is also shown for 1750 (green) and 1995 (orange), as well as observed surface in 1995 (dashed orange). Outlet front positions as known from dated (Midtdalsbreen) and assumed contemporary (i.e., not dated; Rembesdalskåka) terminal moraines are indicated with triangles. Note that the top of Rembesdalskåka (Hardangerjøkulen's summit) does not coincide with the top of Midtdalsbreen's flowline (Fig. 9e).

For the historic run, the ensemble spread in surface elevation is larger in the vicinity of the ELA than at the margins (Fig. 7). Recall that the continuity equation (Eq. 4) requires that thickness change occurs ($\frac{\partial H}{\partial t} \neq 0$) when ice flow and mass balance are not balanced ($\nabla \cdot (\bar{u} H) \neq \dot{M}$). Therefore, softer ice or higher sliding cause ice thickness to decrease, meaning ice spends less time in the accumulation zone. Similarly, faster flow downstream of the ELA also requires thinning. The insensitivity of the frontal positions is likely due to high ablation near the margins overwhelming other effects and, for 1995, also frontal positions pinned by bedrock topography.

Flowers et al. (2008) simulated Holocene behavior of the Langjökull ice cap on Iceland using

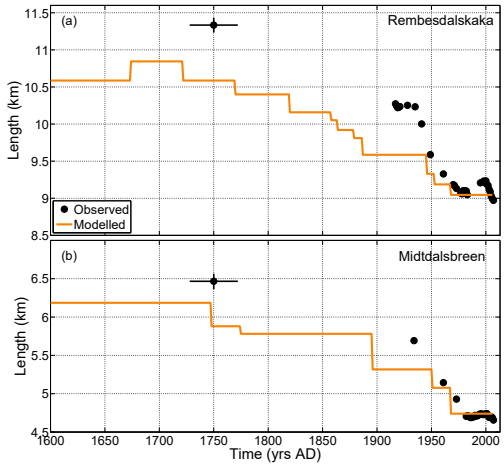

Figure 8. Modeled and observed length of outlet glaciers **(a)** Rembesdalskåka and **(b)** Midtdalsbreen. Temporal uncertainty for 1750 is indicated based on a 10 % age error (Innes, 1986) on the dated moraine at Midtdalsbreen (Andersen and Sollid, 1971) and assuming that the Rembesdalskåka moraine is contemporary. Uncertainties in measured lengths in the 1900s and 2000s are smaller than the marker size.

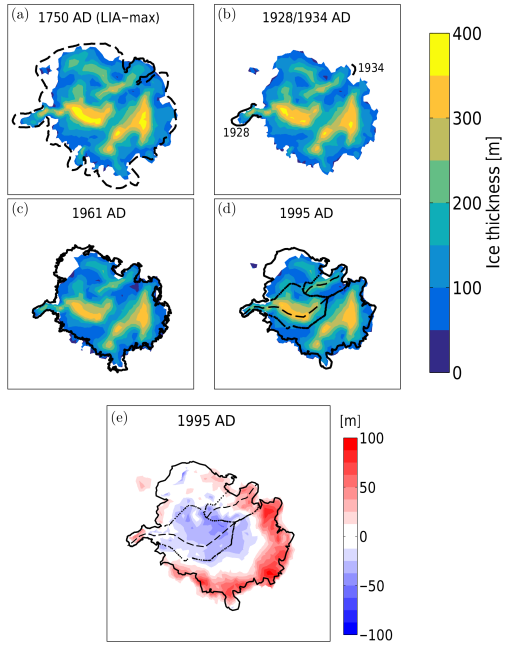

Figure 9. Modeled ice thickness of Hardangerjøkulen in **(a)** AD 1750, **(b)** 1928, **(c)** 1961 and **(d)** 1995. Shown is also the difference between modeled and observed surface in 1995 **(e)**, where positive (negative) values indicate that the model overestimates (underestimates) surface elevation. Observed ice cap extents (Andersen and Sollid, 1971; Sollid and Bjørkenes, 1978; A. Nesje, personal communication, 2014; H. Elvehøy, personal communication, 2014; Cryoclim.net/NVE) for corresponding years are shown where available. For 1750, assumed LIA extent from geomorphological evidence (dashed line) and dated LIA extent (solid line) is shown. For 1928/1934, the modeled thickness displayed is for 1928, though the observed front shown for Mitdalsbreen is from 1934. Drainage basins and flowlines of Rembesdalskåka and Midtdalsbreen are shown for 1995.

$\beta = 2.5 \times 10^{-4}\,\mathrm{m\,a^{-1}\,Pa^{-1}}$, which is within our ensemble range. Somewhat in contrast to this study, they noted a low sensitivity to β. However, seasonal speedups are absent at Langjökull while they have been observed at Hardangerjøkulen (Willis, 1995; Willis et al., 2012), which probably explains the differing sensitivities.

In line with our study, Hubbard et al. (2006) obtained a shallow, dynamic Icelandic ice sheet at the Last Glacial Maximum, associated with high sliding. Similarly, Golledge et al. (2008) obtained a thin, more extensive Younger Dryas ice sheet in Scotland with increased sliding. As also explained above from a theoretical perspective (mass continuity), a shallow geometry is associated with high sliding.

A future expansion of this work would be a multiple regression of the dynamical parameters for Hardangerjøkulen and its outlet glaciers. This could disentangle whether their importance changes over time, for example depending on mass balance regime or whether the glacier is retreating or advancing. However, the available (velocity) data are not sufficient to constrain the dynamic parameters to a narrower range, and thus more data would be needed to make such an analysis insightful. Better knowledge of the bed properties at Hardangerjøkulen by means of radar, seismic or borehole studies, along with modeling of the subglacial drainage system, would also be steps toward understanding the (transient) behavior of basal slipperiness.

5.2 Mass balance parameterization

We deliberately chose to use a simple mass balance formulation to focus on first-order ice dynamical responses to spatially homogeneous changes in the forcing. The evolution of Hardangerjøkulen through the 20th century has been simulated by Giesen (2009) using the simple mass balance profile used here, as well as with a spatially distributed mass and energy balance model (Giesen and Oerlemans, 2010). Differences in ice volume and outlet glacier lengths produced with the two mass balance configurations were present, but small, justifying the use of the simple mass balance profile. In this section, we discuss some of the results presented in Giesen

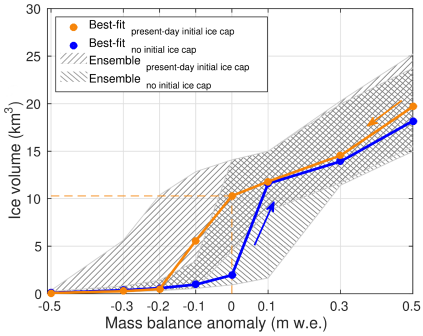

Figure 10. Steady-state ice volumes reached using step perturbations of the 1963–2007 mass balance, using an ensemble of dynamical parameter combinations, starting from the present-day ice cap and ice-free conditions.

(2009) and Giesen and Oerlemans (2010) that are relevant for our study.

Similar to the present study, Giesen and Oerlemans (2010) were not able to match both the modeled lengths of Rembesdalskåka and Midtdalsbreen with modern observations. Since they used a sophisticated mass balance model including an albedo scheme, a spatial precipitation gradient, and aspect and shading effects on insolation, this suggests that the mismatch should not be attributed to the mass balance forcing but rather to other factors.

The two single years (2001–2002; Krantz, 2002) with mass balance measurements on Midtdalsbreen are not enough to systematically assess differences in the mass balance regimes of Rembesdalskåka and Midtdalsbreen. Nonetheless, differing mass balance regimes were suggested based on surface elevation changes from 1961 to 1995 (Andreassen and Elvehøy, 2001) and also served as an explanation for differing glacier reconstructions between the southwestern and northeastern margins of the ice cap (Dahl and Nesje, 1994; Nesje et al., 1994). Coupled glacier and precipitation reconstructions based on multiproxy approaches on lacustrine sediments (e.g., Vasskog et al., 2012) could give more insight into differing continentality of the outlet glaciers of Hardangerjøkulen. Snow and mass balance field studies covering the entire ice cap would also be valuable to better understand the spatial mass balance variability.

Apart from spatial variations in the mass balance profile, temporal changes in climate or ice cap geometry may affect the mass balance function. For example, solar insolation patterns may change with strongly altered ice cap geometry, by shading effects of valley walls. However, Hardangerjøkulen has a gently sloping surface and is not surrounded by high mountains. Therefore, topographic effects on the insolation result in small spatial variations of the mass balance between -0.1 and $+0.1$ m w.e. for the vast majority of the ice cap, and only two outlet glaciers oriented south show larger deviations locally. Even in a considerably warmer climate with a smaller ice cap, with continuously updated topographic effects on solar radiation, the mass balance profile with elevation remained close to the present-day value. Furthermore, solar irradiance at 4000 BP, when we start our simulation, was at most 5 % larger in the summer months than today (Giesen, 2009) and is therefore expected to have a minor effect on mass balance. In addition, Giesen and Oerlemans (2010) show that lowering the ice albedo from 0.35 to 0.20 under a realistic 21st century scenario only leads to a 5 % larger volume decrease of the ice cap. We conclude that using a mass balance profile only dependent on elevation is a good approximation for Hardangerjøkulen, even in a different climate with a smaller or larger ice cap.

It is not clear why *observed* mass balance decreases at the uppermost elevations (Fig. 2), but likely explanations are snow redistribution by wind or orographic precipitation effects. Snow erosion and redeposition may be parameterized based on surface curvature, which is a good indicator of regions with wind-induced snow redistribution (Blöschl et al., 1991; Huss et al., 2008). Giesen (2009) tested a surface-curvature approach for Hardangerjøkulen, but the plateau was too flat for snow redistribution to occur in the model. An orographic precipitation model has not yet been applied to Hardangerjøkulen and is outside the scope of our study.

Glaciological measurements of mass balance have inherent uncertainties and biases, related to instrumentation, survey practices and techniques (Cogley et al., 2011). Andreassen et al. (2016) performed a reanalysis of glaciological and geodetic mass balance for Norwegian glaciers, including Rembesdalskåka. For the period 1995–2010, they found a more negative geodetic mass balance (-0.45 m w.e.) than the glaciological one used in this study. We performed an additional simulation with this more negative mass balance for the final years of our simulation (1995–2008) and found that the effect on ice volume is ca. 0.5 km^3, or 5.3 % of modeled ice volume in year 2008.

5.3 Mass balance sensitivity and hysteresis

Hardangerjøkulen is found to be particularly sensitive to mass balance changes: the ice cap disappears completely for the -0.5 m w.e. anomaly forcing and almost doubles in volume for $+0.5$ m w.e. Similar experiments for Nigardsbreen, southwestern Norway (Oerlemans, 1997a), and Franz Josef Glacier, southwestern New Zealand (Oerlemans, 1997b), show much smaller responses ($\sim$ 20–25 %). Our results are consistent with those of Giesen (2009), who also used an SIA model (Van Den Berg et al., 2008), but with different implementation of dynamical parameters and numerical methods.

Hardangerjøkulen's high sensitivity can be explained by its hypsometry and surface topography. Rivera and Casassa (1999) attributed differing responses of three Patagonian glaciers to contrasting hypsometries and thereby sensitivity

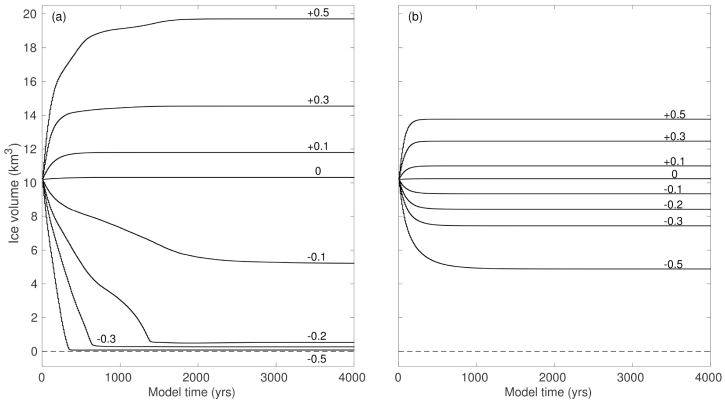

Figure 11. Ice volume evolution for selected mass balance perturbations (−0.5 to 0.5 m w.e.) relative to the mean mass balance 1963–2007, using our best-fit dynamical parameter combination, for **(a)** with and **(b)** without a mass balance–altitude feedback. A mass balance anomaly of −0.2 m w.e. is added for greater detail of Hardangerjøkulen's disappearance.

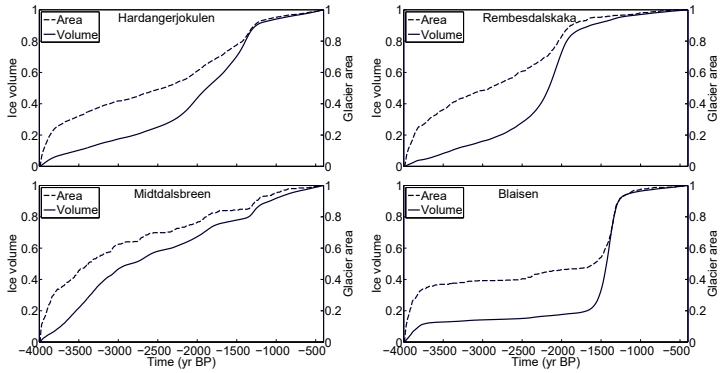

Figure 12. Simulated ice volume and area evolution for **(a)** Hardangerjøkulen, and the outlet glaciers **(b)** Rembesdalskåka, **(c)** Midtdalsbreen, and **(d)** Blåisen, from 4000 to 400 BP (AD 1600). Quantities are non-dimensionalized relative to final volume and area in year AD 1600.

to ELA change. Nesje et al. (2008a) noted that the difference between Hardangerjøkulen's ELA and maximum elevation is particularly small (∼ 180 m) compared to other glaciers and ice caps in Norway. Furthermore, the ice cap is relatively flat with little area distribution in altitude. A comparison with Franz Josef Glacier, New Zealand (Woo and Fitzharris, 1992), Nigardsbreen, Norway (Oerlemans, 1997a), and Vatnajökull, Iceland (Aðalgeirsdóttir et al., 2003), confirms that Hardangerjøkulen has the most extreme hypsometry (Fig. 14a). Furthermore, the present ELA is located close to the altitudes where area is large, resulting in an unusually vulnerable ice cap. For example, an ELA increase of 100 m at Hardangerjøkulen is equivalent to a 16.9 % decrease in area. Corresponding values for Nigardsbreen (9.9 %), Franz Josef Glacier (1.5 %) and Vatnajökull (6.1 %) are much smaller, confirming this explanation (Fig. 14b).

The high sensitivity to mass balance changes found for Hardangerjøkulen supports abrupt changes inferred from lake sediment records for the Holocene for both the northern and southern side of the ice cap (Dahl and Nesje, 1994; Nesje et al., 1994). One example is the so-called "Finse event", when an advance to a maximum extent beyond that of present day of the northern Blåisen outlet glacier ∼ 8300 BP was followed by a complete disappearance of this glacier within less than a century. Our results show that for a mass balance anomaly of −0.5 m w.e., the present-day ice cap disappears in ∼ 300 years. Depending on the ice cap volume at the Finse event, we find that an anomaly between −2.0 and 2.4 m w.e. melts away Hardangerjøkulen within a century.

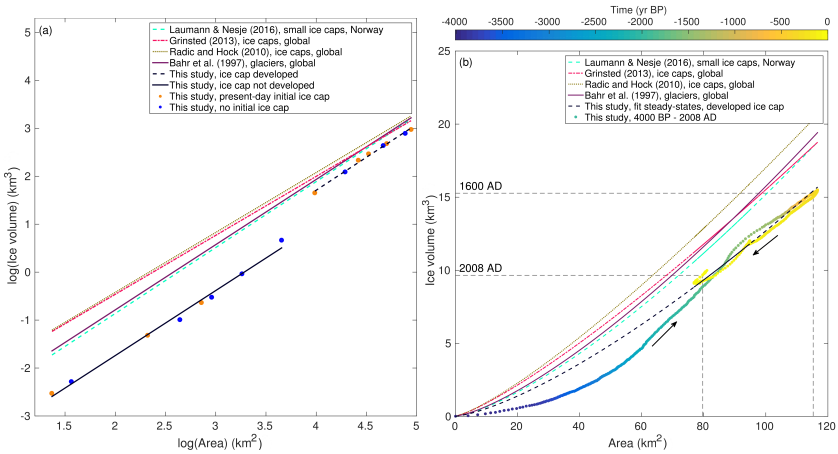

Figure 13. **(a)** Logarithmic values of volume and area for steady-state experiments using mass balance anomalies within −0.5 to +0.5 m w.e. relative to the AD 1963–2007 reference mass balance. Both steady states reached from the present-day ice cap and from ice-free conditions are shown. Steady states are grouped into two cases, depending on whether an ice cap has developed or ice is only present on high ridges. Commonly used volume–area relations from the literature are also shown (Bahr et al., 1997; Radić and Hock, 2010; Grinsted, 2013; Laumann and Nesje, 2017). **(b)** Volume and area combinations for our simulation from 4000 BP to AD 2008, along with the volume–area relation derived from simulated developed steady-state ice caps in **(a)**.

Nonetheless, the advanced ice cap at the Finse event was likely not fully grown and in a steady state, so an anomaly of ∼ 1.5 m w.e. is more likely.

Given a mass balance sensitivity of around −0.9 m w.e. K^{-1} (Giesen and Oerlemans, 2010) and no change in precipitation, the air temperature increase responsible for the ice cap disappearance after the Finse event must have been at least 1.5 K. Reconstructed summer temperature after the Finse event suggest a sharp increase of 1.0–1.2 K (Dahl and Nesje, 1996). A 10 % precipitation decrease would compensate for this difference, since the sensitivity to precipitation for Hardangerjøkulen is around +0.3 m w.e. K^{-1} (Giesen and Oerlemans, 2010). Despite uncertainties in the reconstruction and model simulations, it is encouraging that both give consistent results, suggesting that ice flow models coupled with reconstructions may be used to constrain past climate conditions.

We can also view our results on mass balance sensitivity in light of future climate change. The mean mass balance in the last decade was −0.3 m w.e. Since Hardangerjøkulen was in approximate balance over the preceding decades, this decrease primarily reflects changes in meteorological conditions, and not dynamical adjustments. With the mass balance of the last decade, our experiments suggest that Hardangerjøkulen disappears within 750 years (Fig. 11). However, future projections indicate further warming for southern Norway. Giesen and Oerlemans (2010) imposed future climate scenarios on a surface energy balance mass balance model coupled to an SIA model, suggesting that Hardangerjøkulen will vanish almost completely before 2100. Similar conclusions have been reached for glaciers in Iceland (Aðalgeirsdóttir et al., 2006, 2011; Guðmundsson et al., 2009), French Alps (Le Meur et al., 2007), Swiss Alps (Jouvet et al., 2011) and Canadian Rocky Mountains (Clarke et al., 2015). Given the aforementioned temperature and precipitation sensitivities for Hardangerjøkulen, our estimate of −2.2 m w.e. to remove the present-day ice cap in 100 years translates to a temperature increase of ∼ 2.7 °C, given a 10 % increase in precipitation. This is close to future projections for southern Norway (Hansen-Bauer et al., 2015).

Hardangerjøkulen's strong hysteresis highlights the importance of accurately representing the initial state in transient simulations of small ice caps, as previously suggested for ice sheets (e.g Aschwanden et al., 2013; Aðalgeirsdóttir et al., 2014). Starting from ice-free conditions, Hardangerjøkulen grows to only 20 % of its present-day volume under a modern climate. This is in stark contrast to the Juneau Icefield in Alaska, an ice field in a similar climatic setting, which in model simulations regrows close to modern ice volume under present-day mass balance conditions (Ziemen et al., 2016). The authors attribute this insensitivity to initial conditions to the complex topography of the Juneau Icefield, with numerous outlet glaciers able to retreat up to high altitudes where positive mass balance areas persist even under future warming scenarios. This behavior is not observed at Yakutat Icefield, a low-lying maritime ice field in

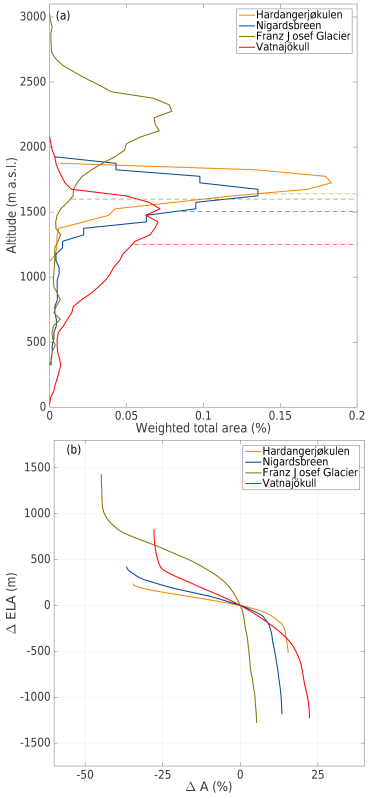

Figure 14. **(a)** Hypsometry of present-day Hardangerjøkulen (Giesen and Oerlemans, 2010) and Nigardsbreen, Norway (Oerlemans, 1997a), Franz Josef Glacier, New Zealand (Woo and Fitzharris, 1992), and Vatnajökull, Iceland (Aðalgeirsdóttir et al., 2003). Respective ELAs are indicated with dashed lines. Areas are weighted by the total area, and altitude bins are 25 m. **(b)** Effect of a step change in ELA on area for respective glacier.

southeast Alaska (Trüssel et al., 2015), which cannot be sustained under present-day climate conditions. Its topography is relatively flat, comparable to the one of Hardangerjøkulen, which might explain its high sensitivity under modern climate scenarios. Similarly, Gilbert et al. (2016) suggested that Barnes Ice Cap, Baffin Island, Canada, is not sustainable under present mass balance conditions. While they did not perform regrowth experiments, their findings of the Barnes Ice Cap being a remnant of the Laurentide Ice Sheet suggest a hysteresis similar as we show for Hardangerjøkulen.

5.4 Holocene to LIA buildup

In the early part of the modeled period (ca. 4000–3800 BP), ice grows preferentially on high bed topography, and Midtdalsbreen and Blåisen start to develop earlier than Rembesdalskåka (Fig. 5, also see Fig. 1). While the model resolution here is coarse (300–500 m), we expect that ice dynamics at this stage plays a minor role, since the ice present is split up into several small separate glaciers (< 2 km long, < 100 m thick). Instead, the initial ice growth at high bed ridges is due to buildup of ice above the present-day ELA, which is used as initial mass balance forcing.

The actual rate of advance may differ from what is modeled here because the SIA has limitations in the steep terrain (Le Meur et al., 2004) where Rembesdalskåka terminates during the period of fast ice volume increase (ca. 3800–2300 BP, Fig. 4c). However, the effects of ice flow mechanics are likely small compared to those of the mass balance on the long timescales considered here.

During the period of modeled rapid ice cap growth (ca. 2300–1300 BP), reconstructed precipitation in western Norway is slightly lower than the general increasing mass balance trend applied here (Dahl and Nesje, 1996; Bjune et al., 2005). At the same time, glacier reconstructions from southern Hardangerjøkulen indicate a slight decrease in glacier size (Nesje et al., 1994). Unfortunately, there is to our knowledge no geomorphological or other evidence that can be used as tie points for modeled ice cap extent or volume during this period.

Our simulated preferential ice cap growth on the northern and western side, illustrated in Fig. 5b at 2300 BP, is in line with reconstructions showing an early glacierization of the north (Dahl and Nesje, 1994) versus the south (Nesje et al., 1994).

We are aware that bed topography for Hardangerjøkulen is uncertain in places, though less so for Midtdalsbreen and Rembesdalskåka, which are of prime interest. Moreover, the proglacial lake in front of Rembesdalskåka may have modulated LIA frontal behavior, as suggested for Icelandic glaciers (Hannesdóttir et al., 2015). However, we expect this effect to be minor compared to other model uncertainties.

Further data for model validation are required to add more detail to our modeled history of Hardangerjøkulen. However, given the limited knowledge about ice cap activity between the ice-free conditions at 4000 BP and the LIA maximum around AD 1750, we consider our continuous model simulation to be a good first estimate of Hardangerjøkulen's growth from inception to its maximum extent during the LIA.

Moreover, we have provided a plausible ice cap history over several thousand years as the starting point for our simulations from the LIA until today, in contrast to several previous studies (e.g., Giesen and Oerlemans, 2010; Aðalgeirsdóttir et al., 2011; Zekollari et al., 2014) that reach desired initial LIA conditions by perturbing a present-day ice cap.

5.5 Nonlinearity, asymmetry and their implications

The initial present-day mass balance forcing ($\Delta B(t) = 0$ m w.e.) at 4000 BP likely explains the rapid increase in ice volume over the first few hundred years, since this forcing essentially represents a step change in mass balance at 4000 BP. However, this effect diminishes after a few hundred years, after which the response is due to the linear mass balance forcing. $\Delta B(t) = 0$ m w.e. starting from ice-free conditions produces a steady-state ice volume of only $\sim 2\,\mathrm{km}^3$ (Fig. 10), a volume exceeded at 3300 BP, so any additional ice volume cannot be explained by the initial step change in mass balance at 4000 BP. Most importantly, the nonlinear ice volume response between 2300 and 1300 BP is thus entirely forced by the linear mass balance increase during this period.

Analogous to the Holocene simulations, we performed experiments with a slowly *decreasing* mass balance over multiple millennia (from $\Delta B(t) = 0.4$ to 0 m w.e.), allowing the ice cap to dynamically adjust, starting with the AD 1600 ice cap state. We find that the western ice cap disappears first, while ice in the eastern part of the ice cap is more persistent. Hence, the western and northern parts of the ice cap grow first and disappear first, whereas the eastern part grows last and disappears last. Further, our experiments show that a gradual (linear) climatic change results in a nonlinear change in ice volume. This nonlinear, asynchronous growth and retreat illustrates that proxy records representing different parts of an ice cap at different times may lead to substantially different conclusions about ice cap size through time.

Previous work has highlighted glacier hypsometry, overdeepenings and proglacial lakes in altering glacier *retreat* to climate forcing (Kuhn et al., 1985; Jiskoot et al., 2009; Aðalgeirsdóttir et al., 2011). Adhikari and Marshall (2013) and Hannesdóttir et al. (2015) showed that overdeepened basins loose mass by thinning rather than retreat. Here we suggest that a similar behavior applies to an *advancing* glacier. In particular, overdeepened areas delay frontal advance and lead to preferential glacier thickening. However, note that the effect of higher order stresses, not captured by our simplified dynamic model, may be more important for an advancing glacier (Adhikari and Marshall, 2013).

Regarding volume–area scaling (Sect. 4.4), Bahr et al. (2015) argue that the fundamental difference between valley glaciers and ice caps, and hence the reason for different scaling exponents (γ), is the influence of bedrock topography, specifically that ice thickness is large compared to the relief of underlying topography. The bedrock topography below Hardangerjøkulen consists of deep subglacial valleys and high ridges controlling the ice flow, as also noted by Laumann and Nesje (2017) for other Norwegian ice caps. In fact, our simulations confirm that bed topography is vital in controlling the growth and retreat of Hardangerjøkulen. The relatively thin ice at the ice cap summit does not correspond to the classical ice cap with the thickest ice in the center, which explains why volume–area exponents for valley glaciers ($\gamma = 1.375$) rather than ice caps ($\gamma = 1.25$) are found for Hardangerjøkulen. However, the overestimation of c by commonly used volume–area scaling relations for ice caps is more surprising. The low c we find compared to literature values for ice caps suggests that literature volume–area scaling parameters may not be accurate for relatively small ice caps.

Importantly, glacier reconstructions using proglacial lake sediments are generally based on assumed changes in glacier (erosive) area rather than volume (Hallet et al., 1996), while we show that volume and area can become decoupled for several centuries (Fig. 12). We also demonstrate that the degree of volume–area coupling varies for different outlet glaciers, implying that each outlet glacier should be considered individually. For example, a differing response to identical climate forcing is illustrated when Midtdalsbreen advances only modestly from 2300 to 1300 BP (Fig. 5b–d), while Hardangerjøkulen triples its ice volume during the same period due to ice growth elsewhere (mainly in the east, south and southwest).

Our nonlinear response and out-of-phase volume and area call for reassessment of some glacier and climate reconstruction methodologies. To extract a climate signal, linear assumptions between ice extent (area), ice volume (mass balance), climate and their geomorphological or proxy signal are commonly assumed in glacier reconstructions (e.g., Liestøl in Sissons, 1979; Bakke et al., 2005). Linearity is also commonly assumed in simplified models used to extract climate information from glacier variations (e.g., Harrison et al., 2001; Oerlemans, 2005; Lüthi, 2009; Roe, 2011). However, we find that these assumptions do not hold for Hardangerjøkulen and its outlet glaciers. For a growing ice cap, two scenarios may arise for which the linear assumption between area (proxy) and volume (climate) fails: (i) area changes faster than volume (first few hundred years of our Holocene simulation), meaning the interpreted signal becomes biased towards a climate favorable for glacier growth (wetter/colder), or (ii) volume changes faster than area (2300–1300 BP in our simulation), and the climate signal is missed or underestimated because the preferential thickening is not translated into a corresponding frontal change. We expect that ice caps with comparable geometry in, for example, Norway, Iceland, Alaska, Patagonia and peripheral Greenland may display similar behavior.

These results highlight the need for model–data integration in paleostudies. Ice sheet modelers require glacier records for calibration and validation and climate reconstructions for model forcing. Based on our experiments, we advise that glacier-derived climate records are tagged with explicitly stated glaciological assumptions and associated uncertainties. In particular, we would like to recommend future model–data studies which directly constrain geometric contributions to the glaciological uncertainties involved in sedimentary glacier proxies.

6 Conclusions

We have used a two-dimensional ice flow model with a simple mass balance parameterization to simulate the evolution of Hardangerjøkulen ice cap since the mid-Holocene, from ice-free conditions up to the present day. Until the LIA, the model is forced by a linear mass balance increase based on reconstructions of temperature and precipitation. From the LIA onwards, an optimized mass balance history is employed, and direct mass balance measurements are used after 1963.

We used an ensemble approach to assess sensitivity to sliding and ice deformation parameters during both calibration and transient runs. We find that small differences in model ice rheology at the calibration stage increase significantly with time. This time dependence has implications for other model studies of long-term dynamics of glaciers and ice caps. Such studies would benefit from using a "transient calibration" rather than a "snapshot" approach and thereby reduce temporal biases arising from data quality issues or a particular dynamic or climatic state.

More data in both space and time are needed to further constrain the dynamic model parameters and mass balance for Hardangerjøkulen.

In our simulations, Hardangerjøkulen evolves from no ice in the mid-Holocene to its LIA maximum in different stages, where the fastest stage (2200–1300 BP) involves a tripling of ice volume in less than 1000 years. Notably, our linear climate forcing during this time gives a nonlinear response in ice cap volume and area. This growth occurs in a spatially asymmetric fashion, where Midtdalsbreen reaches its maximum first, while advances of Rembesdalskåka and the eastern ice cap are delayed. These different responses are caused by local bed topography and the mass balance–altitude feedback.

Following the simulated Holocene growth of Hardangerjøkulen, we successfully reproduce the main features of the LIA extent of the main outlet glaciers, given temporal and spatial uncertainties in moraine evidence. In the early 1900s the simulated glacier positions are slightly underestimated, whereas the ice extent closely resembles the observed margins available starting from 1960, and the surface topography fits well with the 1995 surface survey.

Hardangerjøkulen is found to be highly sensitive to mass balance changes. A reduction by 0.2 m w.e. or more relative to the mass balance from the last decades induces a strong mass balance–altitude feedback and makes the ice cap disappear completely. Conversely, an anomaly of $+0.5$ m w.e. almost doubles total ice volume.

Volume and area for Hardangerjøkulen and several of its outlet glaciers vary out-of-phase for several centuries during the Holocene. This disequilibrium varies in time and among the outlet glaciers, showing that ice cap reconstruction methodologies carrying linear assumptions between ice extent and volume may not hold. Based on the nonlinear, asynchronous response we find for Hardangerjøkulen, these paleoglaciological studies may decrease their uncertainty by (i) quantifying the effect of bedrock topography on ice flow and mass balance, using a numerical model, (ii) performing reconstructions on at least two outlet glaciers, preferably with distinct dynamics and bedrock topography, and (iii) reporting glaciological assumptions and proxy uncertainties to ice sheet modelers using their data.

Our experiments suggest that the present-day ice cap is in a mass balance regime where it will not regrow once it has disappeared. We thus find that Hardangerjøkulen displays strong hysteresis and that the interaction between hypsometry and mass balance–altitude feedback controls its behavior. By combining our modeled sensitivities with past climatic and glacier information, we also illustrate that ice flow models can further constrain past climates and glacier states. This highlights the need to understand the long-term history of glaciers and ice caps and calls for further integrated model–data studies.

7 Data availability

Data of length changes and surface mass balance can be accessed at http://glacier.nve.no/viewer/CI/en/cc/ClimateIndicatorInfo/2964 (Midtdalsbreen) and http://glacier.nve.no/viewer/CI/en/cc/ClimateIndicatorInfo/2968 (Rembesdalskåka). The model code can be freely downloaded from http://issm.jpl.nasa.gov. Model scripts and other datasets can be obtained upon request from the corresponding author.

Author contributions. Henning Åkesson, Kerim H. Nisancioglu, Rianne H. Giesen and Mathieu Morlighem designed the research, Henning Åkesson performed the model runs with significant input from Kerim H. Nisancioglu and Rianne H. Giesen, Mathieu Morlighem provided the ice sheet model and added necessary implementations together with Henning Åkesson and Henning Åkesson created all figures and wrote the paper, with substantial contributions from all the authors.

Competing interests. The authors declare that they have no conflict of interest.

Acknowledgements. We wish to acknowledge NVE for access to mass balance data, glacier outlines and surface and bed DEMs. Thanks also to Norwegian Meteorological Institute for providing climate data (eklima.no). We are also grateful to Atle Nesje for sharing detailed knowledge about Hardangerjøkulen and for reading the manuscript prior to submission. The research leading to these results has received funding from the European Research Council under the European Community's Seventh Framework Programme (FP7/2007-2013)/ERC grant agreement 610055 as

part of the ice2ice project. This research is also supported by the Research Council of Norway via the NOTUR project NN4659K "Models of past ice and climate". Henning Åkesson was supported by the Research Council of Norway (project no. 229788/E10), as part of the research project Eurasian Ice Sheet and Climate Interactions (EISCLIM) and has also received travel support from BKK AS. We wish to thank Andy Aschwanden, Nicholas R. Golledge, two anonymous reviewers and the Editor Andreas Vieli, whose thorough comments greatly improved the original manuscript.

Edited by: A. Vieli
Reviewed by: A. Aschwanden, N. R. Golledge, and two anonymous referees

References

Aðalgeirsdóttir, G., Gudmundsson, G. H., and Björnsson, H.: A regression model for the mass-balance distribution of the Vatnajoökull ice cap, Iceland, Ann. Glaciol., 37, 189–193, 2003.

Aðalgeirsdóttir, G., Jóhannesson, T., Björnsson, H., Pálsson, F., and Sigurðsson, O.: Response of Hofsjökull and southern Vatnajökull, Iceland, to climate change, J. Geophys. Res.-Ea. Surf., 111, F03001, doi:10.1029/2005JF000388, 2006.

Aðalgeirsdóttir, G., Guðmundsson, S., Björnsson, H., Pálsson, F., Jóhannesson, T., Hannesdóttir, H., Sigurðsson, S. P., and Berthier, E.: Modelling the 20th and 21st century evolution of Hoffellsjökull glacier, SE-Vatnajökull, Iceland, The Cryosphere, 5, 961–975, doi:10.5194/tc-5-961-2011, 2011.

Aðalgeirsdóttir, G., Aschwanden, A., Khroulev, C., Boberg, F., Mottram, R., Lucas-Picher, P., and Christensen, J.: Role of model initialization for projections of 21st-century Greenland ice sheet mass loss, J. Glaciol., 60, 782–794, 2014.

Adhikari, S. and Marshall, S. J.: Influence of high-order mechanics on simulation of glacier response to climate change: insights from Haig Glacier, Canadian Rocky Mountains, The Cryosphere, 7, 1527–1541, doi:10.5194/tc-7-1527-2013, 2013.

Andersen, J. and Sollid, J.: Glacial chronology and glacial geomorphology in the marginal zones of the glaciers, Midtdalsbreen and Nigardsbreen, south Norway, Norsk Geografisk Tidskrift, 25, 1–38, 1971.

Andreassen, L. and Elvehøy, H.: Volume change – Hardangerjøkulen, in: chap. Glaciological investigations in Norway in 2000, NVE Report No. 2, Norwegian Water Resources and Energy Directorate, Oslo, 101–102, 2001.

Andreassen, L., Elvehøy, H., and Kjøllmoen, B.: Laser scanning of Norwegian mass balance glaciers 2007–2011, in: EGU General Assembly Conference Abstracts, vol. 14, p. 10941, http://ncoe-svali.org/xpdf/andreassen_et_al_egu2012.pdf (access date: 29 May 2014), 2012.

Andreassen, L. M., Elvehøy, H., Kjøllmoen, B., Engeset, R. V., and Haakensen, N.: Glacier mass-balance and length variation in Norway, Ann. Glaciol., 42, 317–325, 2005.

Andreassen, L. M., Elvehøy, H., Kjøllmoen, B., and Engeset, R. V.: Reanalysis of long-term series of glaciological and geodetic mass balance for 10 Norwegian glaciers, The Cryosphere, 10, 535–552, doi:10.5194/tc-10-535-2016, 2016.

Arendt, A., Bliss, A., Bolch, T., Cogley, J., Gardner, A., Hagen, J.-O., Hock, R., Huss, M., Kaser, G., Kienholz, C., Pfeffer, W., Moholdt, G., Paul, F., Radic, V., Andreassen, L., Bajracharya, S., Barrand, N., Beedle, M., Berthier, E., Bhambri, R., Brown, I., Burgess, E., Burgess, D., Cawkwell, F., Chinn, T., Copland, L., Davies, B., De Angelis, H., Dolgova, E., Earl, L., Filbert, K., Forester, R., Fountain, A., Frey, H., Giffen, B., Glasser, N., Guo, W., Gurney, W., Hagg, W., Hall, D., Haritashya, U., Hartmann, G., Helm, C., Herreid, S., Howat, I., Kapustin, G., Khromova, T., König, M., Kohler, J., Kriegel, D., Kutuzov, S., Lavrentiev, I., LeBris, R., Liu, S., Lund, J., Manley, W., Marti, R., Mayer, C., Miles, E., Li, X., Menounos, B., Mercer, A., Mölg, N., Mool, P., Nosenko, G., Negrete, A., Nuimura, T., Nuth, C., Pettersson, R., Racoviteanu, A., Ranzi, R., Rastner, P., Bau, F., Raup, B., Rich, J., Rott, H., Sakai, A., Schneider, C., Seliverstov, Y., Sharp, M., Sigurdsson, O., Stokes, C., Way, R., Wheate, R., Winsvold, S., Wolken, G., Wyatt, F., and Zheltyhina, N.: Randolph Glacier Inventory – A Dataset of Global Glacier Outlines: Version 5.0, Glims technical report, Global Land Ice Measurements from Space, Digital Media, Boulder, Colorado, USA, 2015.

Aschwanden, A., Aðalgeirsdóttir, G., and Khroulev, C.: Hindcasting to measure ice sheet model sensitivity to initial states, The Cryosphere, 7, 1083–1093, doi:10.5194/tc-7-1083-2013, 2013.

Bahr, D. B., Meier, M. F., and Peckham, S. D.: The physical basis of glacier volume-area scaling, J. Geophys. Res., 102, 20355–20362, 1997.

Bahr, D. B., Pfeffer, W. T., and Kaser, G.: A review of volume-area scaling of glaciers, Rev. Geophys., 53, 95–140, 2015.

Bakke, J., Øivind, L., Nesje, A., Dahl, S. O., and Paasche, Ø.: Utilizing physical sediment variability in glacier-fed lakes for continuous glacier reconstructions during the Holocene, northern Folgefonna, western Norway, Holocene, 15, 161–176, doi:10.1191/0959683605hl797rp, 2005.

Berthier, E., Schiefer, E., Clarke, G. K., Menounos, B., and Rémy, F.: Contribution of Alaskan glaciers to sea-level rise derived from satellite imagery, Nat. Geosci., 3, 92–95, 2010.

Bjune, A. E., Bakke, J., Nesje, A., and Birks, H. J. B.: Holocene mean July temperature and winter precipitation in western Norvay inferred from palynological and glaciological lake-sediment proxies, Holocene, 15, 177–189, doi:10.1191/0959683605hl798rp, 2005.

Blöschl, G., Kirnbauer, R., and Gutknecht, D.: Distributed snowmelt simulations in an alpine catchment: 1. Model evaluation on the basis of snow cover patterns, Water Resour. Res., 27, 3171–3179, doi:10.1029/91WR02250, 1991.

Church, J., Clark, P., Cazenave, A., Gregory, J., Jevrejeva, S., Levermann, A., Merrifield, M., Milne, G., Nerem, R., Nunn, P., Payne, A., Pfeffer, W., Stammer, D., and Unnikrishnan, A.: Sea Level Change, in: chap. Climate Change 2013: The Physical Science Basis, Contribution of Working Group I to the Fifth Assessment Report of the Intergovernmental Panel on Climate Change, Cambridge University Press, Cambridge, UK and New York, NY, USA, 2013.

Clarke, G. K., Jarosch, A. H., Anslow, F. S., Radić, V., and Menounos, B.: Projected deglaciation of western Canada in the twenty-first century, Nat. Geosci., 8, 372–377, doi:10.1038/ngeo2407, 2015.

Cogley, J., Hock, R., Rasmussen, L., Arendt, A., Bauder, A., Braithwaite, R., Jansson, P., Kaser, G., Möller, M., Nicholson, L., and

Zemp, M.: Glossary of glacier mass balance and related terms, IHP-VII technical documents in hydrology No. 86, IACS Contribution No. 2, UNESCO-IHP, Paris, 2011.

Cuffey, K. M. and Paterson, W. S. B.: The physics of glaciers, Acad. Press, Cambridge, Mass., 2010.

Dahl, S. O. and Nesje, A.: Holocene glacier fluctuations at Hardangerjøkulen, central-southern Norway: a high-resolution composite chronology from lacustrine and terrestrial deposits, Holocene, 4, 269–277, doi:10.1177/095968369400400306, 1994.

Dahl, S. O. and Nesje, A.: A new approach to calculating Holocene winter precipitation by combining glacier equilibrium-line altitudes and pine-tree limits: a case study from Hardangerjøkulen, central southern Norway, Holocene, 6, 381–398, doi:10.1177/095968369600600401, 1996.

Davies, B. J., Golledge, N. R., Glasser, N. F., Carrivick, J. L., Ligtenberg, S. R., Barrand, N. E., Van Den Broeke, M. R., Hambrey, M. J., and Smellie, J. L.: Modelled glacier response to centennial temperature and precipitation trends on the Antarctic Peninsula, Nat. Clim. Change, 4, 993–998, 2014.

Elvehøy, H., Kohler, J., Engeset, R., and Andreassen, L.: Jøkullaup fra Demmevatn, NVE Report 17, NVE, Oslo, 1997.

Flowers, G. E., Björnsson, H., Geirsdóttir, Á., Miller, G. H., Black, J. L., and Clarke, G. K.: Holocene climate conditions and glacier variation in central Iceland from physical modelling and empirical evidence, Quaternary Sci. Rev., 27, 797–813, doi:10.1016/j.quascirev.2007.12.004, 2008.

Giesen, R.: The ice cap Hardangerjøkulen in the past, present and future climate, PhD thesis, IMAU, Utrecht University, Utrecht, 2009.

Giesen, R. and Oerlemans, J.: Response of the ice cap Hardangerjøkulen in southern Norway to the 20th and 21st century climates, The Cryosphere, 4, 191–213, doi:10.5194/tc-4-191-2010, 2010.

Gilbert, A., Flowers, G. E., Miller, G. H., Rabus, B. T., Van Wychen, W., Gardner, A. S., and Copland, L.: Sensitivity of Barnes Ice Cap, Baffin Island, Canada, to climate state and internal dynamics, J. Geophys. Res.-Ea. Surf., 121, 1516–1539, doi:10.1002/2016JF003839, 2016.

Glen, J. W.: The creep of polycrystalline ice, P. Roy. Soc. Lond. A, 228, 519–538, doi:10.1098/rspa.1955.0066, 1955.

Goldberg, D. N., Heimbach, P., Joughin, I., and Smith, B.: Committed retreat of Smith, Pope, and Kohler Glaciers over the next 30 years inferred by transient model calibration, The Cryosphere, 9, 2429–2446, doi:10.5194/tc-9-2429-2015, 2015.

Golledge, N. R., Hubbard, A., and Sugden, D. E.: High-resolution numerical simulation of Younger Dryas glaciation in Scotland, Quaternary Sci. Rev., 27, 888–904, doi:10.1016/j.quascirev.2008.01.019, 2008.

Greve, R. and Blatter, H.: Dynamics of ice sheets and glaciers, Springer, Berlin, Heidelberg, 2009.

Grinsted, A.: An estimate of global glacier volume, The Cryosphere, 7, 141–151, doi:10.5194/tc-7-141-2013, 2013.

Guðmundsson, G. H.: Transmission of basal variability to a glacier surface, J. Geophys. Res.-Solid Ea., 108, 2253, doi:10.1029/2002JB002107, 2003.

Guðmundsson, S., Björnsson, H., Jóhannesson, T., Adalgeirsdóttir, G., Pálsson, F., and Sigurðsson, O.: Similarities and differences in the response to climate warming of two ice caps in Iceland, Hydrol. Res., 40, 495–502, doi:10.2166/nh.2009.210, 2009.

Hagen, J. O.: Brefrontprosesser ved Hardangerjøkulen (Glacial terminus processes at Hardangerjøkulen), PhD thesis, Department of Geography, University of Oslo, Oslo, Norway, 1978.

Hallet, B., Hunter, L., and Bogen, J.: Rates of erosion and sediment evacuation by glaciers: A review of field data and their implications, Global Planet. Change, 12, 213–235, doi:10.1016/0921-8181(95)00021-6, 1996.

Hannesdóttir, H., Björnsson, H., Pálsson, F., Aðalgeirsdóttir, G., and Guðmundsson, S.: Changes in the southeast Vatnajökull ice cap, Iceland, between 1890 and 2010, The Cryosphere, 9, 565–585, doi:10.5194/tc-9-565-2015, 2015.

Hansen-Bauer, I., Førland, E., Haddeland, I., Hisdal, H., Mayer, S., Nesje, A., Nilsen, J., Sandven, S., Sandø, A., Sorteberg, A., and Ådlandsvik, B.: Klima i Norge 2100 Kunnskapsgrunnlag for klimatilpasning oppdatert i 2015, NCCS report, NCCS, Oslo, Norway, p. 203, 2015.

Harrison, W., Elsberg, D., Echelmeyer, K., and Krimmel, R.: On the characterization of glacier response by a single time-scale, J. Glaciol., 47, 659–664, doi:10.3189/172756501781831837, 2001.

Hecht, F.: BAMG: Bi-dimensional anisotropic mesh generator, Tech. rep., Inria, St. Ismier, France, 2006.

Hindmarsh, R.: A numerical comparison of approximations to the Stokes equations used in ice sheet and glacier modeling, J. Geophys. Res.-Ea. Surf., 109, F01012, doi:10.1029/2003JF000065, 2004.

Hubbard, A., Sugden, D., Dugmore, A., Norddahl, H., and Pétursson, H. G.: A modelling insight into the Icelandic Last Glacial Maximum ice sheet, Quaternary Sci. Rev., 25, 2283–2296, doi:10.1016/j.quascirev.2006.04.001, 2006.

Huss, M. and Hock, R.: A new model for global glacier change and sea-level rise, Front. Earth Sci., 3, 1–22, doi:10.3389/feart.2015.00054, 2015.

Huss, M., Bauder, A., Funk, M., and Hock, R.: Determination of the seasonal mass balance of four Alpine glaciers since 1865, J. Geophys. Res.-Ea. Surf., 113, F01015, doi:10.1029/2007JF000803, 2008.

Hutter, K.: Theoretical glaciology: material science of ice and the mechanics of glaciers and ice sheets, Reidel, Norwell, Mass., 1983.

Innes, J. L.: Dating exposed rock surfaces in the Arctic by lichenometry: the problem of thallus circularity and its effect on measurement errors, Arctic, 39, 253–259, 1986.

Jacob, T., Wahr, J., Pfeffer, W. T., and Swenson, S.: Recent contributions of glaciers and ice caps to sea level rise, Nature, 482, 514–518, 2012.

Jiskoot, H., Curran, C. J., Tessler, D. L., and Shenton, L. R.: Changes in Clemenceau Icefield and Chaba Group glaciers, Canada, related to hypsometry, tributary detachment, length–slope and area–aspect relations, Ann. Glaciol., 50, 133–143, doi:10.3189/172756410790595796, 2009.

Jouvet, G., Huss, M., Blatter, H., Picasso, M., and Rappaz, J.: Numerical simulation of Rhonegletscher from 1874 to 2100, J. Comput. Phys., 228, 6426–6439, 2009.

Jouvet, G., Huss, M., Funk, M., and Blatter, H.: Modelling the retreat of Grosser Aletschgletscher, Switzerland, in a changing climate, J. Glaciol., 57, 1033–1045, doi:10.3189/002214311798843359, 2011.

Kalela-Brundin, M.: Climatic information from tree-rings of Pinus sylvestris L. and a reconstruction of summer temperatures back to AD 1500 in Femundsmarka, eastern Norway, using partial least squares regression (PLS) analysis, Holocene, 9, 59–77, doi:10.1191/095968399678118795, 1999.

Kirchner, N., Ahlkrona, J., Gowan, E. J., Lötstedt, P., Lea, J. M., Noormets, R., von Sydow, L., Dowdeswell, J. A., and Benham, T.: Shallow ice approximation, second order shallow ice approximation, and full Stokes models: A discussion of their roles in palaeo-ice sheet modelling and development, Quaternary Sci. Rev., 135, 103–114, 2016.

Kjøllmoen, B., Andreassen, L. M., Elvehøy, H., Jackson, M., Giesen, R. H., and Winkler, S.: Glaciological investigations in Norway in 2010, NVE Report No. 3, Norwegian Water Resources and Energy Directorate, Oslo, 1–91, 2011.

Konnestad, H.: Moreneformer i fronten av Midtdalsbreen – en glasiologisk og geomorfologisk undersøkelse av dannelsesprosessene (Moraine formation at the terminus of Midtdalsbreen – a glacial and geomorphological study of their creation), PhD thesis, Department of Geography, University of Oslo, Oslo, Norway, 1996.

Krantz, K.: Volume changes and traditional mass balance on two outlet glaciers at Hardangerjøkulen, Norway, Master's thesis, Masters thesis unpublished, Department of Geography, University of Oslo, Oslo, Norway, 2002.

Kuhn, M., Markl, G., Kaser, G., Nickus, U., Obleitner, F., and Schneider, H.: Fluctuations of climate and mass balance: different responses of two adjacent glaciers, Z. Gletscherk. Glazialgeol., 21, 409–416, 1985.

Larour, E., Seroussi, H., Morlighem, M., and Rignot, E.: Continental scale, high order, high spatial resolution, ice sheet modeling using the Ice Sheet System Model (ISSM), J. Geophys. Res.-Ea. Surf., 117, F01022, doi:10.1029/2011JF002140, 2012.

Laumann, T. and Nesje, A.: Spørteggbreen, western Norway, in the past, present and future: Simulations with a two-dimensional dynamical glacier model, Holocene, 24, 842–852, doi:10.1177/0959683614530446, 2014.

Laumann, T. and Nesje, A.: Volume–area scaling parameterisation of Norwegian ice caps: A comparison of different approaches, Holocene, 27, 164–171, 2017.

Le Meur, E. and Vincent, C.: A two-dimensional shallow ice-flow model of Glacier de Saint-Sorlin, France, J. Glaciol., 49, 527–538, doi:10.3189/172756503781830421, 2003.

Le Meur, E., Gagliardini, O., Zwinger, T., and Ruokolainen, J.: Glacier flow modelling: a comparison of the Shallow Ice Approximation and the full-Stokes solution, Comptes Rendus Physique, 5, 709–722, doi:10.1016/j.crhy.2004.10.001, 2004.

Le Meur, E., Gerbaux, M., Schäfer, M., and Vincent, C.: Disappearance of an Alpine glacier over the 21st Century simulated from modeling its future surface mass balance, Earth Planet. Sc. Lett., 261, 367–374, doi:10.1016/j.epsl.2007.07.022, 2007.

Leysinger-Vieli, G.-M. and Gudmundsson, G.: On estimating length fluctuations of glaciers caused by changes in climatic forcing, J. Geophys. Res., 109, F01007, doi:10.1029/2003JF000027, 2004.

Lüthi, M. P.: Transient response of idealized glaciers to climate variations, J. Glaciol., 55, 918–930, 2009.

MacAyeal, D. R.: A tutorial on the use of control methods in ice-sheet modeling, J. Glaciol., 39, 91–98, 1993.

Melvold, K. and Schuler, T.: Mapping of subglacial topography using GPR for determining subglacial hydraulic conditions, in: chap. 14, Applied Geophysics in periglacial environments, Cambridge University Press, Cambridge, 2008.

Morland, L.: Thermomechanical balances of ice sheet flows, Geophys. Astrophys. Fluid Dynam., 29, 237–266, doi:10.1080/03091928408248191, 1984.

Morlighem, M., Rignot, E., Seroussi, H., Larour, E., Ben Dhia, H., and Aubry, D.: Spatial patterns of basal drag inferred using control methods from a full-Stokes and simpler models for Pine Island Glacier, West Antarctica, Geophys. Res. Lett., 37, L14502, doi:10.1029/2010GL043853, 2010.

Morlighem, M., Rignot, E., Seroussi, H., Larour, E., Ben Dhia, H., and Aubry, D.: A mass conservation approach for mapping glacier ice thickness, Geophys. Res. Lett., 38, L19503, doi:10.1029/2011GL048659, 2011.

Nesje, A.: Latest Pleistocene and Holocene alpine glacier fluctuations in Scandinavia, Quaternary Sci. Rev., 28, 2119–2136, doi:10.1016/j.quascirev.2008.12.016, 2009.

Nesje, A. and Dahl, S. O.: Holocene glacier variations of Blåisen, Hardangerjøkulen, central southern Norway, Quatern. Res., 35, 25–40, doi:10.1016/0033-5894(91)90092-J, 1991.

Nesje, A. and Dahl, S. O.: The Little Ice Age – only temperature?, Holocene, 13, 139–145, doi:10.1191/0959683603hl603fa, 2003.

Nesje, A., Dahl, S. O., Løvlie, R., and Sulebak, J. R.: Holocene glacier activity at the southwestern part of Hardangerjøkulen, central-southern Norway: evidence from lacustrine sediments, Holocene, 4, 377–382, doi:10.1177/095968369400400405, 1994.

Nesje, A., Bakke, J., Dahl, S. O., Lie, Ø., and Matthews, J. A.: Norwegian mountain glaciers in the past, present and future, Global Planet. Change, 60 10–27, 2008a.

Nesje, A., Dahl, S., Thun, T., and Nordli, Ø.: The Little Ice Age glacial expansion in western Scandinavia: summer temperature or winter precipitation?, Clim. Dynam., 30, 789–801, doi:10.1007/s00382-007-0324-z, 2008b.

Nordli, P., Lie, Ø., Nesje, A., and Dahl, S. O.: Spring-summer temperature reconstruction in western Norway 1734–2003: a data-synthesis approach, Int. J. Climatol., 23, 1821–1841, doi:10.1002/joc.980, 2003.

Oerlemans, J.: A flowline model for Nigardsbreen, Norway: projection of future glacier length based on dynamic calibration with the historic record, J. Glaciol., 24, 382–389, 1997a.

Oerlemans, J.: Climate sensitivity of Franz Josef Glacier, New Zealand, as revealed by numerical modeling, Arctic Alp. Res., 29, 233–239, doi:10.2307/1552052, 1997b.

Oerlemans, J.: Glaciers and climate change, Balkema, Lisse, 2001.

Oerlemans, J.: Extracting a climate signal from 169 glacier records, Science, 308, 675–677, 2005.

Østen, K.: Radio-ekko undersøkelser på Midtdalsbreen, Sør-Norge, MS thesis unpublished, Department of Geography, University of Oslo, Oslo, Norway, 1998.

Paterson, W.: The physics of glaciers, Pergamon, New York, 1994.

Pfeffer, W. T., Arendt, A. A., Bliss, A., Bolch, T., Cogley, J. G., Gardner, A. S., Hagen, J.-O., Hock, R., Kaser, G., Kienholz, C., Miles, E. S., Moholdt, G., Mölg, N., Paul, F., Radić, V., Rastner, P., Raup, B. H., Rich, J., and Sharp, M. J.: The Randolph Glacier Inventory: a globally complete inventory of glaciers, J. Glaciol., 60, 537–552, 2014.

Radić, V. and Hock, R.: Regional and global volumes of glaciers derived from statistical upscaling of glacier inventory data, J. Geo-

phys. Res.-Ea. Surf., 115, F01010, doi:10.1029/2009JF001373, 2010.

Raper, S. C. B. and Braithwaite, R. J.: Glacier volume response time and its links to climate and topography based on a conceptual model of glacier hypsometry, The Cryosphere, 3, 183–194, doi:10.5194/tc-3-183-2009, 2009.

Rasmussen, L., Andreassen, L., Baumann, S., and Conway, H.: 'Little Ice Age' precipitation in Jotunheimen, southern Norway, Holocene, 20, 1039–1045, doi:10.1177/0959683610369510, 2010.

Reinardy, B. T., Leighton, I., and Marx, P. J.: Glacier thermal regime linked to processes of annual moraine formation at Midtdalsbreen, southern Norway, Boreas, 42, 896–911, doi:10.1111/bor.12008, 2013.

Rignot, E., Rivera, A., and Casassa, G.: Contribution of the Patagonia Icefields of South America to sea level rise, Science, 302, 434–437, 2003.

Rivera, A. and Casassa, G.: Volume changes on Pio XI glacier, Patagonia: 1975–1995, Global Planet. Change, 22, 233–244, 1999.

Roe, G. H.: What do glaciers tell us about climate variability and climate change?, J. Glaciol., 57, 567–578, 2011.

Rutt, I. C., Hagdorn, M., Hulton, N., and Payne, A.: The Glimmer community ice sheet model, J. Geophys. Res.-Ea. Surf., 114, F02004, doi:10.1029/2008JF001015, 2009.

Sellevold, M. and Kloster, K.: Seismic measurements on the glacier Hardangerjøkulen, Western Norway, Norsk Polarinslitutt Arbok 1964, 87–91, 1964.

Seppä, H., Hammarlund, D., and Antonsson, K.: Low-frequency and high-frequency changes in temperature and effective humidity during the Holocene in south-central Sweden: implications for atmospheric and oceanic forcings of climate, Clim. Dynam., 25, 285–297, doi:10.1007/s00382-005-0024-5, 2005.

Shepherd, A., Ivins, E. R., Geruo, A., et al.: A reconciled estimate of ice-sheet mass balance, Science, 338, 1183–1189, doi:10.1126/science.1228102, 2012.

Sissons, J.: The Loch Lomond Stadial in the British Isles, Nature, 280, 199–203, doi:10.1038/280199a0, 1979.

Sollid, J. L. and Bjørkenes, A.: Glacial geology of Midtdalsbreen – Genesis of moraines at Midtdalsbreen, Geomorphological map 1 : 2500, Norsk Geografisk Tidsskrift, 32, 1978.

Sutherland, D. G.: Modern glacier characteristics as a basis for inferring former climates with particular reference to the Loch Lomond Stadial, Quaternary Sci. Rev., 3, 291–309, doi:10.1016/0277-3791(84)90010-6, 1984.

Trüssel, B. L., Truffer, M., Hock, R., Motyka, R. J., Huss, M., and Zhang, J.: Runaway thinning of the low-elevation Yakutat Glacier, Alaska, and its sensitivity to climate change, J. Glaciol., 61, 65–75, 2015.

Uvo, C. B.: Analysis and regionalization of northern European winter precipitation based on its relationship with the North Atlantic Oscillation, Int. J. Climatol., 23, 1185–1194, doi:10.1002/joc.930, 2003.

Vaksdal, M.: Sammenligning av to dreneringssytemer i Midtdalsbreen, Hardangerjøkulen, Sør-Norge (Comparison of two drainage systems at Midtdalsbreen, Hardangerjøkulen, South Norway), MS thesis unpublished, Department of Geography, University of Oslo, Oslo, Norway, 2001.

Van Den Berg, J., van de Wal, R., and Oerlemans, H.: A mass balance model for the Eurasian Ice Sheet for the last 120,000 years, Global Planet. Change, 61, 194–208, doi:10.1016/j.gloplacha.2007.08.015, 2008.

Vasskog, K., Paasche, Ø., Nesje, A., Boyle, J. F., and Birks, H. J. B.: A new approach for reconstructing glacier variability based on lake sediments recording input from more than one glacier, Quatern. Res., 77, 192–204, doi:10.1016/j.yqres.2011.10.001, 2012.

Vaughan, D., Comiso, J., Allison, I., Carrasco, J., Kaser, G., Kwok, R., Mote, P., Murray, T., Paul, F., Ren, J., Rignot, E., Solomina, O., Steffen, K., and Zhang, T.: Observations: Cryosphere, in: Climate Change 2013: The Physical Science Basis, Contribution of Working Group I to the Fifth Assessment Report of the Intergovernmental Panel on Climate Change, edited by: Stocker, T. F., Qin, D., Plattner, G.-K., Tignor, M., Allen, S. K., Boschung, J., Nauels, A., Xia, Y., Bex, V., and Midgley, P. M., Cambridge University Press, Cambridge, UK and New York, NY, USA, 2013.

Velle, G., Brooks, S. J., Birks, H., and Willassen, E.: Chironomids as a tool for inferring Holocene climate: an assessment based on six sites in southern Scandinavia, Quaternary Sci. Rev., 24, 1429–1462, doi:10.1016/j.quascirev.2004.10.010, 2005a.

Velle, G., Larsen, J., Eide, W., Peglar, S. M., and Birks, H. J. B.: Holocene environmental history and climate of Råtåsjøen, a low-alpine lake in south-central Norway, J. Paleolimnol., 33, 129–153, doi:10.1007/s10933-004-2689-x, 2005b.

Weertman, J.: The theory of glacier sliding, J. Glaciol., 5, 287–303, doi:10.1007/978-1-349-15480-7_14, 1964.

Willis, I. C.: Intra-annual variations in glacier motion: a review, Prog. Phys. Geogr., 19, 61–106, doi:10.1177/030913339501900104, 1995.

Willis, I. C., Fitzsimmons, C. D., Melvold, K., Andreassen, L. M., and Giesen, R. H.: Structure, morphology and water flux of a subglacial drainage system, Midtdalsbreen, Norway, Hydrol. Process., 26, 3810–3829, oi10.1002/hyp.8431, 2012.

Winkelmann, R., Martin, M., Haseloff, M., Albrecht, T., Bueler, E., Khroulev, C., and Levermann, A.: The Potsdam parallel ice sheet model (PISM-PIK) – Part 1: Model description, The Cryosphere, 5, 715–726, doi:10.5194/tc-5-715-2011, 2011.

Woo, M.-K. and Fitzharris, B.: Reconstruction of mass balance variations for Franz Josef Glacier, New Zealand, 1913 to 1989, Arct. Alp. Res., 24, 281–290, 1992.

Zekollari, H. and Huybrechts, P.: On the climate–geometry imbalance, response time and volume–area scaling of an alpine glacier: insights from a 3-D flow model applied to Vadret da Morteratsch, Switzerland, Ann. Glaciol., 56, 51–62, doi:10.3189/2015AoG70A921, 2015.

Zekollari, H., Huybrechts, P., Furst, J. J., Rybak, O., and Eisen, O.: Calibration of a higher-order 3-D ice-flow model of the Morteratsch glacier complex, Engadin, Switzerland, Ann. Glaciol., 54, 343–351, doi:10.3189/2013AoG63A434, 2013.

Zekollari, H., Furst, J. J., and Huybrechts, P.: Modelling the evolution of Vadret da Morteratsch, Switzerland, since the Little Ice Age and into the future, J. Glaciol., 60, 1155–1168, doi:10.3189/2014JoG14J053, 2014.

Ziemen, F. A., Hock, R., Aschwanden, A., Khroulev, C., Kienholz, C., Melkonian, A., and Zhang, J.: Modeling the evolution of the Juneau Icefield between 1971 and 2100 using the Parallel Ice Sheet Model (PISM), J. Glaciol., 62, 199–214, 2016.

Appendix B

Popular science contributions

B.1 Outreach activities

Åkesson, H., Steiger, N. Breer, klima og klimagassutslipp - hva er det som skjer? Glacier and climate education for high school students, 24th Feb, 2017, Finse, Norway

Åkesson, H. Breer og klima: hva er det som skjer? - og hvordan vi vet det. Glacier and climate education for high school students, 23rd Mar, 2015, Finse, Norway

Jensen, M.F. Åkesson, H. Hva gjør en klimaforsker?. Møt en klimaforsker, 19th Feb, 2015, VilVite Science Centre, Bergen, Norway

Åkesson, H. et al. Representing the Bjerknes Centre for Climate Research at Forskningsdagene (Research Days), Sep 18th, 2015, public science fair, Bergen, Norway

B.2 Media presence and interviews

Åkesson, H. Breitbart misrepresents research from 58 scientific papers to falsely claim that they disprove human-caused global warming. 7th Jun, 2017, Climate-feedback.org.

Åkesson, H. DELINGPOLE: 'Global Warming' Is a Myth, Say 58 Scientific Papers in 2017. 6th Jun, 2017, Breitbart News

Åkesson, H. Kan smelte bort. 2nd May, 2017, Vi Menn (paper)

Åkesson, H. Hardangerjøkulen: The Real-Life Hoth is Disappearing. 9 Mar, 2017, GlacierHub.org

Åkesson, H. Low snow cover threatens Swiss ski resorts. 27th Feb, 2017, Breaking Property News

Åkesson, H. Low snow cover threatens Swiss ski resorts. 27th Feb, 2017, Climate News Network

Åkesson, H, Engeset, R.V. 300 meter tykk isbre kan være borte om 50 År. 22nd Feb, 2017, Kraftnytt.no.

Åkesson, H. Nisancioglu, K.H.. Hardangerjøkulen kan smelte vekk i løpet av dette Århundret. 16th Feb, 2017, energiogklima.no.

Åkesson, H. Norwegian ice cap 'exceptionally sensitive' to climate change. 14th Feb, 2017, ScienceDaily.

Åkesson, H. Norwegian ice cap 'exceptionally sensitive' to climate change. 14th Feb, 2017, Phys.org.

Åkesson, H., Engeset, R.V.. 300 meter tykk isbre kan være borte om 50 år. 13th Feb, 2017 NRK.no.

Åkesson, H. Denne isbreen kan være borte om 50 År. 13th Feb, 2017, NRK Dagsrevyen (Norwegian public TV).

Åkesson, H., Engeset, R.V. Hardangerjøkulen kan forsvinne. 13th Feb, 2017, NRK Vestlandsrevyen (Norwegian public TV).

Åkesson, H.,Engeset, R.V. Isbreer kan forsvinne dette århundret. 13th Feb, 2017, NRK P2 Nyhetsmorgen (Norwegian public radio).

Åkesson, H., Engeset, Rune Verpe. Isbreer kan forsvinne dette århundret. 13th Feb, 2017, NRK Hordaland (Norwegian public radio).

Åkesson, H., Engeset, R.V. Nesten alle de norske isbreene kan smelte helt bort innen 100 år. 13th Feb, 2017, NRK P3 Nyheter

Åkesson, H., Om 100 år kan de norske isbreene ha smeltet. 13th Feb, 2017, ABC Nyheter.

Paasche, Ø, Åkesson, H. Nordic support for American climate science. 3rd Feb, 2017, UArctic.org

Åkesson, H., Paasche, Ø. Lysbakken: - Trump angriper sannheten og vitenskapen. 2nd Feb, 2017, Bergens Tidende (Norwegian newspaper).

Åkesson, H., Paasche, Ø. Sanker støtte for amerikansk forskning. 1st Feb, 2017, energiogklima.no.

Åkesson, H. Paasche, Ø. Har startet støttekampanje for amerikansk forskning. 1st Feb, 2017, På Høyden (University of Bergen online newspaper).

Bibliography

Amundson, J. M., M. Fahnestock, M. Truffer, J. Brown, M. P. Lüthi, and R. J. Motyka (2010), Ice mélange dynamics and implications for terminus stability, Jakobshavn Isbræ, Greenland, *Journal of Geophysical Research: Earth Surface (2003–2012)*, *115*(F1). 1.3.3

Andersen, B. G. (1981), *Late Weichselian ice sheets in Eurasia and Greenland*, 3–66 pp., Wiley: New York. 1.4.1

Andreassen, L., S. Winsvold, F. Paul, and J. Hausberg (2012), Inventory of Norwegian glaciers, *NVE, Oslo*. 1.4.2

Andreassen, L. M., H. Elvehøy, B. Kjøllmoen, R. V. Engeset, and N. Haakensen (2005), Glacier mass-balance and length variation in Norway, *Annals of Glaciology*, *42*(1), 317–325. 1.4.2

Åström, J., D. Vallot, M. Schäfer, E. Welty, S. O'Neel, T. Bartholomaus, Y. Liu, T. Riikilä, T. Zwinger, J. Timonen, et al. (2014), Termini of calving glaciers as self-organized critical systems, *Nature Geoscience*. 4

Bakke, J., L. Øivind, A. Nesje, S. O. Dahl, and Ø. Paasche (2005), Utilizing physical sediment variability in glacier-fed lakes for continuous glacier reconstructions during the Holocene, northern Folgefonna, western Norway, *The Holocene*, *15*(2), 161–176, doi:10.1191/0959683605hl797rp. 1.4.2

Bamber, J., M. den Broeke, J. Ettema, J. Lenaerts, and E. Rignot (2012), Recent large increases in freshwater fluxes from Greenland into the North Atlantic, *Geophysical Research Letters*, *39*(19). 1.1

Bartholomew, I., P. Nienow, D. Mair, A. Hubbard, M. A. King, and A. Sole (2010), Seasonal evolution of subglacial drainage and acceleration in a Greenland outlet glacier, *Nature Geoscience*, *3*(6), 408–411. 1.3.1

Bassis, J. N., and C. C. Walker (2012), Upper and lower limits on the stability of calving glaciers from the yield strength envelope of ice, *Proceedings of the Royal Society of London A: Mathematical, Physical and Engineering Sciences*, *468*(2140), 913–931, doi:10.1098/rspa.2011.0422. 4

Bassis, J. N., S. V. Petersen, and L. Mac Cathles (2017), Heinrich events triggered by ocean forcing and modulated by isostatic adjustment, *Nature*, *542*(7641), 332–334. 1.3.4

Benn, D. I., C. R. Warren, and R. H. Mottram (2007), Calving processes and the dynamics of calving glaciers, *Earth-Science Reviews*, *82*(3), 143–179. 1.3, 1.3.1, 2

Benn, D. I., J. Åström, T. Zwinger, J. Todd, F. M. Nick, S. Cook, N. R. Hulton, and A. Luckman (2017), Melt-undercutting and buoyancy-driven calving from tidewater glaciers: new insights from discrete element and continuum model simulations, *Journal of Glaciology*, *240*(63), 691–702, doi:10.1017/jog.2017.41. 1.3.2, 4

Bergstrøm, B. (1995), Stratigraphical evidence of a considerable Younger Dryas glacier advance in southeastern Norway, *Nor. Geol. Tidsskr*, *75*, 127–136. 1.4.1

Bersch, M., I. Yashayaev, and K. P. Koltermann (2007), Recent changes of the thermohaline circulation in the subpolar North Atlantic, *Ocean Dynamics*, *57*(3), 223–235. 1.3.1

Bjune, A. E., J. Bakke, A. Nesje, and H. J. B. Birks (2005), Holocene mean July temperature and winter precipitation in western Norvay inferred from palynological and glaciological lake-sediment proxies, *The Holocene*, *15*(2), 177–189. 1.4.2

Bliss, A., R. Hock, and V. Radic (2014), Global response of glacier runoff to twenty-first century climate change, *Journal of Geophysical Research: Earth Surface*pp.n/a–n/a, doi:10.1002/2013JF002931. 1.1

Box, J. E., L. Yang, D. H. Bromwich, and L.-S. Bai (2009), Greenland Ice Sheet Surface Air Temperature Variability: 1840-2007*, *Journal of Climate*, *22*(14), 4029–4049. 1.3.1

Carr, J., C. Stokes, and A. Vieli (2014), Recent retreat of major outlet glaciers on Novaya Zemlya, Russian Arctic, influenced by fjord geometry and sea-ice conditions, *Journal of Glaciology*, *60*(219), 155–170. 1.3.4

Carr, J. R., C. R. Stokes, and A. Vieli (2013), Recent progress in understanding marine-terminating Arctic outlet glacier response to climatic and oceanic forcing: Twenty years of rapid change, *Progress in Physical Geography*, *37*(4), 436–467. 1.3.1, 1.3.3, 1.3.4

Church, J., P. Clark, A. Cazenave, J. Gregory, S. Jevrejeva, A. Levermann, M. Merrifield, G. Milne, R. Nerem, P. Nunn, A. Payne, W. Pfeffer, D. Stammer, and A. Unnikrishnan (2013), *Sea Level Change*chap.Climate Change 2013: The Physical Science Basis. Contribution of Working Group I to the Fifth Assessment Report of the Intergovernmental Panel on Climate Change, Cambridge University Press, Cambridge, United Kingdom and New York, NY, USA. 1.1

Cogley, J., R. Hock, L. Rasmussen, A. Arendt, A. Bauder, R. Braithwaite, P. Jansson, G. Kaser, M. Möller, L. Nicholson, et al. (2011), Glossary of glacier mass balance and related terms, IHP-VII technical documents in hydrology No. 86, IACS Contribution No. 2. 1.2.1

Cook, S., I. Rutt, T. Murray, A. Luckman, T. Zwinger, N. Selmes, A. Goldsack, and T. James (2014), Modelling environmental influences on calving at Helheim Glacier in eastern Greenland, *The Cryosphere*, *8*(3), 827–841. 1.3.2

Cook, S. J., and D. A. Swift (2012), Subglacial basins: Their origin and importance in glacial systems and landscapes, *Earth-Science Reviews*, *115*(4), 332–372. 1.4

Cuffey, K. M., and W. S. B. Paterson (2010), *The physics of glaciers*, Elsevier. 1.2.2, 1.2.2, 1.2.2

Dahl, S. O., and A. Nesje (1994), Holocene glacier fluctuations at Hardangerjøkulen, central-southern Norway: a high-resolution composite chronology from lacustrine and terrestrial deposits, *The Holocene*, *4*(3), 269–277, doi:10.1177/095968369400400306. 1.4.2

Dahl, S. O., and A. Nesje (1996), A new approach to calculating Holocene winter precipitation by combining glacier equilibrium-line altitudes and pine-tree limits: a case study from Hardangerjøkulen, central southern Norway, *The Holocene*, *6*(4), 381–398, doi:10.1177/095968369600600401. 1.4.2

Davies, D., R. Bingham, A. Graham, M. Spagnolo, P. Dutrieux, D. Vaughan, A. Jenkins, and F. Nitsche (2017), High-resolution sub-ice-shelf seafloor records of 20th-century ungrounding and retreat of Pine Island Glacier, West Antarctica, *Journal of Geophysical Research: Earth Surface*. 4

Dokken, T., C. Andersson, and B. Risebrobakken (2015), Relative abundance of planktic foraminifera and calculated SSTs and SST anomaly (11.1-25.5 ka BP) in sediment core MD95-2010, doi:10.1594/PANGAEA.841922. 1.4.1

Dokken, T. M., K. H. Nisancioglu, C. Li, D. S. Battisti, and C. Kissel (2013), Dansgaard-Oeschger cycles: Interactions between ocean and sea ice intrinsic to the Nordic seas, *Paleoceanography*, *28*(3), 491–502. 1.1

Eldevik, T., B. Risebrobakken, A. E. Bjune, C. Andersson, H. J. B. Birks, T. M. Dokken, H. Drange, M. S. Glessmer, C. Li, J. E. Ø. Nilsen, et al. (2014), A brief history of climate–the northern seas from the Last Glacial Maximum to global warming, *Quaternary Science Reviews*, *106*, 225–246. 1.4.1

Enderlin, E., I. Howat, and A. Vieli (2013), High sensitivity of tidewater outlet glacier dynamics to shape, *The Cryosphere*, *7*(3), 1007–1015. 1.3.4

Falkner, K. K., H. Melling, A. M. Münchow, J. E. Box, T. Wohlleben, H. L. Johnson, P. Gudmandsen, R. Samelson, L. Copland, K. Steffen, et al. (2011), Context for the recent massive Petermann Glacier calving event, *Eos, Transactions American Geophysical Union*, *92*(14), 117–118. 1.3, 1.3.4

Fettweis, X., M. Tedesco, M. Broeke, and J. Ettema (2011), Melting trends over the Greenland ice sheet (1958–2009) from spaceborne microwave data and regional climate models, *The Cryosphere*, *5*(2), 359–375. 1.3.1

Fretwell, P., H. D. Pritchard, D. G. Vaughan, J. Bamber, N. Barrand, R. Bell, C. Bianchi, R. Bingham, D. Blankenship, G. Casassa, et al. (2013), Bedmap2: improved ice bed, surface and thickness datasets for Antarctica, *The Cryosphere*, *7*(1). 1.3.4

Goldberg, D., D. M. Holland, and C. Schoof (2009), Grounding line movement and ice shelf buttressing in marine ice sheets, *Journal of Geophysical Research: Earth Surface*, *114*(F4), n/a–n/a, doi:10.1029/2008JF001227, f04026. 1.3.4

Goldberg, D., P. Heimbach, I. Joughin, and B. Smith (2015), Committed retreat of Smith, Pope, and Kohler Glaciers over the next 30 years inferred by transient model calibration, *The Cryosphere*, *9*(6), 2429–2446. 1.3.4

Gomez, N., J. X. Mitrovica, P. Huybers, and P. U. Clark (2010), Sea level as a stabilizing factor for marine-ice-sheet grounding lines, *Nature Geoscience*, *3*(12), 850. 1.3.4

Gudmundsson, G. (2013), Ice-shelf buttressing and the stability of marine ice sheets, *The Cryosphere*, *7*(2), 647. 1.3.4

Gudmundsson, G. H., J. Krug, G. Durand, L. Favier, and O. Gagliardini (2012), The stability of grounding lines on retrograde slopes, *The Cryosphere*, *6*(6), 1497–1505, doi:10.5194/tc-6-1497-2012. 1.3.4

Gump, D. J., J. P. Briner, J. Mangerud, and J. I. Svendsen (2017), Deglaciation of Boknafjorden, south-western Norway, *Journal of Quaternary Science*, *32*(1), 80–90. 1.4.1

Hamborg, M., and J. Mangerud (1981), En rekonstruksjon av isbevegelser under siste istid i Samnanger og Kvam, Hordaland, Vest-Norge, *Norges geologiske undersøkelse*, *369*, 77–98. 1.4.1

Hanna, E., J. M. Jones, J. Cappelen, S. H. Mernild, L. Wood, K. Steffen, and P. Huybrechts (2013), The influence of North Atlantic atmospheric and oceanic forcing effects on 1900–2010 Greenland summer climate and ice melt/runoff, *International Journal of Climatology*, *33*(4), 862–880. 1.3.1

Harrison, W., D. Elsberg, K. Echelmeyer, and R. Krimmel (2001), On the characterization of glacier response by a single time-scale, *Journal of Glaciology*, *47*(159), 659–664. 1.2.3

Hecht, F. (2006), BAMG: Bi-dimensional anisotropic mesh generator, *Tech. rep.*, Inria, St. Ismier, France. 2

Higgins, A. K. (1991), North Greenland glacier velocities and calf ice production, *Polarforschung*, *60*(1), 1–23. 1.3.3

Hogg, A. E., and G. H. Gudmundsson (2017), Impacts of the Larsen-C Ice Shelf calving event, *Nature Climate Change*, *7*(8), 540–542. 1.3.4

Holland, D. M., R. H. Thomas, B. De Young, M. H. Ribergaard, and B. Lyberth (2008), Acceleration of Jakobshavn Isbrae triggered by warm subsurface ocean waters, *Nature Geoscience*, *1*(10), 659–664. 1.3.1, 1.3.2

Howat, I. M., I. Joughin, and T. A. Scambos (2007), Rapid changes in ice discharge from Greenland outlet glaciers, *Science*, *315*(5818), 1559–1561. 1.3, 1.3.1

Howat, I. M., I. Joughin, M. Fahnestock, B. E. Smith, and T. A. Scambos (2008), Synchronous retreat and acceleration of southeast Greenland outlet glaciers 2000–06: Ice dynamics and coupling to climate, *Journal of Glaciology*, *54*(187), 646–660. 1.3.1

Howat, I. M., J. E. Box, Y. Ahn, A. Herrington, and E. M. McFadden (2010), Seasonal variability in the dynamics of marine-terminating outlet glaciers in Greenland, *Journal of Glaciology*, *56*(198), 601–613. 1.3.3

Hughes, A. L., R. Gyllencreutz, Ø. S. Lohne, J. Mangerud, and J. I. Svendsen (2016), The last Eurasian ice sheets–a chronological database and time-slice reconstruction, DATED-1, *Boreas*, *45*(1), 1–45. 1.3.4, 1.4.1, 1.6, 1.4.2

Hughes, N. E., J. P. Wilkinson, and P. Wadhams (2011), Multi-satellite sensor analysis of fast-ice development in the norske øer ice barrier, northeast greenland, *Annals of Glaciology*, *52*(57), 151–160. 1.3.3

Hughes, T. (1986), The Jakobshavn Effect, *Geophysical Research Letters*, *13*, 46–48. 1.3.4

Jackson, R. H., F. Straneo, and D. A. Sutherland (2014), Externally forced fluctuations in ocean temperature at Greenland glaciers in non-summer months, *Nature Geoscience*, *7*(7), 503. 1.3.2

Jakobsson, M., J. B. Anderson, F. O. Nitsche, J. A. Dowdeswell, R. Gyllencreutz, N. Kirchner, R. Mohammad, M. O'Regan, R. B. Alley, S. Anandakrishnan, et al. (2011), Geological record of ice shelf break-up and grounding line retreat, Pine Island Bay, West Antarctica, *Geology*, *39*(7), 691–694. 4

Jamieson, S. S., A. Vieli, S. J. Livingstone, C. Ó. Cofaigh, C. Stokes, C.-D. Hillenbrand, and J. A. Dowdeswell (2012), Ice-stream stability on a reverse bed slope, *Nature Geoscience*, *5*(11), 799–802. 1.3.4

Jenkins, A. (2011), Convection-driven melting near the grounding lines of ice shelves and tidewater glaciers, *Journal of Physical Oceanography*, *41*(12), 2279–2294. 1.3.2

Johannesson, T., C. Raymond, and E. Waddington (1989), A simple method for determining the response time of glaciers, in *Glacier fluctuations and climatic change*pp.343–352, Springer. 1.2.3

Johnsen, I. (2017), Strandforskyvning på Bokn og deglasiasjonen av Boknafjorden, Rogaland [unpublished], Master's thesis, University of Bergen. 1.4.1

Joughin, I., I. Howat, R. B. Alley, G. Ekstrom, M. Fahnestock, T. Moon, M. Nettles, M. Truffer, and V. C. Tsai (2008), Ice-front variation and tidewater behavior on Helheim and Kangerdlugssuaq Glaciers, Greenland, *Journal of Geophysical Research: Earth Surface (2003–2012)*, *113*(F1). 1.3.4

Joughin, I., B. E. Smith, I. M. Howat, D. Floricioiu, R. B. Alley, M. Truffer, and M. Fahnestock (2012), Seasonal to decadal scale variations in the surface velocity of Jakobshavn Isbrae, Greenland: Observation and model-based analysis, *Journal of Geophysical Research: Earth Surface (2003–2012)*, *117*(F2). 1.3.2

Kalela-Brundin, M. (1999), Climatic information from tree-rings of Pinus sylvestris L. and a reconstruction of summer temperatures back to AD 1500 in Femundsmarka, eastern Norway, using partial least squares regression (PLS) analysis, *The Holocene*, *9*(1), 59–77, doi:10.1191/095968399678118795. 1.4.2

Kessler, M. A., R. S. Anderson, and J. P. Briner (2008), Fjord insertion into continental margins driven by topographic steering of ice, *Nature Geoscience*, *1*(6), 365. 1.4

Khan, S. A., J. Wahr, M. Bevis, I. Velicogna, and E. Kendrick (2010), Spread of ice mass loss into northwest Greenland observed by GRACE and GPS, *Geophysical Research Letters*, *37*(6). 1.3

Khan, S. A., K. H. Kjær, M. Bevis, J. L. Bamber, J. Wahr, K. K. Kjeldsen, A. A. Bjørk, N. J. Korsgaard, L. A. Stearns, M. R. van den Broeke, L. Liu, N. K. Larsen, and I. S. Muresan (2014), Sustained mass loss of the northeast Greenland ice sheet triggered by regional warming, *Nature Climate Change*, *4*(4), 292. 1.3

Kimura, S., P. R. Holland, A. Jenkins, and M. Piggott (2014), The effect of meltwater plumes on the melting of a vertical glacier face, *Journal of Physical Oceanography*, *44*(12), 3099–3117. 1.3.2

Kjøllmoen, B., L. M. Andreassen, H. Elvehøy, M. Jackson, R. H. Giesen, and S. Winkler (2011), Glaciological investigations in Norway in 2010, NVE Report No 3, *Norwegian Water Resources and Energy Directorate, Oslo*pp.1–91. 1.4.2

Larour, E., H. Seroussi, M. Morlighem, and E. Rignot (2012), Continental scale, high order, high spatial resolution, ice sheet modeling using the Ice Sheet System Model (ISSM), *Journal of Geophysical Research: Earth Surface (2003–2012)*, *117*(F1), doi:0.1029/2011JF002140. 2

Leclercq, P. W., J. Oerlemans, H. J. Basagic, I. Bushueva, A. Cook, and R. Le Bris (2014), A data set of worldwide glacier length fluctuations, *The Cryosphere*, *8*(2), 659–672. 1.2.3

Liakka, J., J. Nilsson, and M. Löfverström (2012), Interactions between stationary waves and ice sheets: linear versus nonlinear atmospheric response, *Climate dynamics*, *38*(5-6), 1249–1262. 1.1

Löfverström, M., R. Caballero, J. Nilsson, and J. Kleman (2014), Evolution of the large-scale atmospheric circulation in response to changing ice sheets over the last glacial cycle, *Climate of the Past*, *10*(4), 1453–1471. 1.1

Lohne, Ø. S., S. Bondevik, J. Mangerud, and J. I. Svendsen (2007), Sea-level fluctuations imply that the Younger Dryas ice-sheet expansion in western Norway commenced during the Allerød, *Quaternary Science Reviews*, *26*(17), 2128–2151. 1.4.1

Luckman, A., and T. Murray (2005), Seasonal variation in velocity before retreat of Jakobshavn Isbræ, Greenland, *Geophysical Research Letters*, *32*(8). 1.3

Luckman, A., T. Murray, R. De Lange, and E. Hanna (2006), Rapid and synchronous ice-dynamic changes in East Greenland, *Geophysical Research Letters*, *33*(3). 1.3

MacAyeal, D. R. (1993), A tutorial on the use of control methods in ice-sheet modeling, *J. Glaciol*, *39*(131), 91–98. 1.2.2

MacAyeal, D. R., J. Freed-Brown, W. W. Zhang, and J. M. Amundson (2012), The influence of ice melange on fjord seiches, *Annals of Glaciology*, *53*(60), 45–49. 1.3.3

Mangerud, J. (1977), Late Weichselian marine sediments containing shells, foraminifera, and pollen, at Ågotnes, western Norway, *Norsk Geologisk Tidsskrift*, *57*(1977), 23–54. 1.4.1

Mangerud, J., R. Gyllencreutz, Ö. Lohne, and J. I. Svendsen (2011), Glacial history of Norway, *Dev. Quat. Sci.*, (15), 279–298. 1.4.1

Marzeion, B., J. G. Cogley, K. Richter, and D. Parkes (2014), Attribution of global glacier mass loss to anthropogenic and natural causes, *Science*, *345*(6199), 919–921. 1.2.3

McFadden, E. M., I. M. Howat, I. Joughin, B. E. Smith, and Y. Ahn (2011), Changes in the dynamics of marine terminating outlet glaciers in west Greenland (2000–2009), *Journal of Geophysical Research: Earth Surface (2003–2012)*, *116*(F2). 1.3.1

Mengel, M., A. Levermann, K. Frieler, A. Robinson, B. Marzeion, and R. Winkelmann (2016), Future sea level rise constrained by observations and long-term commitment, *Proceedings of the National Academy of Sciences*, *113*(10), 2597–2602. 1.1

Mercer, J. (1961), The response of fjord glaciers to changes in the firn limit, *Journal of Glaciology*, *3*(29), 850–858. 1.3.4

Mercer, J. H. (1978), West Antarctic ice sheet and CO 2 greenhouse effect- A threat of disaster, *Nature*, *271*(5643), 321–325. 1.3.4

Millan, R., E. Rignot, V. Bernier, M. Morlighem, and P. Dutrieux (2017), Bathymetry of the Amundsen Sea Embayment sector of West Antarctica from Operation IceBridge gravity and other data, *Geophysical Research Letters*, *44*(3), 1360–1368. 1.3.4

Moon, T., I. Joughin, B. Smith, and I. Howat (2012), 21st-century evolution of Greenland outlet glacier velocities, *Science*, *336*(6081), 576–578. 1.3.1

Morlighem, M., E. Rignot, H. Seroussi, E. Larour, H. Ben Dhia, and D. Aubry (2010), Spatial patterns of basal drag inferred using control methods from a full-Stokes and simpler models for Pine Island Glacier, West Antarctica, *Geophysical Research Letters*, *37*(14), doi:10.1029/2010GL043853. 1.2.2

Morlighem, M., E. Rignot, J. Mouginot, H. Seroussi, and E. Larour (2014), Deeply incised submarine glacial valleys beneath the Greenland ice sheet, *Nature Geoscience*. 1.3.4

Mouginot, J., E. Rignot, B. Scheuchl, I. Fenty, A. Khazendar, M. Morlighem, A. Buzzi, and J. Paden (2015), Fast retreat of Zachariæ Isstrøm, northeast Greenland, *Science*, *350*(6266), 1357–1361. 1.3, 1.3.4

Nesje, A. (2009), Latest Pleistocene and Holocene alpine glacier fluctuations in Scandinavia, *Quaternary Science Reviews*, *28*(21), 2119–2136, doi:10.1016/j.quascirev.2008.12.016. 1.4.2

Nesje, A., and S. O. Dahl (2003), The Little Ice Age - only temperature?, *The Holocene*, *13*(1), 139–145, doi:10.1191/0959683603hl603fa. 1.4.2

Nesje, A., and J. A. Matthews (2012), The briksdalsbre event: A winter precipitation-induced decadal-scale glacial advance in southern norway in the ad 1990s and its implications, *The Holocene*, *22*(2), 249–261. 1.2.3

Nesje, A., S. O. Dahl, R. Løvlie, and J. R. Sulebak (1994), Holocene glacier activity at the southwestern part of Hardangerjøkulen, central-southern Norway: evidence from lacustrine sediments, *The Holocene*, *4*(4), 377–382, doi:10.1177/095968369400400405. 1.4.2

Nesje, A., J. Bakke, S. O. Dahl, Ø. Lie, and J. A. Matthews (2008a), Norwegian mountain glaciers in the past, present and future, *Global and Planetary Change*, *60*(1), 10–27. 1.4.2

Nesje, A., S. Dahl, T. Thun, and Ø. Nordli (2008b), The Little Ice Age glacial expansion in western Scandinavia: summer temperature or winter precipitation?, *Climate Dynamics*, *30*(7-8), 789–801, doi:10.1007/s00382-007-0324-z. 1.4.2

Nick, F., C. Van der Veen, A. Vieli, and D. Benn (2010), A physically based calving model applied to marine outlet glaciers and implications for the glacier dynamics, *Journal of Glaciology*, *56*(199), 781–794. 1.3.1, 1.3.4, 2

Nick, F. M., A. Vieli, M. L. Andersen, I. Joughin, A. Payne, T. L. Edwards, F. Pattyn, and R. S. van de Wal (2013), Future sea-level rise from Greenland's main outlet glaciers in a warming climate, *Nature*, *497*(7448), 235–238. 2

Nordli, P., Ø. Lie, A. Nesje, and S. O. Dahl (2003), Spring-summer temperature reconstruction in western Norway 1734-2003: a data-synthesis approach, *International Journal of Climatology*, *23*(15), 1821–1841, doi:10.1002/joc.980. 1.4.2

O'Leary, M., and P. Christoffersen (2013), Calving on tidewater glaciers amplified by submarine frontal melting, *The Cryosphere*, *7*(1), 119. 1.3.2

Pattyn, F., L. Favier, S. Sun, and G. Durand (2017), Progress in Numerical Modeling of Antarctic Ice-Sheet Dynamics, *Current Climate Change Reports*, *3*(3), 174–184. 1.1, 1.3.4, 1.4

Peck, V., I. Hall, R. Zahn, H. Elderfield, F. Grousset, S. Hemming, and J. Scourse (2006), High resolution evidence for linkages between NW European ice sheet instability and Atlantic Meridional Overturning Circulation, *Earth and Planetary Science Letters*, *243*(3), 476–488. 1.1

Pfeffer, W. (2003), Tidewater glaciers move at their own pace, *Nature*, *426*(6967), 602–602. 1.3.1, 1.3.4

Pfeffer, W. (2007), A simple mechanism for irreversible tidewater glacier retreat, *Journal of Geophysical Research: Earth Surface (2003–2012)*, *112*(F3). 1.3.1, 1.3.4

Pollard, D., R. M. DeConto, and R. B. Alley (2015), Potential Antarctic Ice Sheet retreat driven by hydrofracturing and ice cliff failure, *Earth and Planetary Science Letters*, *412*, 112–121. 1.3.1, 1.3.4

Post, A., S. O'Neel, R. J. Motyka, and G. Streveler (2011), A complex relationship between calving glaciers and climate, *Eos, Transactions American Geophysical Union*, *92*(37), 305–306. 1.3.1

Rasmussen, L., L. Andreassen, S. Baumann, and H. Conway (2010), 'Little Ice Age' precipitation in Jotunheimen, southern Norway, *The Holocene*, *20*(7), 1039–1045, doi:10.1177/0959683610369510. 1.4.2

Rasmussen, S. O., M. Bigler, S. P. Blockley, T. Blunier, S. L. Buchardt, H. B. Clausen, I. Cvijanovic, D. Dahl-Jensen, S. J. Johnsen, H. Fischer, et al. (2014), A stratigraphic framework for abrupt climatic changes during the Last Glacial period based on three synchronized Greenland ice-core records: refining and extending the INTIMATE event stratigraphy, *Quaternary Science Reviews*, *106*, 14–28. 1.4.1

Reeh, N., H. H. Thomsen, A. K. Higgins, and A. Weidick (2001), Sea ice and the stability of north and northeast Greenland floating glaciers, *Annals of Glaciology*, *33*(1), 474–480. 1.3, 1.3.3

Rignot, E., and P. Kanagaratnam (2006), Changes in the velocity structure of the Greenland Ice Sheet, *Science*, *311*(5763), 986–990. 1.3

Rignot, E., I. Fenty, Y. Xu, C. Cai, and C. Kemp (2015), Undercutting of marine-terminating glaciers in West Greenland, *Geophysical Research Letters*, *42*(14), 5909–5917. 1.3.2

Robel, A. A. (2017), Thinning sea ice weakens buttressing force of iceberg mélange and promotes calving, *Nature Communications*, *8*. 1.3, 1.3.3

Roe, G. H., and R. S. Lindzen (2001), The mutual interaction between continental-scale ice sheets and atmospheric stationary waves, *Journal of Climate*, *14*(7), 1450–1465. 1.1

Sæle, T. H. (2017), Skuringsstriper og isbevegelse for Hordaland [unpublished], Master's thesis, University of Bergen. 1.4.1

Scambos, T. A., J. Bohlander, C. u. Shuman, and P. Skvarca (2004), Glacier acceleration and thinning after ice shelf collapse in the Larsen B embayment, Antarctica, *Geophysical Research Letters*, *31*(18). 1.3.4

Schoof, C. (2007), Ice sheet grounding line dynamics: Steady states, stability, and hysteresis, *Journal of Geophysical Research: Earth Surface*, *112*(F3), n/a–n/a, doi:10.1029/2006JF000664. 1.3.4

Schoof, C. (2010), Ice-sheet acceleration driven by melt supply variability, *Nature*, *468*(7325), 803–806. 1.3.1

Schoof, C., A. D. Davis, and T. V. Popa (2017), Boundary layer models for calving marine outlet glaciers, *The Cryosphere Discussions*, (in review), doi:https://doi.org/10.5194/tc-2017-42. 1.3.4

Sejrup, H. P., E. Larsen, H. Haflidason, I. M. Berstad, B. O. Hjelstuen, H. E. Jonsdottir, E. L. King, J. Landvik, O. Longva, A. Nygård, et al. (2003), Configuration, history and impact of the Norwegian Channel Ice Stream, *Boreas*, *32*(1), 18–36. 1.3.4, 1.4.1

Seroussi, H., M. Morlighem, E. Larour, E. Rignot, and A. Khazendar (2014), Hydrostatic grounding line parameterization in ice sheet models, *The Cryosphere*, *8*(6), 2075–2087, doi:10.5194/tc-8-2075-2014. 2

Slater, D. A., D. N. Goldberg, P. W. Nienow, and T. R. Cowton (2016), Scalings for submarine melting at tidewater glaciers from buoyant plume theory, *Journal of Physical Oceanography*, *46*(6), 1839–1855. 1.3.2

Sole, A. J., D. W. F. Mair, P. W. Nienow, I. Bartholomew, M. King, M. J. Burke, and I. Joughin (2011), Seasonal speedup of a Greenland marine-terminating outlet glacier forced by surface melt–induced changes in subglacial hydrology, *Journal of Geophysical Research: Earth Surface (2003–2012)*, *116*(F3). 1.3.1

Sørensen, R. (1992), The physical environment of Late Weichselian deglaciation of the Oslofjord region, southeastern Norway, *SGU series Ca. Research paper*, (81), 339–346. 1.4.1

Stokes, C. R., and L. Tarasov (2010), Ice streaming in the Laurentide Ice Sheet: A first comparison between data-calibrated numerical model output and geological evidence, *Geophysical Research Letters*, *37*(1). 1.3.4

Stokes, C. R., G. D. Corner, M. C. Winsborrow, K. Husum, and K. Andreassen (2014), Asynchronous response of marine-terminating outlet glaciers during deglaciation of the Fennoscandian Ice Sheet, *Geology*, *42*(5), 455–458. 1.3.4

Straneo, F., and P. Heimbach (2013), North Atlantic warming and the retreat of Greenland's outlet glaciers, *Nature*, *504*(7478), 36–43. 1.3.1

Straneo, F., G. S. Hamilton, D. A. Sutherland, L. A. Stearns, F. Davidson, M. O. Hammill, G. B. Stenson, and A. Rosing-Asvid (2010), Rapid circulation of warm subtropical waters in a major glacial fjord in East Greenland, *Nature Geoscience*, *3*(3), 182–186. 1.3.2

Straneo, F., R. G. Curry, D. A. Sutherland, G. S. Hamilton, C. Cenedese, K. Våge, and L. A. Stearns (2011), Impact of fjord dynamics and glacial runoff on the circulation near Helheim Glacier, *Nature Geoscience*, *4*(5), 322–327. 1.3.2

Straneo, F., P. Heimbach, O. Sergienko, G. Hamilton, G. Catania, S. Griffies, R. Hallberg, A. Jenkins, I. Joughin, R. Motyka, et al. (2013), Challenges to understanding the dynamic response of Greenland's marine terminating glaciers to oceanic and atmospheric forcing, *Bulletin of the American Meteorological Society*, *94*(8), 1131–1144. 1.2, 1.3, 1.3.1, 1.3.2

Stroeven, A. P., C. Hättestrand, J. Kleman, J. Heyman, D. Fabel, O. Fredin, B. W. Goodfellow, J. M. Harbor, J. D. Jansen, L. Olsen, et al. (2016), Deglaciation of Fennoscandia, *Quaternary Science Reviews*, *147*, 91–121. 1.4.1, 1.4.2

Svendsen, J. I., H. Alexanderson, V. I. Astakhov, I. Demidov, J. A. Dowdeswell, S. Funder, V. Gataullin, M. Henriksen, C. Hjort, M. Houmark-Nielsen, et al. (2004), Late Quaternary ice sheet history of northern Eurasia, *Quaternary Science Reviews*, *23*(11), 1229–1271. 1.4.1

Svendsen, J. I., J. P. Briner, J. Mangerud, and N. E. Young (2015), Early break-up of the Norwegian Channel Ice Stream during the Last Glacial Maximum, *Quaternary Science Reviews*, *107*, 231–242. 1.4.1, 1.6

Tarasov, L., and W. Peltier (2005), Arctic freshwater forcing of the Younger Dryas cold reversal, *Nature*, *435*(7042), 662. 1.1

Tsai, V. C., A. L. Stewart, and A. F. Thompson (2015), Marine ice-sheet profiles and stability under Coulomb basal conditions, *Journal of Glaciology*, *61*(226), 205–215, doi:10.3189/2015JoG14J221. 1.3.4

Van Den Broeke, M., J. Bamber, J. Ettema, E. Rignot, E. Schrama, W. J. van de Berg, E. van Meijgaard, I. Velicogna, and B. Wouters (2009), Partitioning recent Greenland mass loss, *science*, *326*(5955), 984–986. 1.3.1

Van Der Veen, C., J. Plummer, and L. Stearns (2011), Controls on the recent speed-up of Jakobshavn Isbrae, West Greenland, *Journal of Glaciology*, *57*(204), 770–782. 1.3.1

Velle, G., S. J. Brooks, H. Birks, and E. Willassen (2005), Chironomids as a tool for inferring Holocene climate: an assessment based on six sites in southern Scandinavia, *Quaternary Science Reviews*, *24*(12), 1429–1462, doi:10.1016/j.quascirev.2004.10.010. 1.4.2

Vieli, A., and F. M. Nick (2011), Understanding and modelling rapid dynamic changes of tidewater outlet glaciers: issues and implications, *Surveys in geophysics*, *32*(4-5), 437–458. 1.3.2, 1.3.3

Vieli, A., M. Funk, and H. Blatter (2001), Flow dynamics of tidewater glaciers: a numerical modelling approach, *Journal of Glaciology*, *47*(159), 595–606. 2

Weertman, J. (1974), Stability of the junction of an ice sheet and an ice shelf, *Journal of Glaciology*, *13*, 3–11. 1.3.4

Xu, Y., E. Rignot, D. Menemenlis, and M. Koppes (2012), Numerical experiments on subaqueous melting of Greenland tidewater glaciers in response to ocean warming and enhanced subglacial discharge, *Annals of Glaciology*, *53*(60), 229–234. 1.3.2

Xu, Y., E. Rignot, I. Fenty, D. Menemenlis, and M. Flexas (2013), Subaqueous melting of Store Glacier, west Greenland from three-dimensional, high-resolution numerical modeling and ocean observations, *Geophysical Research Letters*, *40*(17), 4648–4653. 1.3.2

Yokoyama, Y., J. B. Anderson, M. Yamane, L. M. Simkins, Y. Miyairi, T. Yamazaki, M. Koizumi, H. Suga, K. Kusahara, L. Prothro, et al. (2016), Widespread collapse of the Ross Ice Shelf during the late Holocene, *Proceedings of the National Academy of Sciences*, *113*(9), 2354–2359. 4